Parametric Study of a Commercial-Scale Biomass Downdraft Gasifier: Experiments and Equilibrium Modeling

by

Gopal Gautam

A thesis submitted to the Graduate Faculty of
Auburn University
in partial fulfillment of the
requirements for the Degree of
Master of Science

Auburn, Alabama
December 13, 2010

Keywords: biomass, emissions, gasifier, gasification, modeling, thermodynamics

Approved by

Sushil Adhikari, Co-chair, Assistant Professor of Biosystems Engineering
Sushil Bhavnani, Co-chair, Professor of Mechanical Engineering
Daniel Mackowski, Associate Professor of Mechanical Engineering

Abstract

Biomass has already emerged in the renewable energy arena as one of the promising candidates for the future. Biomass has been a major source of fuel for human from the existence of mankind. Rapid urbanization and widespread use of fossil fuels in the industrial world has relegated it to the status of a minor source of energy. The rejuvenation, however, started with increasing concerns over reducing carbon footprints and also due to strong causative connections between non-renewable fossil fuels and "global warming". Biomass gasification is a thermo-chemical process of converting biomass into the producer gas or syngas (used interchangeably) which can be subsequently used for heat, power and liquid fuels production through various synthesis processes. The major objective of this study was to better understand the effect of various parameters on the syngas composition from a stratified downdraft gasifier. The study is primarily experimental but supplemented by the mathematical modeling that explains various steps in terms of existing scientific principles.

Chapter 1 provides basic literature review on the gasification process, various types of gasifiers and elaborated discussion about the effect of various parameters on syngas composition for different types of gasifiers. The effects were primarily discussed for updraft, downdraft and fluidized bed gasifiers which currently cover more than 98% of the total biomass gasification market.

Chapter 2 presents a thermodynamic model of the process inside the gasifier. Syngas composition is predicted assuming thermodynamic equilibrium condition inside the gasifier. The

thermodynamic equilibrium can be assumed because residence time is high in the fixed bed gasification process. The effect of moisture content as well as temperature was determined. The model was run for nearly 100 samples. Based upon the results of the simulations, using linear regression analysis, equations were derived to predict the syngas composition of the biomass based on their elemental composition and moisture.

Chapter 3 is an experimental study on the effect of selected process parameters such as moisture content and biomass flow rate on syngas composition in the downdraft gasifier. Parameters studied are moisture content and biomass flow rate inside the gasifier. A mass, energy and exergy analysis is also done to corroborate the experimental results as well as to visualize the carbon, heat, and availability loss inside the gasifier in the process.

Chapter 4 discusses tar downdraft gasifier. Although the amount of tar from a downdraft gasifier is always assumed to be small, it is more stable and might adversely affect when used for power generation. Significant amount of toluene, o/p-xylene, naphthalene, phenol, styrene and indene was observed. Tar concentration in the syngas from the gasifier was found to be 0.34-0.68 mg/Nm^3.

Acknowledgments

I would like to express my sincere gratitude to Dr. Sushil Adhikari and Dr. Sushil Bhavnani for their constant support, guidance and help throughout this thesis work. Discussions with them have formed the basic background for this work. Without their help, this thesis could have never achieved its current form.

I am also very grateful to the Center for Bioenergy and Bioproducts and Alabama Agricultural Experiment Station of Auburn University for providing funding for some portion of this study. I would like to thank Mr. Christian Broadbeck for his immense help while conducting the experiments with the gasifier. Without his help, much of this thesis would have remained undone. Also Jonathan Griffith deserves special thanks for helping me with the gasification experiments. I would also like to acknowledge the help from my colleague, Ms. Suchithra Thangalazhy-Gopakumar for help in various experimental works conducted for this thesis.

Finally, I would like to thank my parents for being the source of motivation and support for me throughout my entire academic career. They are always the source of my perseverance, understanding and willingness to accept the challenges I have faced.

Table of Contents

List of Tables

List of Figures

CHAPTER 1

LITERATURE REVIEW

In this chapter, various aspects of biomass gasification were reviewed. The most widely used configurations of biomass gasifiers and the effect of various operating parameters on the quality of syngas are discussed in detail.

1.1   INTRODUCTION

Biomass has evolved as one of the most promising sources of fuel for the future. This has spurred the growth of research and development efforts in both federal and private sectors [1]. This impetus is motivated by several factors; dwindling fossil fuels and thus an increase need of energy security, environmental concerns and promotion of socioeconomic benefits to rural areas. Another important fact is somewhat uniformly distributed nature of biomass worldwide which means it is available locally and is helpful in reducing the dependence upon the fossil fuel [2]. The United States target has potential to produce 60 billion gallons of bioethanol per year if all the available biomass is converted to produce bioethanol [2]. This requires one billion tons of dry biomass per year which can be reasonably achieved. A recent study shows that the United States has a potential of 1.3 billion tons of dry biomass per year from its forest and agricultural resources [2-3]. Studies show the world-wide recoverable residues to be 31 exajoules per year which is almost equivalent to 10% of the commercial energy use [4-5]. Figure 1.1 shows the distribution of different renewable energy generation in the United States. The energy derived

1

from biomass is significant and accounts for more than half of all the renewable energy generation among which, two-thirds is used for heat, power or combined heat and power (CHP) [6].
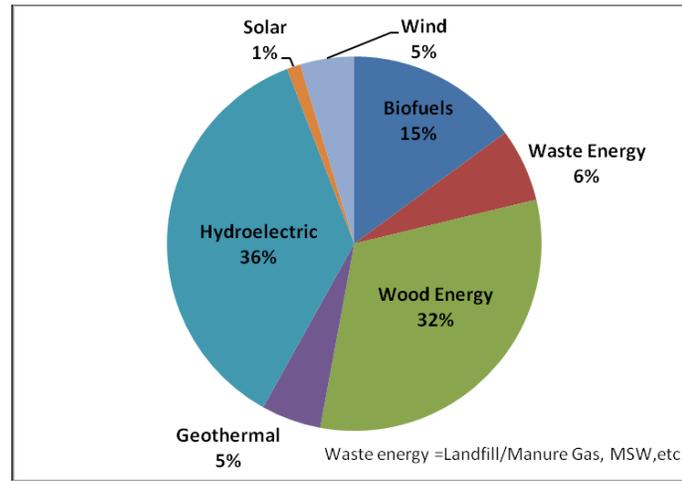
Figure 1.1 Total U.S renewable energy consumption [6]

The end-use of products from biomass conversion can be mainly in any one of heat and power applications, transportation fuels (biodiesel, bioethanol) and chemicals for subsequent processing [7]. Up to present, the only long-term solution for the carbon based fuels and chemical is biomass and can be effectively converted into solid, liquid and gas [8-9]. Huber et al. [10] opine that among all the renewable energy sources, biomass is the most optimal long-term fuel for transportation. Biomass can be converted into biofuels using either thermal or chemical processes. Among thermal conversion processes, gasification has received the most attention. This is due to the higher efficiency compared to processes such as direct combustion, pyrolysis and liquefaction [11-13]. Figure 1.2 shows the power generation from overall gasification (including coal and biomass) from 1970 to 2004 [14]. This industrial rate of power generation

2

using gasification process can be expected to rise with advances in clean coal technologies and more economically feasible techniques for biomass gasification.

Different forms of thermal treatment of biomass are distinguished from each other by the amount of air supplied, residence time, temperature, and consequently the heat transfer rate in the process. Supplying excess air results in combustion while treatment without air/oxygen results in pyrolysis products [15]. Gasification is the conversion of biomass into the mixture of combustible and non-combustible gases (referred as syngas hereafter) by partial oxidation at high temperature around 800-900°C in the presence of a gasifying medium such as air, oxygen or steam. Syngas from biomass is a mixture of carbon monoxide (CO), carbon dioxide (CO_2), hydrogen (H_2), water (H_2O) and a small amount of methane (CH_4). The use of syngas for power generation is widely accepted and considered mature technology [16].
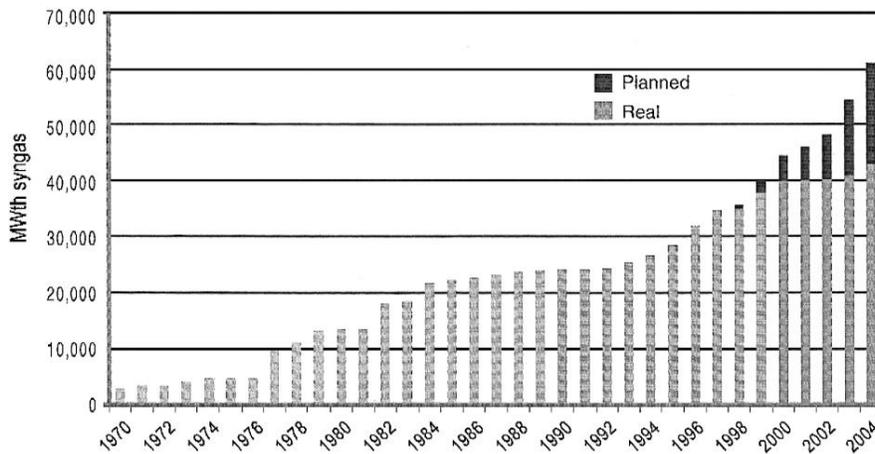
Figure 1.2 Worldwide power generation from gasification (Simbeck [14])

1.2   GASIFIER TYPES AND PROCESSES

Warnecke [17] has classified the gasifiers in four categories which are based on the fluid and/or solid movement inside the reactor.

3

i.   Quasi non-moving or self-moving feedstock

ii.   Mechanically-moved feedstock

   a.   Downdraft gasifier

   b.   Updraft gasifier

   c.   Cross-draft gasifier

iii.   Fluidically-moved feedstock

   a.   Bubbling bed (BB) gasifier

   b.   Circulating fluidized bed (CFB) gasifier

   c.   Entrained-bed gasifier

iv.   Special reactors

   a.   Spouted bed gasifier

   b.   Cyclone gasifier

Among those listed above, downdraft, updraft, BB and CFB gasifiers are the most common as also shown by studies [18]. Figures 1.3-1.6 show schematics of various gasifiers that are widely used in the commercial market. Commercially, about 75% of the gasifiers sold are downdraft gasifiers, 20% fluidized bed, 2.5% updraft, and 2.5% of the other types [18].

The updraft gasifier is popular for application choice when the primary purpose of gasification is heating only (below 10 MWt) due to its high thermal efficiency and ability to handle feedstock with wide variation in size and moisture content as high as 50% [19]. Downdraft gasifiers are preferred for small scale power generation due to low amount of tar content in the syngas. The problem with fixed-bed gasifiers is their inability to maintain uniform radial temperature which results in local slag, bridging and clinkering problems. Lack of uniform

radial temperature is one of the reasons why this kind of gasifier cannot be scaled up rendering them inflexible and of limited use [19].

Fluidized bed gasifier provides higher throughput than those with a fixed bed. Fluidization enhances mass and heat transfer from the fuel thereby increasing heating value of the output and higher efficiency rendering it excellent for low-rank coal and biomass gasification. Entrained bed gasification is similar to fluidized bed gasification except for the operation range temperature which is usually higher than 1900°C. This type can have a even higher throughput capacity but is limited to coal use only due to the particle size constraint on the feedstock (less than 0.15 mm) [20].
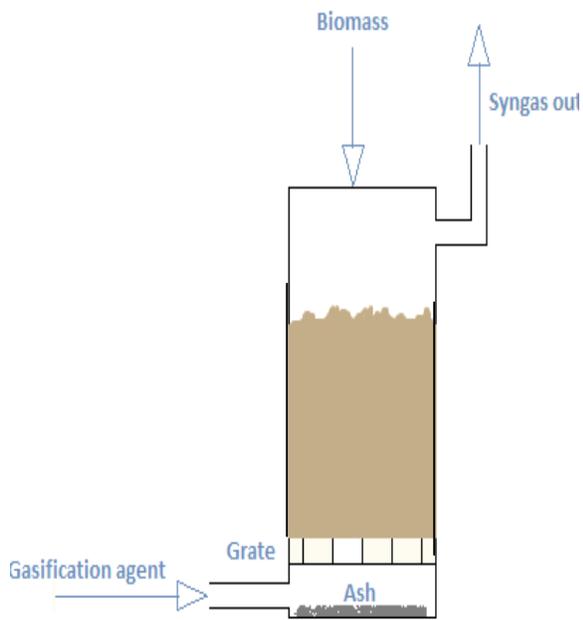
Figure 1.3 Updraft gasifier   Figure 1.4 Downdraft gasifier
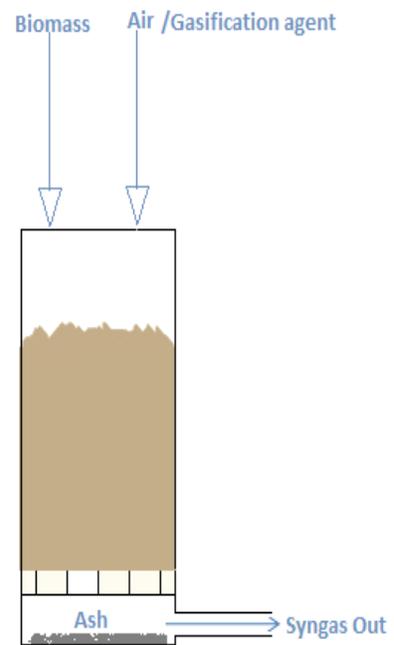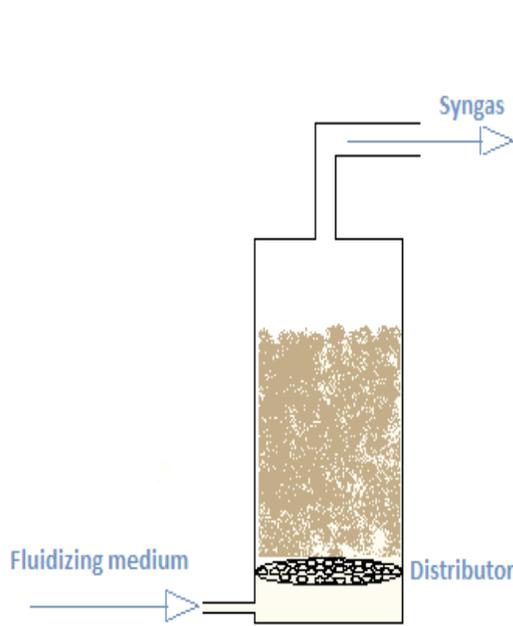
Figure 1.5 Bubbling bed fluidized gasifier   Figure 1.6 Circulating fluidized bed gasifier
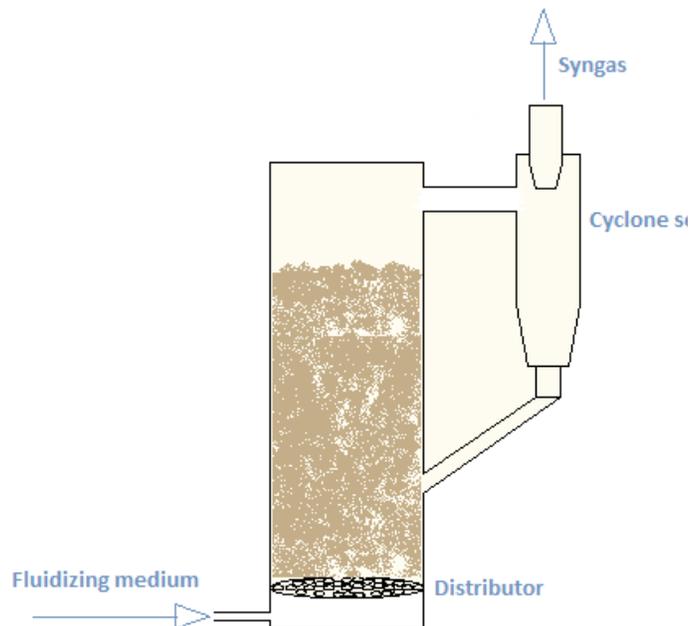
The various types of gasifiers shown in Figure 1.3-1.6 are discussed in the sections below. BB and CFG gasifiers are discussed in a single section as fluidized gasifier due to minor differences between them.

1.2.1 UPDRAFT GASIFIER

The movement of the feedstock and the gasifying agent are in opposite directions in this kind of gasifier (also called a counter-current gasifier). Since the syngas formed is not forced to pass through the hot high temperature zone, the tar content is high in the syngas from this gasifier. On the other hand, the temperature of syngas exiting from this gasifier is lower around (200-300°C) and hence the thermal efficiency of this kind of gasifier is high. Due to high tar content in the syngas, a subsequent tar cleaning system is needed, which can become a major investment if the end-process requires tar-free syngas.

6

1.2.2 DOWNDRAFT GASIFIER

In a downdraft gasifier, the feedstock and gasifying agent both move in the same direction. The gases have to pass through the high-temperature so amount of tar is significantly lower than that in an updraft gasifier. The particulate content is however higher for downdraft gasifier and the thermal efficiency is lower since syngas draws an appreciable amount of energy while passing through the high-temperature zone inside the gasifier.

1.2.3 FLUIDIZED GASIFIER

In fluidized bed gasifiers, feedstock is fluidized with some bed material like sand/silica with a gasifying medium which can be air or steam. Fluidized bed gasifiers can further be classified into two types: bubbling and circulating. Circulating fluidized bed adds one more feature to bubbling bed such that solid material trapped in the gas phase is trapped and re-circulated back to the gasification bed. This provides the significant advantages over the bubbling bed gasifier in terms of mass conversion efficiency and reduces particulate content in the syngas output [20].

Table 1.1 Various characteristics, properties and difference between common types of gasifier ([17, 20-22])

Characteristics	Gasifier Type			
	Downdraft	Updraft	BBG	CFBG
Gasifier size	High space requirement for higher throughput due to modular design of the gasifier and high residence time		Less space required due to enhanced heat transfer resulting in much faster gasification and lower residence time inside the gasifier	
Temperature Profile	Not uniform temperature distribution in the radial distribution		Uniform temperature distribution inside the gasifier	
Permissible particle size/ Size sensitivity	< 50 mm/good		< 5 mm/more sensitive to feedstock size	
Reaction zone temperature	800-1100°C		800-1000°C	
Ability to handle fine paricles	Limited		Good	
Moisture content	Very flexible	Flexible	Flexible	
Gas exit temperature	600-800°C	250°C	850°C	
Tar concentration	very low (0.01-6 g/Nm^3)	very high (50 g/Nm^3)	6-12 g/Nm^3	
Carbon conversion efficiency	Very good		Fair	Very good
Thermal efficiency	Very good	Excellent	good	Very good
LHV of syngas	poor	poor	poor	Fair
Cold gas efficiency	>80%		>90%	
Gas clean-up	High cleaning required	relatively clean gas	Clean-up required for dust and tar	
Dust content in syngas	High	Low	Higher dust content	
Energy requirement for operation	Low		High due to requirement of fans for fluidization	
Investment	Higher investment for the energy generation compared to BBG/CFBG (for large scale output)		Lower investment	
Process control	Cannot be controlled effectively as BBG/CFBG		Easy process control	
Applications	Small to medium scales		Large scales	

1.3 CHEMICAL REACTIONS IN THE GASIFICATION PROCESS

Gasification is a highly complex chemical process. Bridgewater described the gasification sequence as drying and evaporating processes of biomass followed by pyrolysis, and finally oxidation and reduction [23]. However, the overall process can be reasonably described by the reactions described below [22, 24-25].

$$Biomass \xrightarrow{heat(300-400^oC)} gases\ (CO, CO_2, H_2, light\ HC's) + pyrolyzed\ vapors + char \tag{1}$$

$$Pyrolyzed\ vapors \xrightarrow{(heat+high\ residence\ time)} gases\ (CO, CO_2, H_2, light\ HC's) \tag{2}$$

$$C + O_2 \leftrightarrow CO_2, \Delta H = -393.5\ kJ/mol \tag{3}$$

$$C + (1/2)O_2 \leftrightarrow CO, \Delta H = -110.5\ kJ/mol \tag{4}$$

$$C + CO_2 \leftrightarrow 2CO, \Delta H = 172.4\ kJ/mol \tag{5}$$

$$C + H_2O \leftrightarrow H_2 + CO, \Delta H = 131.3\ kJ/mol \tag{6}$$

$$C + 2H_2 \leftrightarrow CH_4, \Delta H = -74.8\ kJ/mol \tag{7}$$

$$CO + H_2O \leftrightarrow H_2 + CO_2, \Delta H = -41.1\ kJ/mol \tag{8}$$

$$CO + 2H_2 \leftrightarrow CH_4 + H_2O, \Delta H = 206.1\ kJ/mol \tag{9}$$
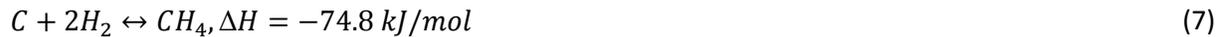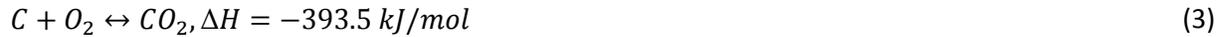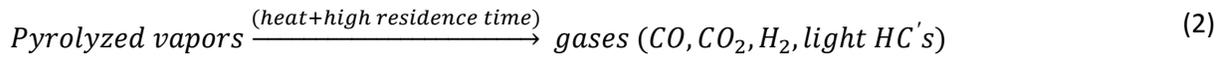
Among the reactions described above, the char-oxidation (Eq. 3) and partial-oxidation (Eq. 4) reactions are slowest, and consequently the rate controlling factor in the overall gasification process [24]. Pyrolysis also results in liquid which is resistant to the cracking due to temperature increase though most of the pyrolyzed liquid does so at higher temperature. This

requires subsequent cleaning set-up for the tar, which can be a substantial investment in many cases [23].

1.4   EFFECT OF VARIOUS PARAMETERS IN THE GASIFICATION PROCESS

Syngas composition varies widely and mostly depends upon the gasifier type, feedstock, feedstock pre-treatment, gasifying medium and operating parameters like temperature, pressure, and nature of interaction between reactants in the gasification process [20, 26]. The effects of major parameters affecting the quality of syngas are discussed in the sections below.

1.4.1   MOISTURE CONTENT

Biomass contains moisture in both ways: intrinsically by its nature, and extrinsically wherein moisture is absorbed from the surrounding atmosphere [27-28]. Moisture content in the biomass, during gasification, increases CO_2 concentration by the water-shift reaction (Eq. 8) which consumes CO and liberates H_2 [27, 29-30]. While the equilibrium constant for water-shift reaction varies little over a wide range of temperatures, the direction tends to reverse at higher temperature. Since more heat is required for moisture evaporation than the small amount of heat gained due to the exothermic behavior of the water-shift reaction, thermal energy inside the gasifier reduces when gasifying biomass with higher moisture content [24]. Thus, the decrease in temperature further exacerbates the scenario and forms more CO_2 since the water-shift reaction is improved at lower temperature. The overall effect is the reduction in calorific value of syngas because, the small increase in H_2 is not sufficient to compensate the loss of significant amount of CO with increase in moisture content [27, 29-33]. However, the negative effect of moisture content on the calorific value of syngas is lower at lower equivalence ratio (ER). The ER is the ratio of actual air fuel ratio to the stoichiometric air fuel ratio which provides the basis for

10

evaluating the amount of air supplied for the gasification with respect to the amount of air required for the complete combustion of the feedstock. Roy et al. [27] have observed that, in a downdraft gasifier, when the moisture content is increased from 0 to 40%, heating value of syngas decreases by 8.72% at ER of 0.45 while the decrease was of 4.7% when the ER used was 0.29. This result was reported from their equilibrium model and thus is applicable to any gasification process. Table 1.2 summarizes the effect of moisture content in three common gasifier types.

Table 1.2 Effect of moisture content upon major syngas constituents

Parameter	Gasifier type	CO	CO_2	H_2	CH_4	Maximum limit (% w.b)
Moisture Content (M.C)	Updraft	- [a]	+ [b]	+	~ [c]	<50 [19]
	Downdraft	-	+	+	~	<40 [34]
	Fluidized	-	+	+	~	<10 [20]
[a] decreases with increase in M.C, [b] increases with increase in M.C, [c] no significant change						

A limiting condition called auto-thermal limit is reported as 65% moisture content in literature beyond which self-sustaining gasification is not possible due to an enthalpy deficiency for vaporization. In fact, supplemental fuel is required for most of the combustor when the moisture content is greater than 50% on a wet basis [35-36]. Moisture content up to 30% (wet basis) can be used for downdraft gasifier [21, 34]. When air is used as the gasification agent, the amount of methane produced is small and stays almost constant with change in moisture content [29, 37]. Thus the temperature decrease inside the gasifier due to moisture also results lower mass conversion efficiency and increases tar content [30, 38-40]. Sheth et al. [41] report the decrease in biomass consumption rate with increase in moisture content which is due to the higher amount of heat necessary for drying those wood chips inside the reactor before they can

be pyrolyzed. However, some moisture content is always desirable since it enhances steam reforming and helps to crack tar, and at higher temperature, also enhances other reactions such as char gasification [42-43]. Steam injection is widely used in industrial applications to adjust syngas composition in the gasification process but often, in the presence of higher temperature provided by some external source [44].

1.4.2   EQUIVALENCE RATIO

Equivalence ratio (ER) is the most influential parameter in any gasification process and often has significant impact on syngas composition. Increase in ER increases the temperature inside the gasifier while ER decrease increases char formation inside the gasifier.   As can be seen from Figure 1.7, all combustible products reduce with an increase in ER with the formation of higher amount of CO_2 as well as total gas yield greatly diminishing the heating value of the final syngas [45-48]. Zainal et al. [49] compared the best optimal value for the downdraft gasifier with respect to equivalence ratio using furniture wood and wood chips as feedstock. The effect of equivalence ratio for each syngas component was analyzed with the conclusion of an optimal equivalence ratio of 0.38 for the gasifier performance for that particular feedstock. At this equivalence ratio, CO, CH_4 and calorific value each attain their maximum outputs while CO_2 reaches its minimum.
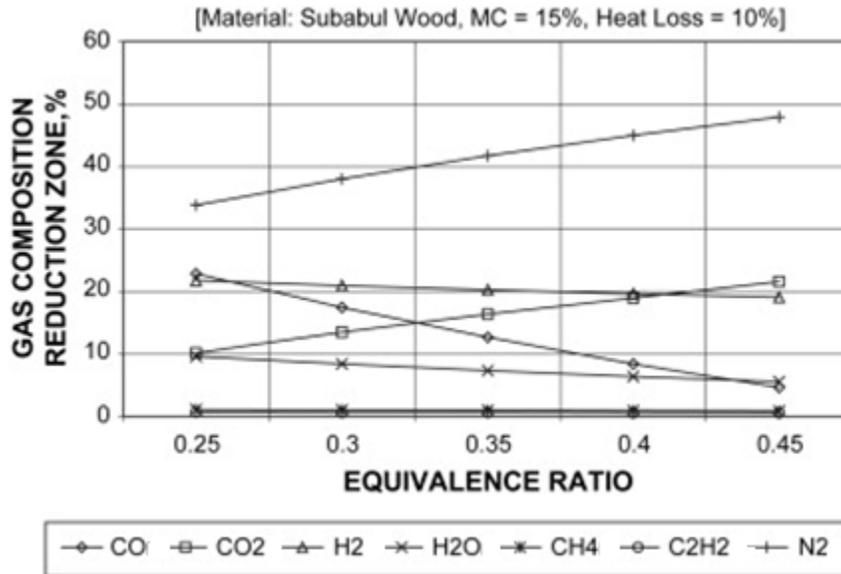
Figure 1.7 Effect of ER upon syngas composition in the reduction zone [39]

Heat conduction inside the gasifier is often limited by the thermal diffusivity of charcoal particles- 0.7×10^{-7} m^2/s which is lower than that of wood [50]. The optimum equivalence ratio is necessary for accelerating pyrolysis and drying rate due to conduction and convection process which also increases the biomass consumption rate [41].

Both Skoulou et al. [51] and Sheth et al. [41] report an optimal equivalence ratio of 0.2 for downdraft gasification of olive kernels and olive tree cutting and furniture wood. The optimum equivalence ratio varies for different biomass due to the amount of oxygen elementally present in the biomass as well as the ash content. For example, coal requires far more oxygen than common biomass materials for gasification due to its lower oxygen content [40]. The existing literature shows that equivalence ratio should be around 0.3-0.4 for the successful gasification. Table 1.3 shows the optimal equivalence ratio for selected feedstocks. Also from

Table 1.3, difference in optimal ER can also be observed for the feedstock with same elemental composition (pine wood chips and saw dust) in fluidized bed. This is due to the difference in gasification temperature which was lower for pine saw dust (780-830°C) than pine wood chips (>900°C). Optimal equivalence ratio for an updraft gasifier is not shown in the table due to the limitations of available literature for updraft configuration.

Table 1.3 Optimal ER for some feedstocks in downdraft and fluidized gasifiers

Gasifier type	Feedstock	Optimal ER	References
Downdraft	Furniture wood + charcoal	0.38	[49]
	Olive kernels and olive tree cutting	0.2	[51]
	Hazelnut shells	0.28	[34]
	Furniture waste	0.2	[41]
Fluidized bed	Rice husk	0.2-0.55	[52]
	Pine wood chips	0.3	[53]
	Pine saw dust	0.2	[42]

Any compound with molecular weight greater than that of benzene is called tar [54]. Tar concentration decreases with increase in ER. This is mainly due to two reasons: (a) higher temperature as a result of higher ER increases reaction rates of the chemical products; and (b) high ER supplies additional oxygen for cracking of tar into lower hydrocarbons, CO_2 and H_2O. Thus, at some point between the applicable ranges (0.15-0.4), a shift between types of tar is also reported. Light tar increases while heavy tar decreases [46, 55]. Corella et al. [56] suggests an equivalence ratio above 0.36 for pine wood in a fluidized bed to reduce the tar content below 2 g/m^3, a level below which coke formation does not exceeds its removal rate.

The effect of superficial velocity (SV) is worthy of discussion under the topic of equivalence ratio due to its direct relation with the amount of gasification/fluidization medium injected inside the gasifier. The SV is the ratio of volume flow rate of syngas to the cross-sectional area of the gasifier and can be thought as one independent parameter unconstrained to a particular gasifier size. Higher SV promotes burning as well as reaction rate and decreases the residence time of biomass in the system [57]. Higher burning rate increases the temperature of the gasifier. Yamazaki et.al [58] recommended SV greater than 0.4 m/s for syngas appropriate for internal combustion engines. An overall increase in combustibles (except CH_4 which shows no appreciable change) is reported with increase in SV. An initial decrease reaching the minimum level followed by an increase is reported with SV, the optimum SV being 0.4 m/s. Increase tar after the increase beyond optimum SV is due to the short residence time of the tar vapors inside the gasifier and slowing down cracking.

1.4.3   TEMPERATURE

Increase in temperature reduces the tar content as well as decreases char inside the gasifier [51, 59]. Gas yield increases due to higher tar cracking. One of the means of increasing temperature is by internal recirculation of syngas [60]. Tar cracking temperatures are often reported to be around 1000-1100°C with some dependency on gasifier design [34, 54]. Other methods of tar cracking are also employed such as multi-stage gasifiers [61-63]. Multi-stage gasifiers, as shown in Figure 1.8, have separated pyrolysis and gasification zones and make use of partial oxidation of pyrolysis gas obtained in the pyrolysis zone for tar cracking and thus, tar content can be reduced as low as 15mg/Nm^3 (Nm^3 –volume at STP) [61]. CO content increases with increase in temperature because endothermic reactions are more favored at higher temperature [64]. Mass conversion efficiency decreases with decrease in temperature [60]. An

15

oxidation zone below a temperature of 725°C gives significantly lower mass conversion efficiency [65].
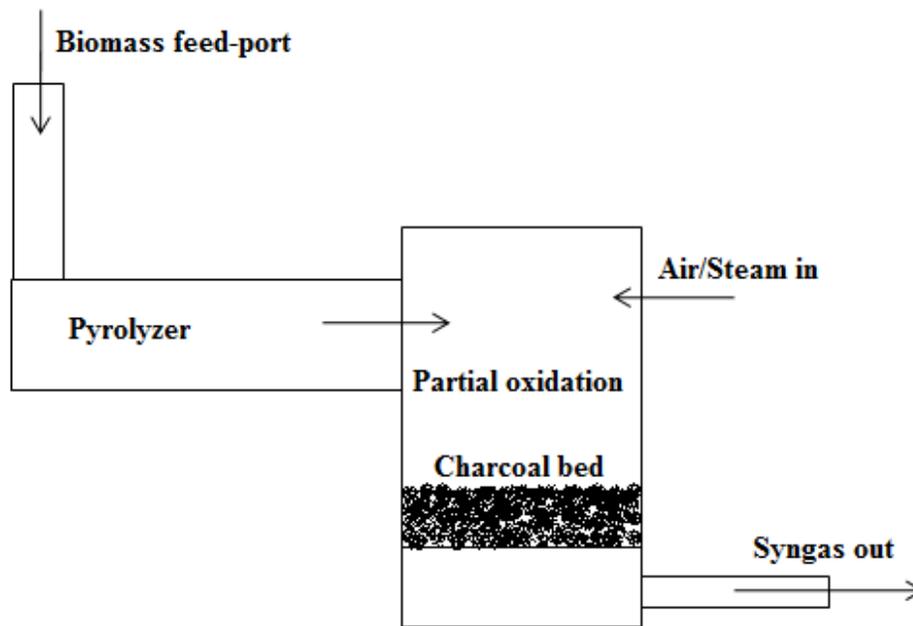
Figure 1.8 Multi-stage downdraft gasifier

Uniformity of temperature in a radial as well as in axial direction inside the reactor is very important for efficient mixing in a fluidized bed. Generally, less than 100°C difference in total riser height is acceptable [43]. Heating value as well as syngas yield is found to increase due to increase in combustibles, particularly at temperatures above 800°C with an increase in operating temperature driven by an external supply of heat in the gasifier for constant ER [43, 45, 47, 66-67]. However, this is different when the temperature is increased due to increase in ER inside the reactor which actually reduces the combustibles [47]. Temperature control cannot

be independent in any gasification process and is an output variable, with the exception of small lab-scale or pilot plants which can be heated with external heat. The temperature of the reactor is dependent on various factors such as moisture content of the fuel, ER, heat losses from the system, and amount of steam added [56, 68-69]. Thus, the temperature inside the gasifier should represent an optimal compromise with ER. The best approach is the proper insulation of the reactor and using waste heat. Higher temperature also reduces tar content significantly due to thermal cracking [43, 45, 47, 67, 70-72]. In addition, Cao et al. [70] report higher reduction in tar with same increase in top part of reactor than in bottom section. However, Drift et al. [55] suggest that the tar that is cracked due to temperature is mostly the heavy tar while light tar is not decomposed. Heavy tars are the product of pyrolysis process which has not gone through cracking while light tars are the cracking products of heavy tar. In certain cases, light tar seems to increase due to the subsequent breakdown of heavy tar into light tar and other compounds. Typical temperatures suggested for biomass gasification in a fluidized bed are around 800-900°C by various studies [67, 72-73]. Although, high temperature increases carbon conversion efficiency of the overall gasification system, consideration should be given to prevent the formation of ash-melt, made not to form ash-melting, especially when used to gasify biomass material with high ash content like rice husk [55]. Seggiani [74] has developed the empirical relations that can be used to predict ash-fusion temperature of biomass-ash based on its elemental composition under reducing conditions. Eq. (10) shows the general form of the relation.

$$T = \alpha_O + \alpha_1 X_1 + \alpha_2 X_2 + \cdots + \alpha_{49} X_{49} \tag{10}$$

In the above relation, α_0 to α_{49} are the coefficients for calculating ash fusion temperature and X_1 to X_{49} are the various chemical compounds present in biomass-ash.

17

1.4.4   BIOMASS TYPE

Biomass elemental composition has a significant effect on syngas composition. The release of pyrolysis gas is highly dependent on hydrogen/carbon ratio as well as oxygen/carbon ratio and increases when these ratios increase, especially with an increase in Hydrogen/Carbon ratio [35]. A higher oxygen concentration in biomass needs lower ER for gasification because of its inherent oxygen that will also be available for gasification [40].

Table 1.4 Ash content and its elemental composition for some common feedstocks

(% dry basis)

Feedstock	Ash	CaO	K_2O	MgO	Na_2O	SiO_2
Pine	3.1	13	7.9	4.5	1.9	52
Poplar	3.4	33	18	3.7	0.14	2.8
Rice straw	13.1	8.9	16	3.5	2.8	51.0
Wheat straw	5.9	8.1	18	2.4	0.22	44.0
Switch-grass	8.97	2.03	11.6	3.0	0.58	65.18

Another important factor is the ash content of the feedstock. Table 1.4 provides the ash content (% dry basis) and the elemental composition of various common biomass feedstocks [35, 75]. Although formation of clinkers can cause problems for the gasifier operation with biomass having ash-content above 5%, successful gasification with ash-content up to 25% is reported [22, 76]. Higher ash content causes slagging, and consequently ash agglomeration due to fusion, the rate of which is dependent upon the ash content in biomass and ash composition [35, 77-78]. Thus high ash content biomass should be gasified at the temperature below the oxidation or reducing temperature of the minerals constituents in the ash, often which is not possible if the constituents have relatively low ash-fusion temperature [54, 62]. Common ash minerals in

biomass are silica, potassium, calcium, aluminum, magnesium, iron, sodium and chlorine. These minerals present in biomass can exist as salts and vaporize during the gasification process contaminating the syngas. Also, it is highly possible for these minerals to react with silicon in presence of oxygen to create low-temperature melting silicates which can create a severe deposition problem. Alkali metals such as potassium and calcium silicates have melting temperatures even below 700^0C [35]. One other way to tackle the problem is to resort to some kind of removal process like leaching for alkali metal removal which has been reported to reduce these minerals by more than 80%. Removal of these alkali metals will increase the ash fusion temperature thus facilitating gasification [35].

The presence of ash in biomass requires careful control over the operating temperature. Neither should it be high enough to fuse minerals in the ash forming a barrier to further gasification by formation of clinkers, nor too low leading to unburnt carbon resulting in lower carbon conversion efficiency.

1.4.5   PARTICLE SIZE

Fixed bed gasifiers have lower biomass feedstock size restrictions compared to fluidized bed gasifiers. Usually, feed size less than 51 mm and 6 mm is recommended for fixed bed and fluidized bed, respectively [20]. Use of larger size feedstock has been tried and reported by several authors [79-81]. Saravanakumar et al. [80] have successfully gasified long sticks with length of 68 cm and diameter of 6 cm successfully in a top-lit updraft gasifier. The maximum particle size suggested for a conventional downdraft gasifier with throated design is one-eighth of the reactor throat diameter [82]. The larger particles form bridges preventing the efficient flow

19

of biomass inside a gasifier while smaller particles interferes with the air/gasifying agent passage creating high pressure drop and consequently can result in gasifier shut-down [22].

Sharma [83] reports increase in the temperature of oxidation and reduction zone with decrease in particle size of the biomass feedstock in a downdraft gasifier. Decrease in particle size reduces the heat loss due to radiation and enhances the thermal conductivity in the oxidation and reduction zones. On the other hand, decrease in particle size increases pressure drop inside the gasifier. Burning rate and thus the char oxidation period of fuel particles decrease with increase in bulk density and particle size [33, 77]. Biomass consumption rate is inversely related to particle size [57]. In other words, higher residence time is recommended for larger biomass particle size. Decrease in CO with increase in CO_2 concentration is observed. Ryu et al. [84] report decrease from 18% to 13.5% CO when the size of wood cubes used in the experiments were increased from 10 mm to 35 mm. Their model predicts a decrease in CH_4 and an increase in H_2 with increase in size of biomass particles. Also, the temperature gradient decreases thus increasing time taken for diffusion of heat. This will result in poor temperature distribution which is also one of the reasons for the increase in CO_2 concentration with increase in particle size.

Carbon conversion efficiency is not strongly affected by particle size except the lower biomass size increases tar concentration because of high entrainment susceptibility during fluidization [85]. This is because particles can be easily transported to the upper part of the reactor, leaving little time for tar cracking. Multi-staging can prevent this as demonstrated the novel concept developed by Kersten et.al [86] using a gasifier design consisting of several cone shaped structures welded together with the base of each connected to the next tubes of equal diameters. The design, as shown in Figure 1.9, makes it possible to maintain numerous fluidized

sections in one reactor, and thus effectively control back-mixing of solids and gases. On the other hand, the axial temperature drop increases significantly with decrease in size. This is due to the easy passage of feed particles from the feed point and thus little or no reaction taking place below the feed point. Thus, the homogeneity of the bed material cannot be maintained throughout the reactor [55, 69]. Wiman and Almstedt [87] report increase in gas-particle interactions with decrease in particle size in a fluidized bed reactor.
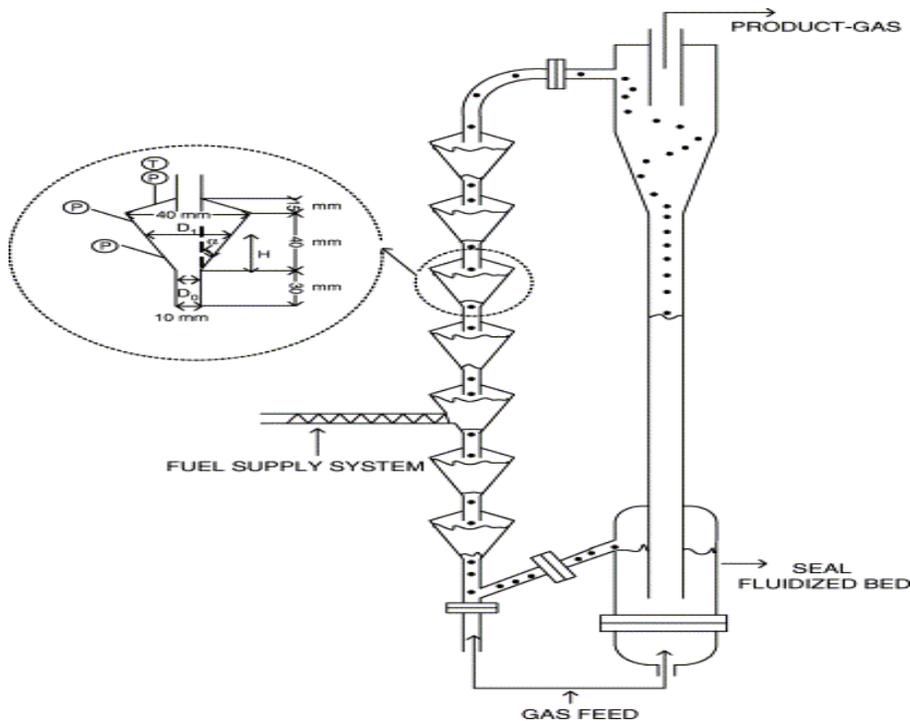
Figure 1.9 Novel multistage fluidized bed biomass gasifier [86]

1.4.6 PRESSURE

High-pressure gasification reduces the size of the reactor for the same amount of feedstock and can act to reduce the need for further compression when the gasification products are intended for subsequent use in Fischer-Tropsch process or other chemical synthesis which requires high pressure [88]. Pressure drop across the gasifier increases with smaller particle size

21

due to increased porosity [77]. The general recommendation of biomass particles size for various gasifiers is listed in Table 1.1.

Increase in pressure in a fluidized bed increases turbulence and thus increase in gas-particle interaction is observed. Increase in pressure also results in bubble instability and bubble splitting in fluidized bed. Wiman and Almstedt [87] have defined a parameter called bed expansion ratio (δ) as follows:

$$\delta = \frac{H_{f1} - H_{mf}}{H_{f1}}$$

Where, H_{f1}= fluidization height at given condition

H_{mf}= minimum fluidization height

Their finding shows a significant increase in δ with increase in pressure. However, the rate of increase drops with increase in pressure and levels off once the pressure reaches around 1 MPa. Among the two particles size of 0.45 mm and 0.70 mm selected for their experiment, δ is lower for the larger size particle [87].

Valin et al. [88] have studied the effect of pressure upon syngas composition with pressure from 2 to 10 bar in fluidized bed with wood sawdust as a feedstock. With increase in pressure, an increase in CO_2, CH_4 and H_2 were observed, while CO decreased. In their lab-scale reactor using steam and N_2 as the gasification medium, with increase in pressure from 2 to 10 bars, an increase of 16%, 53% and 38% of H_2, CO_2 and CH_4, respectively and decrease of CO by 33% was reported. Overall, increase in dry gas yield increase is reported to be 20% with increase

in pressure from 2 to 7 bars after which the gas yield remains constant. The increase in various gases and total gas yield is due to the increase in char hold-up rate which increases catalytic activity of char as well as improved reaction kinetics due to high pressure.

1.4.7   GASIFICATION MEDIUM AND SECONDARY AIR

Biomass gasification can be done with any of the following medium:

- Air

- Oxygen

- Steam

Gasification with air results in syngas with low higher heating value (HHV) due to inherent dilution with N_2 present in the air. Conversely, gasification with oxygen yields syngas with a heating value of 10-12 MJ/Nm^3 and steam gasification results in syngas with heating value even higher, 15-20 MJ/Nm^3 [23]. Air gasification is widely used compared to oxygen and steam due to its economical and operational advantages [89].

Secondary air reduces the tar content in the syngas due to partial combustion of syngas. This in turn establishes local high temperature zone due to exothermic reactions. Thermal cracking of tar is thus due to these high temperature zones in the periphery of the secondary air. Since heat is obtained from the combustion, HHV decreases with increase in secondary air [43, 70-71]. Pan et al. [71] suggest 20% secondary air (% of the primary air) for the minimum tar in forest waste residues.

1.4.8   GASIFICATION OF WASTES AND BIOMASS CO-GASIFICATION

Bacaicoa et al. [90] have studied the co-gasification of a biomass and high density polyethylene (HDPE) mixture in a downdraft gasifier. As expected, biomass consumption rate decreased with increase in HDPE fraction in the mixture. Since HDPE vaporizes instantly at high gasification temperature, the biomass consumption rate is determined by the amount of lignocellulose present in the mixture. A higher fraction of HDPE in the mixture consumes more oxygen from the air supplied and thus leaves less air for lignocellulose to gasify consequently reducing the biomass flow rate. They also report increase in CH_4 and CO concentration with increase in HDPE fraction, while H_2 varies only slightly and CO_2 decreases. This is attibuted in other study to the strong affinity of HDPE towards a Boudouard reaction (Eq. 5) compared to a water-shift reaction (Eq. 8) [91].

Research has also been conducted with co-gasification biomass and coal [91-96]. Pan et al. [97] have gasified poor quality coal (carbon content less than 38%) and biomass (pine wood chips) in a CFB gasifier using air/steam as the gasifying agent. They have done experiments with varying biomass/coal ratio from 0 to 1 at the interval of 0.25. Low temperature resulted when the proportion of pine chips was increased in the blend due to increase in endothermic reaction rate between wood charcoal of high reactivity and that of steam. The poor quality coal, when used alone was not able to sustain gasification and only produced flue gas (gas consisting mostly CO_2, water vapors and nitrogen from the air). Increased combustibles, gas yield and increase in heating value were reported with increase in the proportion of pine chips.

In another research by Poholery et al. [98] co-gasification of polyethyleneterephthalate (PET) and brown coal was examined in a bench-scale FB with 10% O_2 and 90% N_2 as the

gasifying agent. The blend consists of 23% PET and 77% brown coal since difficulties in gasification were reported when the proportion of PET was increased beyond 23%. The effect of bed temperature and freeboard temperature was reported. Increase in CO and H_2 was found while CH_4 showed slight decrease with increase in fluidized bed temperature. On the contrary, free-board temperature had almost no effect on syngas composition, especially at higher fluidized bed temperature. It is due to the fact that all reactions will be completed in close proximity to the fluidized bed at higher temperature.

Xiao et al. [99] have studied plastic waste gasification in a FB gasifier with air as the gasifying medium. Higher ER led to an increase in temperature in the reactor. The temperature distribution inside the reactor showed gradual decrease of temperature from bed to freeboard. Temperature difference reported by them is 80-100°C. Gas yield also increased with ER, while char and tar concentration decreased. The effect of bed height is also examined and an optimum bed height suggested ensuring long residence time to facilitate the effective cracking of heavy tar and char gasification. CO and H_2 increased initially with an increase in ER due to efficient thermal cracking at higher temperature obtained by higher ER and then subsequently decreased with further increase in ER due to combustion of these products. As expected, HHV decreased with increase in ER. The effect of bed height was also examined on syngas composition. Fluidization velocity at constant ER decreased amount of combustibles, except CH_4, as well as gas yield [99].

Velez et al. [100] report the co-gasification results with sub-bituminous coal and biomass (sawdust, rice husk, coffee husk) in a fluidized bed gasifier with air/steam mixture with the objective of finding the optimum proportion of biomass/coal yielding highest heating value. Tests were run at 6%-15% of biomass beyond which proper fluidization was not possible due to

density difference in two fuel types resulting in fuel segregation upon gasification. Reactor temperature decreases with increase in biomass concentration due to the lower heating value of biomass compared to that of coal. Increase in H_2 and CO was obtained with increase in steam/mixture ratio. Ash agglomeration and sintering was also reported in their study.

Mclendon et al. [101] report lower gas yield from co-gasification of coal and biomass with respect to biomass gasified alone. Another interesting research on waste gasification is the gasification of waste tires. Similar effect of various parameters on syngas composition and product yield, consistent with the above discussion were reported from the gasification studies with waste tires [85, 102].

Recently, co-firing of biomass in coal-fired plants has also emerged as one of the biomass utilization options. Though biomass has higher reactivity than coal and can provide some improvements in overall coal gasification process, there are several problems associated with co-firing of biomass in conventional coal-power plants [103]. The major issues associated with using biomass in conventional coal power plants is tabulated below.

- High moisture content in biomass entails the need for prior drying before using into coal-powered plant.
- Biomass has low bulk density than coal and thus, might require additional handling system as well as some modifications in an existing configuration of the plant.
- The ash in biomass has low melting point than those compared to coal. In addition, biomass-ash is aggressive in nature and might corrode the gasifier and associated gas supply system.

- Biomass is hydrophilic and a non-friable which makes it very difficult in deal in conventional coal feed system.

Impacts of these problems depend upon various factors such as coal/biomass ratio, actual configuration of the coal-powered plant and properties of coal.

1.4.9   BED MATERIAL

Proper consideration of bed material in a fluidized bed is important for achieving proper homogenization of feed particles and efficient heat transfer so that minimum temperature gradient is realized within the riser. In many cases, bed material can itself act as a catalyst facilitating efficient tar cracking [46, 56]. Skoulou et al. [46] compared the effect of olivine over silica sand, latter of which is reported to have adverse effect upon effective fluidization due to agglomeration and tar formation when operating at the temperature below 800^0C. Pfeifer et al. [104] have studied in-bed catalysts in a dual bed fluidized bed reactor with Ni/olivine as the catalyst and observed significant tar reduction. Use of catalyst for tar cracking is itself a vast subject and further discussion is avoided here to remain within the scope of the review. The excellent reviews in can be found in references [54, 105-106].

1.5   SUMMARY AND OBJECTIVES OF THIS STUDY

Although biomass gasification is not a new concept by itself, current energy scenario and significant interests in renewable energy has spurred the industrial and academic research in this field. Various configurations of biomass gasifiers have been studied to achieve the maximum efficiency from the process. An exhaustive amount of literature can be found in this field. The summary of this literature review is tabulated below:

- Proper utilization of biomass through gasification can increases the energy security and creates opportunities in the renewable energy sector.

- Moisture content is one of the major technical challenges in biomass gasification. Drying is usually cost-intensive. Utilization of waste heat to dry biomass can be very helpful.

- The equivalence ratio plays important role in determining the overall syngas quality. While using air as the gasifying agent, high amount of sensible energy is lost in heating the nitrogen from air. Although steam or oxygen gasification is possible, the cost associated with the process make them economically unfeasible. Identifying and operating a gasifier in an optimal equivalence ratio can greatly increase the efficiency of the gasifier.

- Tar content has remained as one of the major issues in biomass gasification. Although primary or secondary tar treatment can be done to reduce the level of tar from the biomass gasifier, costs associated with the process might be considerable. Hence, identification of cost-efficient tar removal techniques can be a major breakthrough in the field of biomass gasification.

- The effect of temperature has significant impact in overall gasification process. Higher temperature cannot be achieved without increasing equivalence ratio which in turn, reduces quality of the syngas. Preventing heat losses from the gasifier by proper insulation can reduce air need to maintain the sustainable gasification temperature.

- The type of biomass affects significantly in the overall syngas composition and sometimes, also in the operational issues in the biomass gasification plants. High ash

content material is not desirable. However, many pre-treatment processes exists that can be used to cure the biomass before feeding into the reactor.

- High pressure gasification is very significant in decreasing the overall reactor size and increasing the quality of syngas from the gasifier. However, costs and maintenance problems can be a major issue.

- Fluidized beds offer an excellent advantage over fixed bed gasifier in terms of scalability. However, the constraints on particle size and moisture content often make it unsuitable at some cases. On other hand, fixed beds are suited more for small-scale application. Particle size constraints can impose enough restriction due to economical issues associated with grinding the particles.

- Co-gasification of biomass is an emerging concept and though not have achieved wide industrial acceptance, might be a excellent means of increasing the use of biomass in power plants in near future.

- The increase in investments in gasification power plants is rapidly increasing. Even though the focus of this new power plants may be more efficient utilization of coal rather than biomass, current status of "global warming" and public awareness in utilizing renewable energy, may create ample opportunities for biomass co-firing.

The objectives of this study are:

- To develop a model that can predict syngas composition for wide variety of feedstocks based on their ultimate analysis and moisture content.

- To study the selected operating parameters and their effect on syngas composition in a stratified downdraft biomass gasifier

- To conduct detail study on tar concentration in the syngas from a stratified downdraft gasifier

1.6   REFERENCES

[1] H.L. Chum, R.P. Overend, Biomass and renewable fuels, Fuel Processing Technology, 71 (2001) 187-195.

[2] R.D. Perlack, L.L. Wright, A.F. Turhollow, R.L. Graham, B.J. Stokes, D.C. Erbach, Biomass as feedstock for a bioenergy and bioproducts industry: the technical feasibility of a billion-ton annual supply. Oak Ridge National Laboratory, Oak Ridge, 2005.

[3] A. Demirbas, Biofuels sources, biofuel policy, biofuel economy and global biofuel projections, Energy Conversion and Management, 49 (2008) 2106-2116.

[4] S.P. Babu, Thermal gasification of biomass technology developments: End of task report for 1992 to 1994, Biomass and Bioenergy, 9 (1995) 271-285.

[5] A. Demirbas, Biomass resource facilities and biomass conversion processing for fuels and chemicals, Energy Conversion and Management, 42 (2001) 1357-1378.

[6] D. Peterson, S. Haase, Market assessment of biomass gasification and combustion technology for small- and medium-scale applications, in, National Renewable Energy Laboratory, Golden, CO, 2009.

[7] K.B. Cantrell, T. Ducey, K.S. Ro, P.G. Hunt, Livestock waste-to-bioenergy generation opportunities, Bioresource Technology, 99 (2008) 7941-7953.

[8] H. Boerrigter, R. Rauch, Syngas production and utilization; Review of applications of gases from biomass gasification, in: H.A.M. Knoef (Ed.) Handbook biomass gasification, Biomass technology group (BTG), Netherland, 2005.

[9] New renewable energy resources : a guide to the future, Kogan Page, London, 1994.

[10] G.W. Huber, S. Iborra, A. Corma, Synthesis of Transportation Fuels from Biomass: Chemistry, Catalysts, and Engineering, ChemInform, 37 (2006).

[11] A.V. Bridgwater, Renewable fuels and chemicals by thermal processing of biomass, Chemical Engineering Journal, 91 (2003) 87-102.

[12] A. Demirbas, Combustion characteristics of different biomass fuels, Progress in Energy and Combustion Science, 30 (2004) 219-230.

[13] G.J. Stiegel, R.C. Maxwell, Gasification technologies: the path to clean, affordable energy in the 21st century, Fuel Processing Technology, 71 (2001) 79-97.

[14] D.R. Simbeck, Report on SFA Pacific gasification database and world market report, in: Gasification Technologies Conference, San Francisco, CA, 1999.

[15] A. Demirbas, Biofuels securing the planet's future energy needs, Energy Conversion and Management, 50 (2009) 2239-2249.

[16] A. Demirbas, Progress and recent trends in biofuels, Progress in Energy and Combustion Science, 33 (2007) 1-18.

[17] R. Warnecke, Gasification of biomass: comparison of fixed bed and fluidized bed gasifier, Biomass and Bioenergy, 18 (2000) 489-497.

[18] H.A.M. Knoef, Inventory of Biomass Gasifier Manufacturers and Installations, Final Report to European Commission, Contract DIS/1734/98-NL, in, Biomass Technology Group B.V., University of Twente, Enschede, Netherland, 2000.

[19] A.A.C.M. Beenackers, Biomass gasification in moving beds, a review of European technologies, Renewable Energy, 16 (1998) 1180-1186.

[20] P. Basu, Combustion and gasification in fluidized beds, Taylor and Francis Group, LLC, Boca Raton, FL, 2006.

[21] M. Dogru, A. Midilli, C.R. Howarth, Gasification of sewage sludge using a throated downdraft gasifier and uncertainty analysis, Fuel Processing Technology, 75 (2002) 55-82.

[22] P. McKendry, Energy production from biomass (part 3): gasification technologies, Bioresource Technology, 83 (2002) 55-63.

[23] A.V. Bridgewater, Renewable fuels and chemicals by thermal processing of biomass, Chemical Engineering Journal, 91 (2003) 87-102.

[24] S. Lee, Alternative fuels, 1st ed., Taylor & Francis, Washington, (1996). pp.134-44.

[25] R.C. Brown, Biorenewable resources-engineering new products from agriculture, 1st ed., Iowa state press, Ames, Iowa, 2003.

[26] J.M. Prins, Thermodynamic analysis of biomass gasification and torrefaction, in, Eindhoven University of Technology, Netherland, 2005.

[27] P.C. Roy, A. Datta, N. Chakraborty, Modelling of a downdraft biomass gasifier with finite rate kinetics in the reduction zone, International Journal of Energy Research, 33 (2009) 833-851.

[28] P. McKendry, Energy production from biomass (part 1): overview of biomass, Bioresource Technology, 83 (2002) 37-46.

[29] Z.A. Zainal, R. Ali, C.H. Lean, K.N. Seetharamu, Prediction of performance of a downdraft gasifier using equilibrium modeling for different biomass materials, Energy Conversion and Management, 42 (2001) 1499-1515.

[30] A. Melger, J.F. Perez, H. Laget, A. Horillo, Thermochemical equilibrium modeling of a gasifying process, Energy Conversion and Management, 48 (2007) 59-67.

[31] A.K. Sharma, Equilibrium modeling of global reduction reactions for a downdraft (biomass) gasifier, Energy Conversion and Management, 49 (2008) 832-842.

[32] C.R. Altafini, P.R. Wander, R.M. Barretoa, Prediction of the working parameters of a wood waste gasifier through an equilibrium model Energy Conversion and Management, 44 (2003) 2763-2777.

[33] D. Shin, S. Choi, The combustion of simulated waste particles in a fixed bed, Combustion and Flame, 121 (2000) 167-180.

[34] M. Dogru, C.R. Howarth, G. Akay, B. Keskinler, A.A. Malik, Gasification of hazelnut shells in a downdraft gasifier, Energy, 27 (2002) 415-427.

[35] B.M. Jenkins, L.L. Baxter, T.R.M. Jr., T.R. Miles, Combustion properties of biomass, Fuel Processing Technology, 54 (1998) 17-46.

[36] T.B. Reed, A. Das, Handbook of biomass downdraft gasifier engine systems, SERI, Golden, CO, 1988.

[37] G. Gautam, S. Adhikari, S. Bhavnani, Estimation of biomass synthesis gas using equilibrium modeling, Energy and Fuels, 24 (2010) 2692-2698.

[38] T.H. Jayah, L. Aye, R.J. Fuller, D.F. Stewart, Computer simulation of a downdraft wood gasifier for tea drying, Biomass and Bioenergy, 25 (2003) 459-469

[39] J.K. Ratnadhariya, S.A. Channiwala, Three zone equilibrium and kinetic free modeling of biomass gasifier - a novel approach, Renewable Energy, 34 (2009) 1050-1058.

[40] K.J. Ptasinski, M.J. Prins, A. Pierik, Exergetic evaluation of biomass gasification, Energy, 32 (2007) 568-574.

[41] P.N. Sheth, B.V. Babu, Experimental studies on producer gas generation from wood waste in a downdraft biomass gasifier, Bioresource Technology, 100 (2009) 3127-3133.

[42] I. Narvaez, A. Orio, M.P. Aznar, J. Corella, Biomass gasification with air in an atmospheric bubbling fluidized bed. effect of six operational variables on the quality of the produced raw gas, Industrial & Engineering Chemistry Research, 35 (1996) 2110-2120.

[43] X.T. Li, J.R. Grace, C.J. Lim, A.P. Watkinson, H.P. Chen, J.R. Kim, Biomass gasification in a circulating fluidized bed, Biomass and Bioenergy, 26 (2004) 171-193.

[44] X. Li, J.R. Grace, A.P. Watkinson, C.J. Lim, A. Ergüdenler, Equilibrium modeling of gasification: a free energy minimization approach and its application to a circulating fluidized bed coal gasifier, Fuel, 80 (2001) 195-207.

[45] C. Hanping, L. Bin, Y. Haiping, Y. Guolai, Z. Shihong, Experimental Investigation of Biomass Gasification in a Fluidized Bed Reactor, Energy & Fuels, 22 (2008) 3493-3498.

[46] V. Skoulou, G. Koufodimos, Z. Samaras, A. Zabaniotou, Low temperature gasification of olive kernels in a 5-kW fluidized bed reactor for H2-rich producer gas, International journal of hydrogen energy, 33 (2008) 6515-6524.

[47] P.J. van den Enden, E.S. Lora, Design approach for a biomass fed fluidized bed gasifier using the simulation software CSFB, Biomass and Bioenergy, 26 (2004) 281-287.

[48] A. van der Drift, J. van Doorn, J.W. Vermeulen, Ten residual biomass fuels for circulating fluidized-bed gasification, Biomass and Bioenergy, 20 (2001) 45-56.

[49] Z.A. Zainal, A. Rifau, G.A. Quadir, K.N. Seetharamu, Experimental investigation of a downdraft gasifier, Biomass and Bioenergy, 23 (2002) 283-289.

[50] J. Larfeldt, B. Leckner, M.C. Melaaen, Modelling and measurements of heat transfer in charcoal from pyrolysis of large wood particles, Biomass and Bioenergy, 18 (2000) 507-514.

[51] V. Skoulou, A. Zabaniotou, G. Stavropoulos, G. Sakelaropoulos, Syngas production from olive tree cuttings and olive kernels in a downdraft fixed-bed gasifier, International Journal of Hydrogen Energy, 33 (2008) 1185-1194.

[52] E. Natarajan, A. Nordin, A.N. Rao, Overview of combustion and gasification of rice husk in fluidized bed reactors, Biomass and Bioenergy, 14 533-546.

[53] J. Gil, J. Corella, M.P. Aznar, M.A. Caballero, Biomass gasification in atmospheric and bubbling fluidized bed: Effect of the type of gasifying agent on the product distribution, Biomass and Bioenergy, 17 (1999) 389-403.

[54] T.A. Milne, R.J. Evan, Biomass gasification "tars"; their nature, formation and conversion, in, NREL, Golden, 1998.

[55] A.v.d. Drift, J.v. Doorn, Effect of fuel size and process temperature on fuel gas quality from CFB gasification of biomass, in: A.V. Bridgwater (Ed.) Progress in Thermochemical Biomass Conversion, 2008, pp. 265-271.

[56] J. Corella, J.M. Toledo, G. Molina, Calculation of the conditions to get less than 2 g tar/mn3 in a fluidized bed biomass gasifier, Fuel Processing Technology, 87 (2006) 841-846.

[57] F.V. Tinaut, A. Melgar, J.F. Pérez, A. Horrillo, Effect of biomass particle size and air superficial velocity on the gasification process in a downdraft fixed bed gasifier. An experimental and modelling study, Fuel Processing Technology, 89 (2008) 1076-1089.

[58] T. Yamazaki, H. Kozu, S. Yamagata, N. Murao, S. Ohta, S. Shiya, T. Ohba, Effect of superficial velocity on tar from downdraft gasification of biomass, Energy & Fuels, 19 (2005) 1186-1191.

[59] M.M. Küçük, A. Demirbas, Biomass conversion processes, Energy Conversion and Management, 38 (1997) 151-165.

[60] P.R. Wander, C.R. Altafini, R.M. Barreto, Assessment of a small sawdust gasification unit, Biomass and Bioenergy, 27 (2004) 467-476.

[61] P. Brandt, E. Larsen, U. Henriksen, High tar Reduction in a two-stage gasifier, Energy & Fuels, 14 (2000) 816-819.

[62] L. Gerun, M. Paraschiv, R. Vîjeu, J. Bellettre, M. Tazerout, B. Gøbel, U. Henriksen, Numerical investigation of the partial oxidation in a two-stage downdraft gasifier, Fuel, 87 (2008) 1383-1393.

[63] S. Monteiro Nunes, N. Paterson, D.R. Dugwell, R. Kandiyoti, Tar formation and destruction in a simulated downdraft, fixed-bed gasifier: reactor design and initial results, Energy & Fuels, 21 (2007) 3028-3035.

[64] A. Zabaniotou, O. Ioannidou, V. Skoulou, Rapeseed residues utilization for energy and 2nd generation biofuels, Fuel, 87 (2008) 1492-1502.

[65] A. Rogel, J. Aguillón, The 2D eulerian approach of entrained flow and temperature in a biomass stratified downdraft gasifier, American Journal of Applied Sciences, 3 (2006) 2068-2075.

[66] P. Weerachanchai, M. Horio, C. Tangsathitkulchai, Effects of gasifying conditions and bed materials on fluidized bed steam gasification of wood biomass, Bioresource Technology, 100 (2009) 1419-1427.

[67] C. Wu, X. Yin, L. Ma, Z. Zhou, H. Chen, Design and operation of a 5.5 MWe biomass integrated gasification combined cycle demonstration plant, Energy & Fuels, 22 (2008) 4259-4264.

[68] J. Corella, A. Sanz, Modeling circulating fluidized bed biomass gasifiers. A pseudo-rigorous model for stationary state, Fuel Processing Technology, 86 (2005) 1021-1053.

[69] S.R.A. Kersten, W. Prins, A. van der Drift, W.P.M. van Swaaij, Experimental fact-finding in CFB biomass gasification for ECN's 500 kWth pilot plant, Industrial & Engineering Chemistry Research, 42 (2003) 6755-6764.

[70] Y. Cao, Y. Wang, J.T. Riley, W.-P. Pan, A novel biomass air gasification process for producing tar-free higher heating value fuel gas, Fuel Processing Technology, 87 (2006) 343-353.

[71] Y.G. Pan, X. Roca, E. Velo, L. Puigjaner, Removal of tar by secondary air in fluidised bed gasification of residual biomass and coal, Fuel, 78 (1999) 1703-1709.

[72] Z. Wu, C. Wu, H. Huang, S. Zheng, X. Dai, Test results and operation performance analysis of a 1-MW biomass gasification electric power generation system, Energy & Fuels, 17 (2003) 619-624.

[73] R.C. Saxena, D. Seal, S. Kumar, H.B. Goyal, Thermo-chemical routes for hydrogen rich gas from biomass: A review, Renewable and Sustainable Energy Reviews, 12 (2008) 1909-1927.

[74] M. Seggiani, Empirical correlations of the ash fusion temperatures and temperature of critical viscosity for coal and biomass ashes, Fuel, 78 (1999) 1121-1125.

[75] M.J. Fernandez Llorente, J.E. Carrasco García, Comparing methods for predicting the sintering of biomass ash in combustion, Fuel, 84 (2005) 1893-1900.

[76] X.L. Yin, C.Z. Wu, S.P. Zheng, Y. Chen, Design and operation of a CFB gasification and power generation system for rice husk, Biomass and Bioenergy, 23 (2002) 181-187.

[77] C. Ryu, Y.B. Yang, A. Khor, N.E. Yates, V.N. Sharifi, J. Swithenbank, Effect of fuel properties on biomass combustion: Part I. Experiments--fuel type, equivalence ratio and particle size, Fuel, 85 (2006) 1039-1046.

[78] W.R. Livingston, Biomass ash characteristics and behaviour in combustion, gasification and pyrolysis systems, in, Doosan Babcock Energy Limited, 2007.

[79] K.M. Bryden, K.W. Ragland, Numerical modeling of a deep, fixed bed combustor, Energy & Fuels, 10 (1996) 269-275.

[80] A. Saravanakumar, T.M. Haridasan, T.B. Reed, R.K. Bai, Experimental investigation and modelling study of long stick wood gasification in a top lit updraft fixed bed gasifier, Fuel, 86 (2007) 2846-2856.

[81] R. Bilbao, A. Millera, M.B. Murillo, Temperature profiles and weight loss in the thermal decomposition of large spherical wood particles, Industrial & Engineering Chemistry Research, 32 (1993) 1811-1817.

[82] D.M. Earp, The gasification of biomass in downdraft reactor, in, Aston University, UK, 1988.

[83] A.K. Sharma, Modeling fluid and heat transport in the reactive, porous bed of downdraft (biomass) gasifier, International Journal of Heat and Fluid Flow, 28 (2007) 1518-1530.

[84] Y.B. Yang, V.N. Sharifi, J. Swithenbank, Effect of air flow rate and fuel moisture on the burning behaviours of biomass and simulated municipal solid wastes in packed beds, Fuel, 83 (2004) 1553-1562.

[85] D.Y.C. Leung, C.L. Wang, Fluidized-bed gasification of waste tire powders, Fuel Processing Technology, 84 (2003) 175-196.

[86] S.R.A. Kersten, W. Prins, B. van der Drift, W.P.M. van Swaaij, Principles of a novel multistage circulating fluidized bed reactor for biomass gasification, Chemical Engineering Science, 58 725-731.

[87] J. Wiman, A.E. Almstedt, Influence of pressure, fluidization velocity and particle size on the hydrodynamics of a freely bubbling fluidized bed, Chemical Engineering Science, 53 (1998) 2167-2176.

[88] S. Valin, S. Ravel, J. Guillaudeau, S. Thiery, Comprehensive study of the influence of total pressure on products yields in fluidized bed gasification of wood sawdust, Fuel Processing Technology, In Press, Corrected Proof.

[89] A.V. Bridgwater, The technical and economic feasibility of biomass gasification for power generation, Fuel, 74 (1995) 631-653.

[90] P. García-Bacaicoa, J.F. Mastral, J. Ceamanos, C. Berrueco, S. Serrano, Gasification of biomass/high density polyethylene mixtures in a downdraft gasifier, Bioresource Technology, 99 (2008) 5485-5491.

[91] F. Pinto, C. Franco, R.N. André, C. Tavares, M. Dias, I. Gulyurtlu, I. Cabrita, Effect of experimental conditions on co-gasification of coal, biomass and plastics wastes with air/steam mixtures in a fluidized bed system, Fuel, 82 1967-1976.

[92] D.R. McIlveen-Wright, F. Pinto, L. Armesto, M.A. Caballero, M.P. Aznar, A. Cabanillas, Y. Huang, C. Franco, I. Gulyurtlu, J.T. McMullan, A comparison of circulating fluidised bed combustion and gasification power plant technologies for processing mixtures of coal, biomass and plastic waste, Fuel Processing Technology, 87 (2006) 793-801.

[93] M.L. Mastellone, L. Zaccariello, U. Arena, Co-gasification of coal, plastic waste and wood in a bubbling fluidized bed reactor, Fuel, In Press, Uncorrected Proof.

[94] M.P. Aznar, M.A. Caballero, J.A. Sancho, E. Francés, Plastic waste elimination by co-gasification with coal and biomass in fluidized bed with air in pilot plant, Fuel Processing Technology, 87 (2006) 409-420.

[95] J. Fermoso, B. Arias, M.G. Plaza, C. Pevida, F. Rubiera, J.J. Pis, F. García-Peña, P. Casero, High-pressure co-gasification of coal with biomass and petroleum coke, Fuel Processing Technology, 90 926-932.

[96] M. Lapuerta, J.J. Hernández, A. Pazo, J. López, Gasification and co-gasification of biomass wastes: Effect of the biomass origin and the gasifier operating conditions, Fuel Processing Technology, 89 (2008) 828-837.

[97] Y.G. Pan, E. Velo, X. Roca, J.J. Manyà, L. Puigjaner, Fluidized-bed co-gasification of residual biomass/poor coal blends for fuel gas production, Fuel, 79 (2000) 1317-1326.

[98] M. Pohorelý, M. Vosecký, P. Hejdová, M. Puncochár, S. Skoblja, M. Staf, J. Vosta, B. Koutský, K. Svoboda, Gasification of coal and PET in fluidized bed reactor, Fuel, 85 (2006) 2458-2468.

[99] R. Xiao, B. Jin, H. Zhou, Z. Zhong, M. Zhang, Air gasification of polypropylene plastic waste in fluidized bed gasifier, Energy Conversion and Management, 48 (2007) 778-786.

[100] J.F. Vélez, F. Chejne, C.F. Valdés, E.J. Emery, C.A. Londoño, Co-gasification of Colombian coal and biomass in fluidized bed: An experimental study, Fuel, 88 (2009) 424-430.

[101] T.R. McLendon, A.P. Lui, R.L. Pineault, S.K. Beer, S.W. Richardson, High-pressure co-gasification of coal and biomass in a fluidized bed, Biomass and Bioenergy, 26 (2004) 377-388.

[102] G. Xiao, M.-J. Ni, Y. Chi, K.-F. Cen, Low-temperature gasification of waste tire in a fluidized bed, Energy Conversion and Management, 49 (2008) 2078-2082.

[103] A. Maciejewska, H. Veringa, J. Sanders, S.D. Peteves, Co-firing of biomass with coal: constraints and role of biomass pre-treatment, in, Institute for Energy, Netherlands, 2006.

[104] C. Pfeifer, R. Rauch, H. Hofbauer, In-Bed Catalytic Tar Reduction in a Dual Fluidized Bed Biomass Steam Gasifier, Industrial & Engineering Chemistry Research, 43 (2004) 1634-1640.

40

[105] Z. Abu El-Rub, E.A. Bramer, G. Brem, Review of Catalysts for Tar Elimination in Biomass Gasification Processes, Industrial & Engineering Chemistry Research, 43 (2004) 6911-6919.

[106] L. Devi, K.J. Ptasinski, F.J.J.G. Janssen, A review of the primary measures for tar elimination in biomass gasification processes, Biomass and Bioenergy, 24 (2003) 125-140.

CHAPTER 2

ESTIMATION OF BIOMASS SYNTHESIS GAS COMPOSITION USING EQUILIBRIUM
MODELING

2.1   ABSTRACT

Carbon monoxide (CO), carbon dioxide (CO_2), hydrogen (H_2) and methane (CH_4) are the major gases produced from biomass gasification. The composition of CO, CO_2 and H_2 in syngas from the biomass gasification process was calculated via equilibrium modeling. Methane concentration predicted by the equilibrium model was almost negligible (<0.15 vol. %) at temperatures above 800°C. Nearly one-hundred biomass samples were used to calculate synthesis gas composition and the generalized equations were obtained by multiple regression analysis to predict synthesis gas composition using elemental analysis of biomass. Equilibrium results were compared with the experimental data. Effect of temperature and moisture content on synthesis gas composition is also presented. Although perfect chemical equilibrium conditions cannot be achieved in an actual gasification process, the derived formula generally predicts the syngas composition to a reasonable degree of accuracy.

KEYWORDS: carbon dioxide, carbon monoxide, equilibrium, hydrogen, methane, syngas

2.2   INTRODUCTION

Conversion of biomass to biofuels and biopower has emerged as a promising alternative for meeting future energy demand. In addition, biomass is the only source of carbon-based renewable fuels, and the proper and sustainable exploitation of this resource is essential to secure the United States' energy security. Among various biomass conversion technologies within thermo-chemical and biochemical platforms, this study is focused on a biomass gasification process for syngas production. Biomass gasification has received the highest interest among various biomass conversion technologies because it is almost feedstock-agnostic and can be used to produce electricity and liquid fuels such as "green" gasoline and diesel using the Fisher-Tropsch process.

Further, biomass gasification shows a higher efficiency compared to other processes such as direct combustion, pyrolysis, and liquefaction [1-2]. The product gas (also known as synthesis gas or syngas; hereafter syngas) from the biomass gasification is a mixture of carbon dioxide (CO_2), carbon monoxide (CO), hydrogen (H_2), methane (CH_4), water (H_2O) and nitrogen (N_2) if air is used as a gasifying agent. Syngas has been mostly accepted for power generation and is considered to be more mature technology compared to other biomass conversion processes [3]. Fixed bed reactors are widely used for gasification of coal, biomass including municipal waste utilization, because of their simplicity in design and efficiency [4].The choice of biomass for gasification depends upon demographic factors. In the United States, Midwestern states have abundant agricultural residues such as corn stover and wheat straw, whereas southern states have more forest residues. These biomass feedstocks vary in their composition, which ultimately affects the syngas composition. An exhaustive amount of literature is already present for biomass gasification using various regionally appropriate feedstocks. Most of the time, syngas

composition is unknown until the gasification work is conducted. Experimental work is often resource-intensive (time and money) and a mathematical model predicting syngas composition (concentration of H_2, CO, CH_4, and CO_2) using elemental analysis of biomass would be helpful.

There are several models such as thermodynamic equilibrium, kinetics-free, steady-state, semi-transient and transient that can be used to determine the syngas composition [5]. Among these techniques, the thermodynamic equilibrium model is the simplest of all type and gives syngas composition for various biomass types at selected gasification temperatures with reasonable accuracy. A system is said to be in thermodynamic equilibrium when it is in thermal, mechanical and chemical equilibrium. Chemical equilibrium is the state of minimum Gibbs free energy and maximum system entropy. Mechanical equilibrium occurs when the system is not performing or receiving any work. Thermodynamic equilibrium modeling provides a closer prediction when the reaction temperature is sufficiently higher [6]. Equilibrium conditions are difficult to achieve in practical operating conditions and results obtained from thermodynamic equilibrium modeling can serve as the maximum limit on syngas composition. A few studies have been conducted to determine syngas composition and heating value of syngas using thermodynamic equilibrium modeling on limited biomass types [6-9].

Watkinson et al. [9] have developed a thermodynamic equilibrium model and compared their result with various types of gasifiers used for coal. The study found the best prediction for entrained bed gasifier with a lower degree of accuracy in predicting syngas composition from fluidized bed and moving bed gasifiers. Jarungthammachote and Dutta [7] and Melger et al. [8] have predicted syngas composition from various biomass types using thermodynamic equilibrium modeling at a fixed equivalence ratio. Their studies predicted gasification temperature through an iterative process and the syngas composition at given equivalence ratio.

The objective of this chapter is to develop a mathematical expression to determine syngas composition based on carbon, hydrogen and oxygen that can be applicable to any biomass type. In addition, the analysis also includes the effect of moisture content in the biomass. Thermodynamic results will be compared with the experimental data available for selected biomass types.

2.3   METHODOLOGY

2.3.1   MODEL FORMULATION

Empirical relations were developed for predicting the individual fraction of major combustible species of the syngas, CO and H_2. Although these equations can be used for any type of gasifier, it is more accurate for a downdraft gasifier due to its low tar content. Although there are several factors affecting syngas composition from biomass, it mainly depends on the gasifier type, feedstock and feedstock pre-treatment, gasifying medium and operating parameters such as temperature, pressure and equivalence ratio [10]. In this study, the formulation of the thermodynamic model was based on the following assumptions:

- All carbon content in biomass is converted into gaseous form and the residence time is high enough to achieve thermodynamic equilibrium. This might not be true in an actual gasification process; however the degree of error introduced by this assumption is acceptable and the applicability of this assumption is confirmed in literature [6, 8, 11]. The products taken into account are CO, CO_2, H_2, CH_4, N_2 and water. These are the major gaseous compounds formed during the gasification process. Hydrocarbons other than CH_4 were assumed negligible in syngas and were not taken into account.

- Ash in the feedstock was assumed inert in all gasification reactions although it holds true typically only for reaction temperatures less than 700°C [12]. Herbaceous biofuels contain silicon and potassium as the major mineral content which lowers ash fusion temperature below 700°C whereas gasification generally occurs at temperatures higher than 700°C. Therefore, the relations derived in this study cannot be used effectively for biomass with high mineral content.

- All the gaseous products are assumed to behave as ideal gases. This will lead to insignificant errors because the gasification in downdraft gasifiers is conducted at high temperature and low pressure. Also, the pressure drop inside the gasifier was assumed to be negligible.

- The reaction was auto-thermal and no external source of heat was applied. The process is completely adiabatic so that no heat losses occur from the gasifier. The amount of air was varied to achieve the desired reaction temperature in the gasifier.

- The amount of tar in syngas was assumed to be negligible. This places the restriction upon the use of this model for various configurations of gasifier design. For downdraft gasifier, this assumption is valid since the tar concentration is significantly low compared to other configurations [13-15]. For an updraft gasifier, where the higher hydrocarbons produced are not cracked and hence contain high fraction of tar, the results of this modeling cannot be applied [13]. Modifications such as subtracting the amount of volatiles from the biomass and treating the rest as char for the

gasification can be done to improve the model [9]. However, this will lead to increasing amount of error in terms of the final results. Output from the gasification was assumed only to be permanent gases free of oxygen which is true because the oxygen supplied is far less than that needed for combustion in a gasification process. Sulfur and chlorine content in biomass were also neglected since they are less than 0.6% in most biomass feedstocks [12].

The chemical composition of biomass was taken to be in the form $CH_xO_yN_z$ and the gasification reaction can be written in the following form:

$$CH_xO_yN_z + m_wH_2O + x_g(O_2 + 3.76N_2)$$
$$\rightarrow x_1CO + x_2H_2 + x_3CO_2 + x_4H_2O + x_5CH_4$$
$$+ \left(\frac{z}{2} + x_g3.76\right)N_2 \tag{1}$$
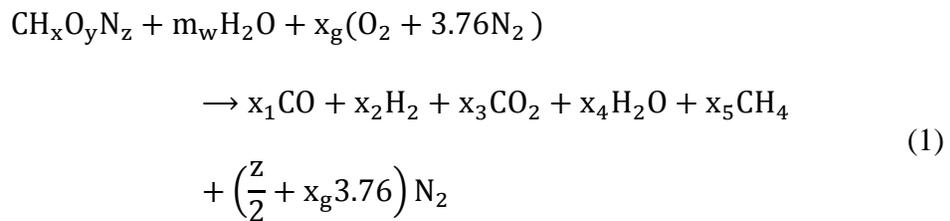
Where m_w in Eqn. (1) can be calculated using the following relation.

$$m_w = \frac{(M_{bio}m)}{18(1-m)} \tag{2}$$

The major reactions that occur inside the downdraft reactor are as follows:

$$C + CO_2 \rightarrow 2CO \tag{3}$$

47

$$C + H_2O \rightarrow CO + H_2 \tag{4}$$

The two reactions shown above can be combined into one single reaction (Eqn.5) known as water-gas shift reaction [6, 8] :

$$CO + H_2O \rightarrow CO_2 + H_2 \tag{5}$$

The other reaction that is prominent in the gasification process is formation of methane as shown below:

$$C + 2H_2 \rightarrow CH_4 \tag{6}$$

Eqns. (5) and (6) are the two major reactions that occur in the gasification process [6-8, 16].The equilibrium constant for these two above equations (5 and 6) as the function of their molar composition can be written as follows:

$$K_1 = \frac{P_{CO_2} \cdot P_{H_2}}{P_{CO} \cdot P_{H_2O}} = \frac{n_{CO_2} \cdot n_{H_2}}{n_{CO} \cdot n_{H_2O}} = \frac{x_3 x_2}{x_1 x_4} \tag{7}$$

$$K_2 = \frac{P_{CH_4}}{\left(P_{H_2}\right)^2} = \frac{n_{CH_4} \cdot n_{tot}}{n_{H_2}^2} = \frac{x_5}{x_2^2} n_{tot} \tag{8}$$

Gibbs free energy is used in determining the value of K_1 and K_2 as presented in Eqn. (9). For the given ideal gas, the Gibbs free energy is a strong function of the reaction temperature and a weak function of pressure [17].

$$\ln K(T) = \frac{-\Delta G_T}{RT} \tag{9}$$

$$\Delta G_T = \sum_i x_i \Delta \bar{g}^o_{f,T,i} \tag{10}$$

Where, $\Delta \bar{g}^o_{f,T,i}$ is empirically calculated according to the Eqn. (19).

Eqns. (11-13) can be written by balancing carbon, hydrogen and oxygen moles, respectively as shown below.

$$x_1 + x_3 + x_5 = 1 \tag{11}$$

$$x + 2m_w = 2x_2 + 2x_4 + 4x_5 \tag{12}$$

$$y + m_w + 2x_g = x_1 + 2x_3 + x_4 \tag{13}$$

Now, there are five equations (7, 8 and 11-13), and six unknowns ($x_1 - x_5$ and x_g). The final equation was obtained by an enthalpy balance inside the gasifier. Total enthalpy content in

49

any chemical species is the sum of its chemical enthalpy and sensible enthalpy and can be written as follows:

$$
\begin{aligned}
H^o_{f-biomass} + m_w \left(H^o_{f_{H_2O(l)}} + H_{vap} \right) + x_g(H^o_{fO_2} + 3.76H^o_{fN_2}) \\
= x_1 \left(H^o_{fCO} + \int_{298}^{T_g} C_{pCO} dT \right) \\
+ x_2 \left(H^o_{fH_2} + \int_{298}^{T_g} C_{pH_2} dT \right) \\
+ x_3 \left(H^o_{fCO_2} + \int_{298}^{T_g} C_{pCO_2} dT \right) \\
+ x_4 \left(H^o_{fH_2O} + \int_{298}^{T_g} C_{pH_2O} dT \right) \\
+ x_5 \left(H^o_{fCH_4} + \int_{298}^{T_g} C_{CH_4} dT \right) \\
+ \left(\frac{z}{2} + x_g 3.76 \right) \int_{298}^{T_g} C_{pN_2} dT
\end{aligned}
\tag{14}
$$

Zainal et al. [6] have used HHV for predicting syngas composition from biomass. However, the use of LHV for finding heat of formation is also common [7-8, 18]. In this study, LHV is used for evaluating heat of formation of biomass. Heat of formation of biomass is calculated by using following equation [18]:

$$H^o_{f,bio} = LHV + \sum_{i=1}^{n} n_i p_i \qquad (15)$$

LHV is calculated in dry basis of biomass and was calculated using the following equation [18]:

$$LHV = 4.187\big(81C + 300H - 26(O - S) - 6(9H + m)\big)(kJ/kg) \qquad (16)$$

The above equation (Eqn. 13) can be reduced to following form since $H^o_{f_{N_2}}$, $H^o_{f_{H_2}}$ and $H^o_{f_{O_2}}$ are zero at the reference temperature and pressure of 298 K and 1 atm.

$$H^o_{f-biomass} + m_w \left(H^o_{f_{H_2O(l)}} + H_{vap}\right)$$

$$= x_1 \left(H^o_{f_{CO}} + \int_{298}^{T_g} C_{p_{CO}}\, dT\right) + x_2 \left(\int_{298}^{T_g} C_{p_{H_2}}\, dT\right)$$

$$+ x_3 \left(H^o_{f_{CO_2}} + \int_{298}^{T_g} C_{p_{CO_2}}\, dT\right)$$

$$+ x_4 \left(H^o_{f_{H_2O}} + \int_{298}^{T_g} C_{p_{H_2O}}\, dT\right) \qquad (17)$$

$$+ x_5 \left(H^o_{f_{CH_4}} + \int_{298}^{T_g} C_{CH_4}\, dT\right)$$

$$+ \left(\frac{z}{2} + x_g 3.76\right) \int_{298}^{T_g} C_{p_{N_2}}\, dT$$

Eqn. (17) acts as the constraint for the gasification process and forms the basis for adjusting the amount of air to be supplied. The amount of air is adjusted in such a way that total enthalpy of the reactants is equal to that of products in gaseous form.

C_p can be determined using an empirical relation that holds for a wide range of temperature.

$$C_p(T) = c_1 + c_2 T + c_3 T^2 + C_4 T^3 (kJ/kg) \qquad (18)$$

The sensible heat of each gas species was found by integrating Eqn. (18) from the ambient temperature to gasification temperature. The value of c_1-c_4 is taken as reported by Reid et.al. [19].

Table 2.1 Coefficients of specific heat capacity for various gases

Species	c_1	c_2	c_3	c_4
N_2	31.2	-1.36×10^{-2}	2.68×10^{-5}	-1.17×10^{-8}
CO_2	19.8	7.34×10^{-2}	-5.60×10^{-5}	1.72×10^{-8}
H_2	29.1	-1.92×10^{-3}	4.00×10^{-6}	-8.70×10^{-10}
CO	30.9	-1.29×10^{-2}	2.79×10^{-5}	-1.23×10^{-8}
CH_4	19.3	5.21×10^{-2}	1.20×10^{-5}	-1.13×10^{-8}
$H_2O_{(g)}$	32.2	1.92×10^{-3}	1.06×10^{-5}	-3.60×10^{-9}

Similarly, the change in Gibbs free energy for an individual gas is given by:

$$\Delta\bar{g}^o_{f,T,i} = \bar{H}^o_{f,i} - aT\ln T - bT^2 - \frac{c}{2}T^3 - \frac{d}{3}T^4 + \frac{e}{2T} + f + gT \qquad (19)$$

The values of a-g are taken from Probstein and Hicks [20] and are shown in Table 2.2 along with enthalpy of formation at standard reference state of 298 K and 1 atm pressure.

Table 2.2 Enthalpy of formation and coefficient for Eqn. (19)

Species	$\bar{H}^o_{f,298}$	a	b	c	d	e	f	g
CH_4	-74.8	-4.62×10^{-2}	1.13×10^{-5}	1.32×10^{-8}	-6.65×10^{-12}	-4.89×10^{2}	14.1	-0.223
CO	-110.5	5.62×10^{-3}	-1.19×10^{-5}	6.38×10^{-9}	-1.85×10^{-12}	-4.89×10^{2}	.868	-0.0613
CO_2	-393.5	-1.95×10^{-2}	3.12×10^{-5}	-2.45×10^{-8}	6.95×10^{-12}	-4.89×10^{2}	5.27	-0.121
H_2O	-241.8	-8.95×10^{-3}	-3.67×10^{-6}	5.21×10^{-9}	-1.48×10^{-12}	0	2.87	-.0172

2.3.2 ALGORITHMS AND GENERAL FORMULA DERIVATION

The model was run with an elemental composition of nearly 100 biomass feedstocks, which were documented in a governmental database [21]. The feedstocks used in the model includes pine, poplar, eucalyptus, corn stover, rice husk and many other common types of biomass. The elemental compositions of these feedstocks were obtained from Syngas composition was determined by solving six equations (Eqns. 7-8, 11-13 and 17) in MATLAB [22]. Newton-Jacobi iteration was used for solving these equations. Complete MATLAB coding for these

overall equilibrium model are attached in Appendix A and B. Once the syngas composition was determined from all feedstocks, a linear equation was developed to calculate the concentration of each gas species. Syngas composition from all biomass feedstocks run in the model along with their elemental and ash wt.% is reported in Appendix C. Multiple linear regression analysis was performed to determine the coefficients for the linear equation using MS-EXCEL spreadsheet.

2.4.   RESULTS AND DISCUSSION

2.4.1   PREDICTION OF CO AND H_2 FROM DIFFERENT BIOMASS TYPES

Table 2.3 shows the prediction of CO and H_2 (combustible gases in syngas) for different common types of biomass on dry basis using equilibrium model. These syngas composition are computed from running the model at $800^{\circ}C$. The equivalence ratio for all of these simulations is automatically adjusted such that the pre-set temperature of $800^{\circ}C$ is achieved. Thus equivalence ratio is not constant but a function of the elemental composition of biomass. Equivalence ratio for the gasification of various biomasses as reported in Table 2.3 is in the range of 0.39-0.48. It was found that increase in oxygen concentration in biomass reduces the equivalence ratio because of inherent supply of oxidizing agent from biomass itself. The composition of syngas predicted by the empirical formula is generally higher than the observed concentration at many cases.

Table 2.3 CO and H_2 composition for most common feedstocks available in the U.S from

MATLAB model.

Type	Ultimate analysis, wt.%			Gas composition, vol.%		Equivalence ratio
	C	H	O	H_2	CO	
Switchgrass	48.5	5.5	38.2	13.8	22.5	0.47
Hybrid Poplar	49.8	5.5	42.4	15.4	25.4	0.42
Eucalyptus	49.5	6.3	42.0	16.1	24.0	0.42
Sugarcane Bagasses	48.4	6.0	41.6	15.4	23.4	0.44
Wood dust	49.2	5.7	41.2	15.1	24.2	0.43
Peanut hulls	45.8	5.5	39.6	13.6	21.3	0.49
Cotton stalks	51.2	5.0	37.1	13.5	24.6	0.46
Pine wood	49.7	6.3	43.7	16.7	24.9	0.40
Oak wood	49.5	6.0	44.5	16.6	25.5	0.40
Corn Stover	46.5	5.8	40.4	14.4	21.7	0.47

2.4.2   FORMULA DERIVATION

Expressions for CO, H_2 and CO_2 were obtained in terms of three variables such as C, H and O except for CO_2 which is expressed as the function of two variables, C and O. The p-value, which shows the significance of a parameter in regression analysis, was less than 0.00002 for each of the independent variables asserting its influence in the individual syngas component.

Goodness of fit (R^2) value obtained is higher than 0.98 showing significance of all independent variables. The obtained relations are as follows:

$$CO(\%vol.) = 0.71C - 1.35H + 0.47O - 22.43 \ (R^2 \text{ value} = 0.98) \qquad (20)$$

$$H_2(\%vol.) = 0.223C + 1.022H + 0.332O - 15.36 \ (R^2 \text{ value} = 0.99) \qquad (21)$$

$$CO_2(\% \ vol.) = -0.41C - 0.04O + 31.65 \ (R^2 \text{ value} = 0.96) \qquad (22)$$

CH_4 is also an important constituent of syngas from biomass gasification. However, the equilibrium modeling prediction was always less than 0.15% for biomass at a temperature of $800^{\circ}C$ and therefore, it is not presented here. Similar observations were reported in other thermodynamic modeling studies [6-8]. Nonetheless, the methane concentration is in the range of 3-4 vol. % in actual gasification. The three relations shown above were derived assuming the gasifier temperature to be $800^{\circ}C$. On the other hand, the equivalence ratio was self-adjusted in the model to maintain $800^{\circ}C$ so that the various gasification reactions inside the gasifier are self-sustained. Temperature inside the gasifier is the optimal compromise between moisture content and equivalence ratio so an adjustment of equivalence ratio to achieve desired temperature is

very likely [23]. The Eqns. (20-22) gives the syngas composition for the temperature of 800°C which is adjusted for the particular biomass at the equivalence ratio enough to sustain endothermic reaction and maintain the pre-set temperature of 800°C. Moisture content can be accounted in above correlation by the use of following values of C, H and O if the data for ultimate analysis are based on wet basis:

$$C^* = \frac{C}{(1 + 0.01m_w)} \qquad (23)$$

$$O^* = \frac{O + 0.889m_w}{(1 + 0.01m_w)} \qquad (24)$$

$$H^* = \frac{H + 0.111m_w}{(1 + 0.01m_w)} \qquad (25)$$

2.4.3   RESULT VALIDATION: COMPARISON WITH EXPERIMENTAL RESULTS

Table 2.4 shows the comparison between the experimental results available from literature and predicted values from equation derived from (20-21). Results are compared with the corresponding references [16, 24-26]. H_2 and CO composition as reported by Zainal et al. [24], is the average of 57 test runs with the temperature around 700-900°C for most of the experimental duration. They used furniture wood as their feedstock with equivalence between 0.268-0.43. H_2 and CO data from Bacaicoa et al. [27] is from experiment conducted in the

downdraft gasifier with capacity of 25-50 kg/hr and equivalence ratio of 0.247. The data taken

from Jayah et al. [25] is among one of their conducted experiments in the downdraft gasifier. The

syngas reported by Jayah et al. is between 18.4-22.1% of CO and 13-18.3% of H_2 with the

temperature of the gasification zone in the range of 700-1000°C. Comparison for both Bacaicoa

et al. [27] and Jayah et al. [25] was done with syngas composition at temperature close to this

model. CO and H_2 composition from Altafini et al. [16] is the average of 10 test runs with the

reaction temperature around 832°C and average air/sawdust ratio of 1.829. As can be seen from

Table 2.4, the predicted result is in good agreement with the experimental results, but the

composition of syngas predicted by the empirical relations is generally higher than the observed

concentration at many cases.

Table 2.4 Comparison of model with experimental values

Moisture Content, wt% (wet basis)	Ultimate analysis, wt.% (dry basis)			H_2, % vol. (moisture free basis)		CO, % vol. (moisture free basis)		Ref.
	C	H	O	P*	E**	P*	E**	
0	47.3	5.8	45	16.1	14.05	24.5	24.04	Zainal et.al. [24]
12	45.8	6	47.9	17.8	15.07	22.3	24.1	Bacaicoa et al. [26-27]
14	50.6	6.5	42	17.6	18.3	22	20.2	Jayah et al. [25]
20	52	6.1	41.6	17.8	14	22.2	20.14	Altafini et al. [16]

P*-Values predicted from Eqn. (20) and (21) for H_2 and CO respectively. E**-Experimental data

2.4.4   EFFECT OF MOISTURE CONTENT ON SYNGAS COMPOSITION

The effect of various parameters are shown in Figure 2.1 to 2.8 for the particular biomass

with 50 wt.% carbon, 6 wt.% hydrogen and 44 wt.% oxygen which is the typical composition of

dry woody biomass. Figure 2.1 shows the effect of moisture content on the syngas composition.

The concentration of H_2 increased from 16.9 vol.% to 17.8 vol.% with the change in moisture

58

content from 0 to 28 wt.% and started decreasing thereafter with further increase in moisture content. The concentration of CO decreased monotonically with increase in moisture content and the change in CO was more pronounced compared to the change in H_2 with the same change in moisture. CO decreased from 23.2 vol.% to 8.9 vol.% with an increase in moisture from 0 to 43 wt.%. As expected, CO_2 concentration increases with increase in moisture content from 9.4 vol.% to 18.1 vol.% as moisture content increases from 0-43 vol.%. The methane concentration is less than 0.15 vol.% for over the entire range of moisture content.
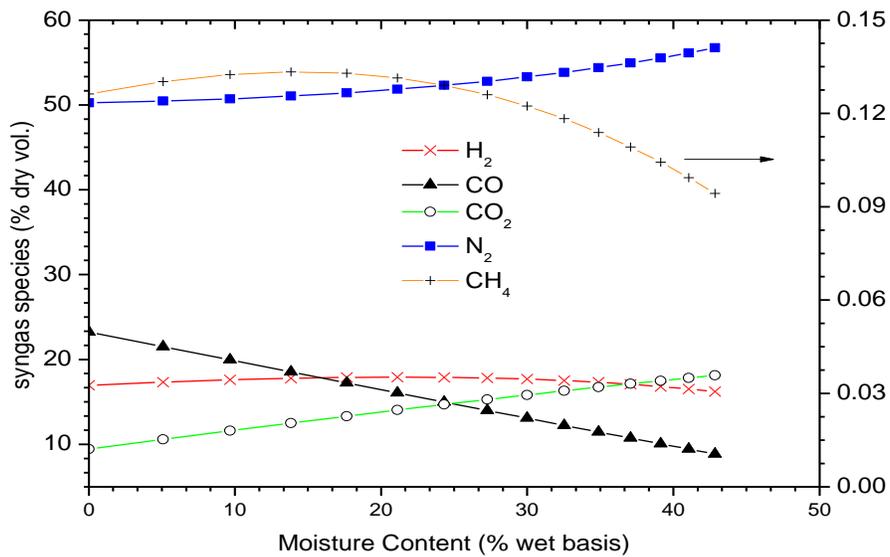
Figure 2.1 Effect of moisture content on syngas composition

(Data for this plot in Appendix D: Table D.1)

The effect of moisture content as shown in Figure 2.1 needs further elaboration at this point. The model is based on the assumption that the process is completely adiabatic thus additional air flow is required with an increase in moisture content to generate the heat required to sustain the desired temperature. This equivalence ratio increases as seen in Figure-2. This can

be seen in the increase in concentration of N_2 with increase in moisture content. In an actual gasification process, if this air flow is not supplemented, decrease in gasifier temperature is observed. The small increase in H_2 concentration is overshadowed by the rapid decrease of CO with increase in moisture content. The overall effect is the decrease in HHV of syngas with increase in moisture content, which can be seen from Figure 2.2. HHV of syngas decreases from 5.1 MJ/m^3 to 3.4 MJ/m^3 with an increase in moisture content from 0 to 43 wt.%.
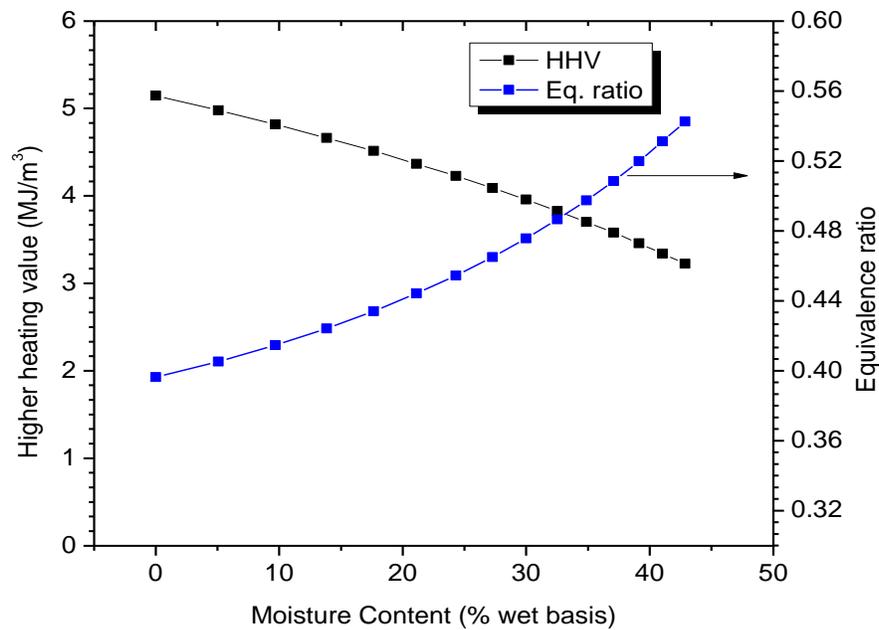
Figure 2.2 Effect of moisture content on HHV of syngas under adiabatic condition

(Data for this plot in Appendix D: Table D.1)

2.4.5   EFFECT OF TEMPERATURE ON SYNGAS COMPOSITION

Figure 2.3 depicts the decrease in volumetric fraction of CO, H_2 and CH_4 (not appreciable due to the inherently small concentration of CH_4) with increase in temperature. This decrease is due to the increase in dilution by N_2 at higher temperature because the equivalence ratio adjusts

60

itself to meet the adiabatic condition set in Eqn. (17). The effect of temperature on equivalence ratio can be seen graphically in Figure 2.5. Figure 2.4 depicts the actual number of moles of each species in syngas composition. Number of moles of CO remained almost constant whereas number of moles of H_2 decreased monotonically. The number of moles of H_2O and CO_2 increased with the increase in temperature. Thus, effect of temperature presented in Figs. 2.3 and 2.4 is not the effect of increasing temperature alone but also the effect of increase in equivalence ratio to maintain adiabatic conditions with increase in temperature.
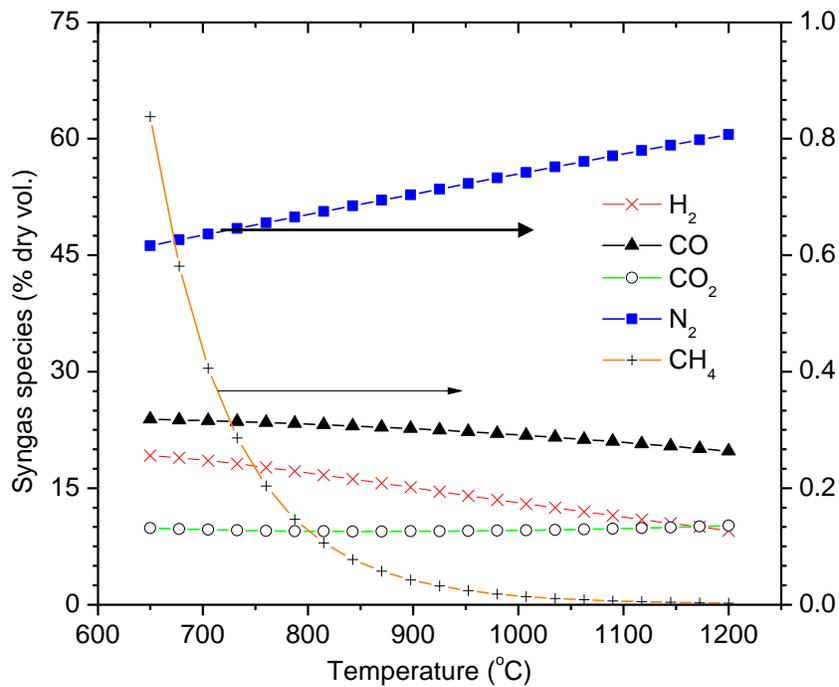
Figure 2.3 Effect of temperature on syngas species concentration (variable x_g)

(Data for this plot in Appendix D: Table D.2)
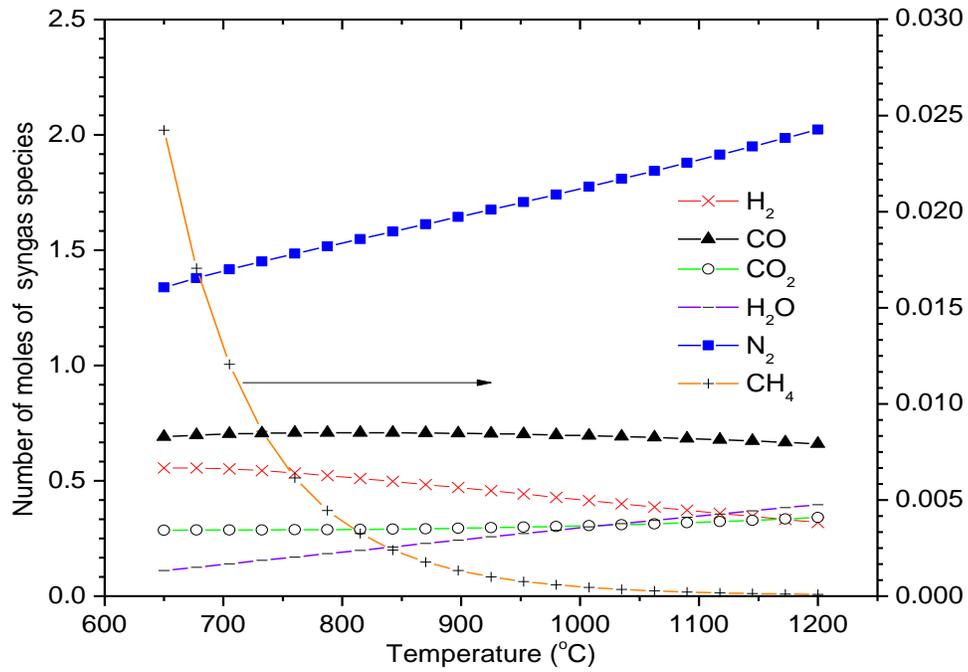
Figure 2.4 Effect of temperature on number of moles of syngas species (variable x_g)

(Data for this plot in Appendix D: Table D.3)
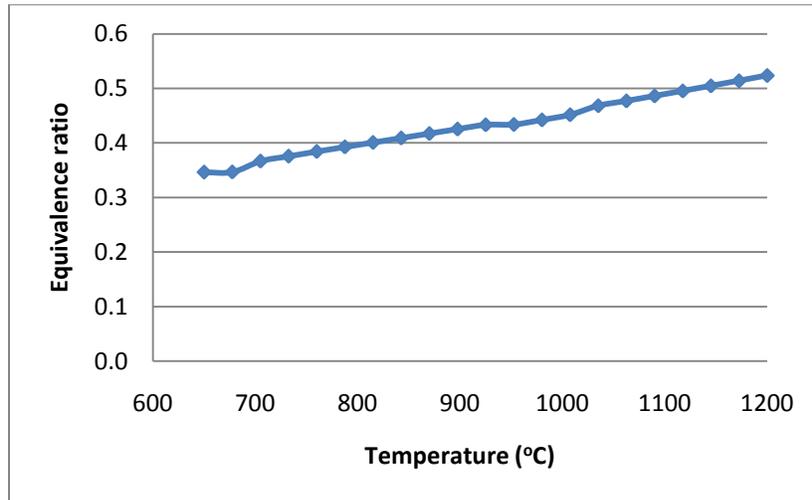
Figure 2.5 Effect of temperature on equivalence ratio in adiabatic condition (variable x_g)

(Data for this plot in Appendix D: Table D.4)

The effect of temperature alone at fixed equivalence ratio (constant x_g) is shown by Figs. 2. 6 and 2.7. The model is run with the equivalence ratio of 0.396. This equivalence ratio is the self-adjusted equivalence ratio for the particular biomass at $800^{\circ}C$. Since the equivalence ratio was fixed for developing Figs. 2.6 and 2.7, adiabatic condition is not valid. The increase in temperature alone at fixed equivalence ratio results in an increase in the volumetric concentration of CO as well as H_2O vapor in syngas, while concentration of CO_2 decreases after reaching its maximum value at around $850^{\circ}C$. Concentration of H_2 and CH_4 decreases with the increase in temperature and the CH_4 concentration reach to negligible amount after $900^{\circ}C$.
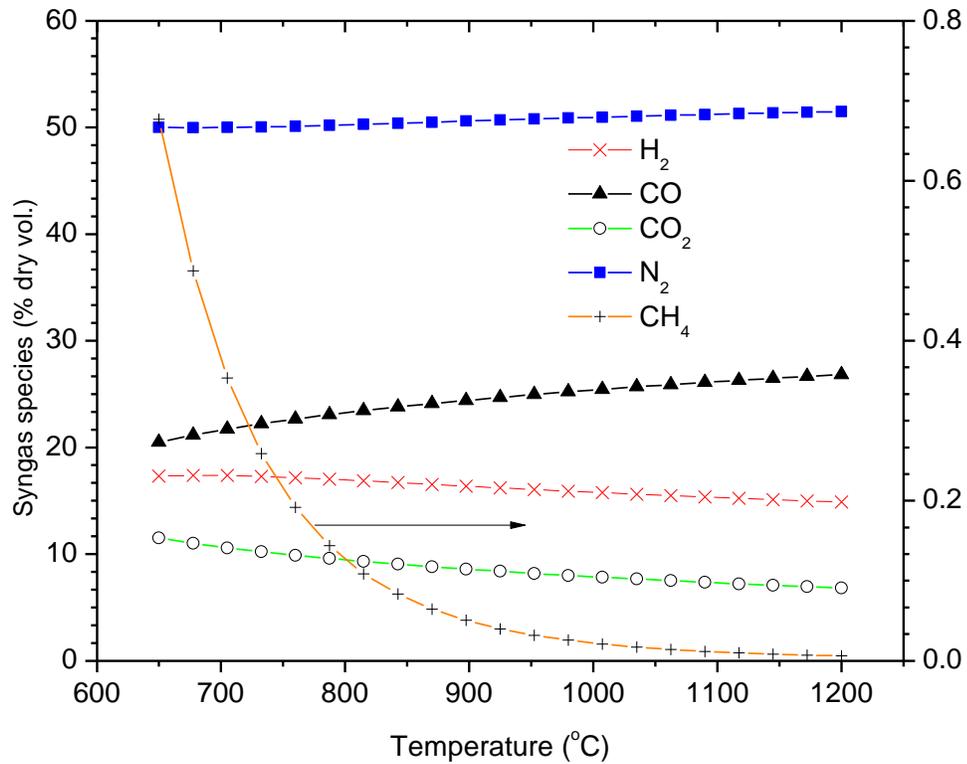
Figure 2.6 Effect of temperature on syngas species at fixed equivalence ratio of 0.396

(Data for this plot in Appendix D: Table D.5)
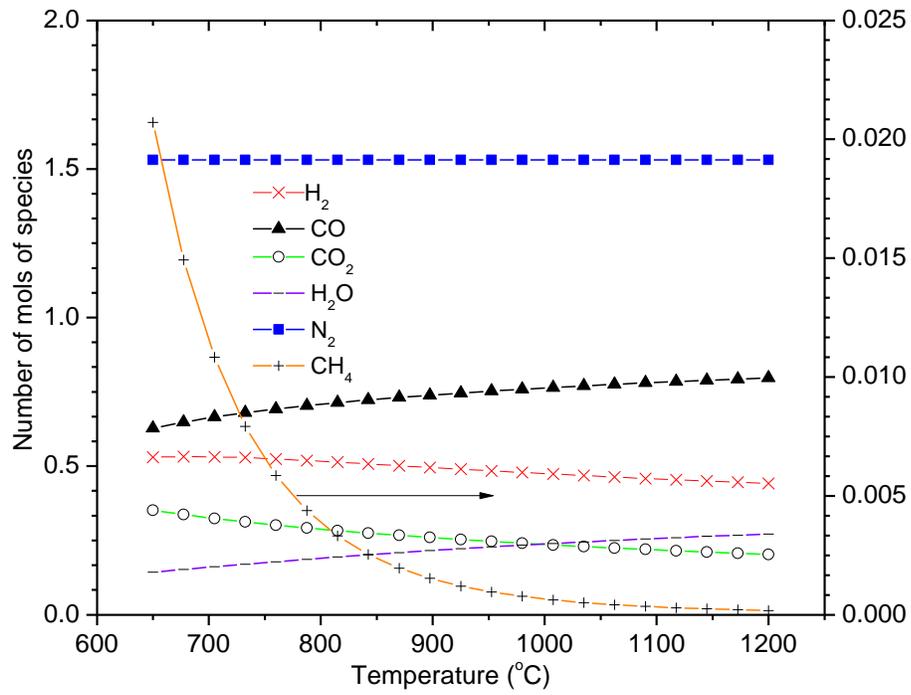
Figure 2.7 Effect of temperature on syngas species at fixed equivalence ratio of 0.396

(Data for this plot in Appendix D: Table D.6)

Figure 2.8 compares the heating value of syngas for constant and variable fuel/air ratios. For self-adjusted value of x_g, HHV decreases rapidly with increase in temperature but increases very slowly for fixed x_g as seen from Figure 2.7.
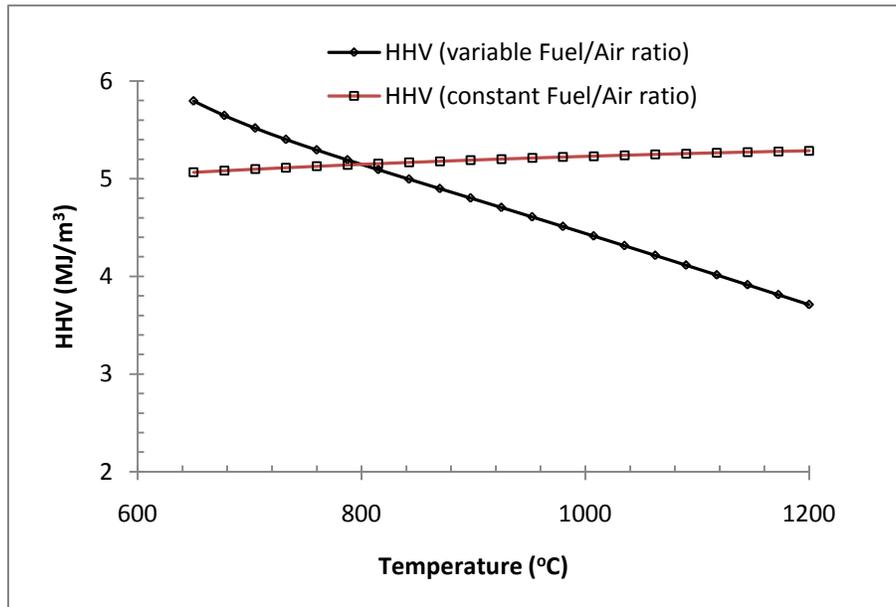
Figure 2.8 Effect of temperature on HHV of syngas under adiabatic condition

(Data for this plot in Appendix D: Table D.2 and D.5)

2.4.6 CH_4 PREDICTION FROM EQUILIBRIUM MODEL

As discussed above, CH_4 predictions from thermodynamic equilibrium modeling are significantly lower than those encountered in practical gasification tests. Typical CH_4 concentration in downdraft gasifiers is 2-5 vol. % (dry basis). This is due to the fact that CH_4 from the thermal cracking of tars and volatiles of biomass is not incorporated in the model. Since CH_4 is a very stable hydrocarbon, it is one of the main products of thermal breakdown of higher-order hydrocarbons. Neglecting this phenomenon results in a lower CH_4 prediction from the equilibrium modeling discussed in this chapter.

2.5   CONCLUSIONS AND FINAL REMARKS

Empirical relations derived for CO, H_2 and CO_2 predict syngas composition with a reasonable degree of accuracy. However, the relations become less accurate with increase in the ash content in the biomass materials because a reaction with ash and heat absorbed by ash is ignored in the model. Also, perfect adiabatic conditions are difficult to achieve in practical gasifiers resulting in some discrepancy between predicted and experimental results. As the temperature increases, the predicted values from this model and relation become more realistic. Moisture content reduces CO fraction in syngas significantly and thus reducing HHV of the gas. Thus, for the gasification process, it is essential to have the moisture content below a threshold that meets the end-requirements. The amount of hydrocarbons produced during the gasification process depends upon the temperature of the gasification and decreases rapidly with increase in temperature. It is also seen that the concentration of CH_4 above $900^{\circ}C$ is negligible as predicted by the equilibrium model.

2.6   NOMENCLATURE

$a - g$ Coefficient for gibbs free energy empirical relation

C, H, O, N, S Carbon, hydrogen, oxygen, nitrogen and sulfur fraction in biomass (dry basis)

C^*, H^*, O^* Carbon, hydrogen and oxygen fraction in biomass (wet basis)

C_{pX} Specific heat capacity of X species (KJ/kmol)

$c_1 - c_4$ Coefficient for specific heat capacity

ΔG_T Gibbs free energy (KJ/kmol))

$\Delta g_{f,T,i}$ Change in Gibbs free energy for individual gas with temperature

HHV   Higher heating value (MJ/kg)

H_{bio} Heat of formation (kJ/kmol)

H_f^o Enthalpy of formation (KJ/kmol)

K_1 Equilibrium constant for water-gas shift reaction

K_2 Equilibrium constant for $C + 2H_2 \rightarrow CH_4$

LHV   Lower heating value (MJ/kg)

M_{bio} Molecular weight of the biomass

m Moisture content in biomass (% dry basis)

m_w Number of moles of water vapor (dry basis)

n_i Number of moles of species i

n_{tot} Total number of gaseous moles in the reactor

P_X Partial pressure of species of I inside the reactor

p_i Products of complete combustion of biomass (kmol) for species i

w   Stoichiometric coefficients of water vapor

x, y, z Normalized coefficient of atomic hydrogen, oxygen and nitrogen for biomass molecule

$x_1 - x_5$ Number of moles of $H_2, CO, CO_2, H_2O, CH_4$ respectively

x_g Number of moles of oxygen for gasification

2.7   REFERENCES

[1] A.V. Bridgewater, Renewable fuels and chemicals by thermal processing of biomass, Chemical Engineering Journal, 91 (2003) 87-102.

[2] A. Demirbas, Combustion characteristics of different biomass fuels, Progress in Energy and Combustion Science, 30 (2004) 219-230.

[3] A. Demirbas, Progress and recent trends in biofuels, Progress in Energy and Combustion Science, 33 (2007) 1-18.

[4] Y.B. Yang, V.N. Sharifi, J. Swithenbank, Effect of air flow rate and fuel moisture on the burning behaviours of biomass and simulated municipal solid wastes in packed beds, Fuel, 83 (2004) 1553-1562.

[5] T.B. Reed, Principles and technology of biomass gasification, in: K.W. Boer, J.A. Duffie (Eds.) Advances in solar energy, An annual review of research and development, Plenum press, New York, 1985.

[6] Z.A. Zainal, R. Ali, C.H. Lean, K.N. Seetharamu, Prediction of performance of a downdraft gasifier using equilibrium modeling for different biomass materials, Energy Conversion and Management, 42 (2001) 1499-1515.

[7] S. Jarungthammachote, A. Dutta, Thermodynamic equilibrium model and second law analysis of a downdraft waste gasifier, Energy, 32 (2007) 1660-1669.

[8] A. Melger, J.F. Perez, H. Laget, A. Horillo, Thermochemical equilibrium modeling of a gasifying process, Energy Conversion and Management, 48 (2007) 59-67.

[9] A.P. Watkinson, J.P. Lucas, C.J. Lim, A prediction of performance of commercial coal gasifiers, Fuel, 70 (1991) 519-527.

[10] J.M. Prins, Thermodynamic analysis of biomass gasification and torrefaction, in, Eindhoven University of Technology, 2005.

[11] M. Ruggiero, G. Manfrida, An equilibrium model for biomass gasification, Renewable Energy, 16 (1999) 1106-1109.

[12] B.M. Jenkins, L.L. Baxter, T.R.M. Jr., T.R. Miles, Combustion properties of biomass, Fuel Processing Technology, 54 (1998) 17-46.

[13] R. Warnecke, Gasification of biomass: comparision of fixed bed and fluidized bed gasifier, Biomass and bioenergy, 18 (2000) 489-497.

[14] S.M. Nunes, N. Paterson, D.R. Dugwell, R. Kandiyoti, Tar formation and destruction in a simulated downdraft, fixed-bed gasifier: reactor design and initial results, Energy and fuels, 21 (2007) 3028-3035.

[15] T. Yamazaki, H. Kozu, S. Yamagata, N. Murao, S. Ohta, S. Shiya, T. Ohba, Effect of superficial velocity on tar from downdraft gasifier, Energy and fuels, 19 (2005) 1186-1191.

[16] C.R. Altafini, P.R. Wander, R.M. Barretoa, Prediction of the working parameters of a wood waste gasifier through an equilibrium model Energy Conversion and Management, 44 (2003) 2763-2777.

[17] J.M. Smith, H.C.V. Ness, M.M. Abbott, Introduction to chemical engineering thermodynamics, 5th ed., McGraw-Hill, 1996.

[18] M.L.d. Souza-Santos, Solid fuels combustion and gasification Modeling, simulation and equipment operation, Marcel Dekker., Inc, New York, 2004.

[19] R.C. Reid, J.M. Prausnitz, B.E. Poling, The properties of gases and liquids, 4 ed., McGraw-Hill, 1987.

[20] R.F. Probstein, R.E. Hicks, Synthetic fuels, McGraw-Hill, 1982.

[21] Biomass Property Database, in, U.S Department of Energy.

[22] MATLAB, in, Mathworks, Inc., 2008.

[23] J. Corella, M.J. Toledo, G. Molina, Calculation of the conditions to get less than 2 g tar/ Nm^3 in a fluidized bed biomass gasifier, Fuel processing technology, 87 (2006) 841-846.

[24] Z.A. Zainal, A. Rifau, G.A. Quadir, K.N. Seetharamu, Experimental investigation of a downdraft gasifier, Biomass and Bioenergy, 23 (2002) 283-289.

[25] T.H. Jayah, L. Aye, R.J. Fuller, D.F. Stewart, Computer simulation of a downdraft wood gasifier for tea drying, Biomass and Bioenergy, 25 (2003) 459-469

[26] P.R. Wander, C.R. Altafini, R.M. Barreto, Assessment of a small sawdust gasification unit, Biomass and Bioenergy, 27 (2004) 467-476.

[27] G.P. Bacaicoa, R. Bilbao, J. Arauzo, M. L. Salvador, Scale-up of downdraft moving bed gasifiers (25-300 kg/h) Designs, experimental aspects and results, Bioresource Technology, 48 (1994) 229-235.

CHAPTER 3

GASIFICATION OF WOOD CHIPS AND AGRICULTURAL RESIDUES USING A

DOWNDRAFT GASIFIER

3.1   ABSTRACT

Auburn University and its collaborator, Community Power Corporation, have developed a mobile 25 kW$_e$ downdraft gasifier. In this study, gasification of various biomass feedstocks such as pine wood chips, commercial wood pellets, saw dust, peanut hulls and poultry litter (the last four in pelletized form) were conducted. Ultimate and proximate analyses were carried out to characterize the biomass feedstock used for gasification. The syngas obtained from various feedstocks and different operating conditions were analyzed using the on-site gas analyzer. Temperature distributions inside the gasifier for different feedstocks and operating conditions were also examined. A minimum temperature difference across the reduction and combustion zone was found in this gasifier. Gasification tests with commercial wood pellets were more closely examined at various flow rates and carbon, enthalpy and exergy analyses were made.

KEYWORDS: carbon dioxide, carbon monoxide, downdraft gasifier, hydrogen, methane, syngas.

3.2   INTRODUCTION

Biomass gasification involves the thermal conversion of biomass into a mixture of combustible gases which can be subsequently used for energy application along with other byproducts, such as volatiles, char and ashes. Under a broad classification, gasification systems can be classified as moving bed and fluidized bed. Moving-bed is the oldest and simplest of all gasification technologies and is generally more suitable for small-scale energy generation with capacity less than 10-15 tons of biomass per hour [1]. When moving bed gasifiers have larger capacities, there is non-uniformity of temperature distribution in the gasifier that results in low quality synthesis gas (hereafter syngas). The gasification process is also more difficult to optimize [2]. The most general forms of moving-bed gasifiers are updraft and downdraft, which are only differentiated by the direction of flow of the gasifying (often called oxidizing agent) agent with respect to fuel. The flow of the oxidizing agent is counter to fuel in the former case whereas it flows along with the fuel in the latter case.

The future prospects of gasification seem to be very promising in the United States. The share of biomass in the total energy supply was 3.23% in 2007 and is expected to increase by an annual average growth rate of 4.2% from 2007-2030, the highest growth rate amongst all other energy sources [3]. The total biomass available in the United States is about 1.3 billion tons per year with the southern states in the country accounting for about 423 million tons/year from forest and agricultural residues [4]. Thus, the proper gasification of these residues will be instrumental in reducing the nation's dependency on fossil fuels, thereby increasing the energy security of the nation.

There are several parameters such as equivalence ratio, temperature, pressure, and moisture content that influence the quality of synthesis gas produced from biomass gasification. Equivalence ratio is one of the most studied parameters affecting syngas composition. It is defined as the ratio of amount of air supplied to the biomass to the amount of stoichiometric amount of air needed for complete combustion. Zainal et al. [5] observed the influence of equivalence ratio upon the constituents of syngas as well as the calorific value and gas output rate. The optimum equivalence ratio suggested was 0.38 for the downdraft gasification of woodchips. Skoulou et al. [6] also investigated the effect of equivalence ratio and temperature upon the quality of syngas in the downdraft gasifier for olive tree kernels and olive tree cuttings and concluded an equivalence ratio of 0.42 optimal for the downdraft gasification of olive tree cuttings and kernels. Based on previous studies, it can be assumed that the optimum equivalence ratio is feedstock dependent [5-6]. The experiment conducted in the temperature range of 750-950°C also showed an increase in carbon monoxide (CO) and hydrogen (H_2) with increase in gasifier temperature; the overall effect was an increase in the heating value of syngas. Jayah et al. [7] used a computer model calibrated by experimental results obtained from a typical medium-scale downdraft gasifier for examining the effects of various parameters upon the biomass conversion efficiency. A longer gasification zone, lower heat losses from the gasifier, lower moisture content and higher air-inlet temperature all had a positive impact upon the conversion efficiency. Longer gasification zone (hence increase in residence time of carbonaceous material) inside the gasifier facilitates the conversion process but also increases the cost of building a new plant. A gasification zone of 330 mm with a capacity of 80 kW was suggested for the downdraft gasifier [7]. Bacaicoa et al. [8] studied the gasification of polyethylene and wood particle mixtures in a downdraft gasifier with varying ratios of wood chips/polyethylene chips as well as

air flow rate. They found an increase in the calorific value of syngas with an increase in polyethylene/biomass ratio due to an increase in CO to carbon dioxide (CO_2) ratio. An increase in cold gas efficiency (ratio of chemical energy in the syngas to that of fuel) was also observed. Lin et al. [9] gasified rice-husk in a downdraft gasifier in a baseline experiment for a pilot plant design and concluded that the husk feed rate should be about 28 kg/hr for obtaining 10 kW of power in a downdraft gasifier. Experiments by Wander et al. [10] with a downdraft, stratified, open top gasifier showed independence between air/biomass ratio and mass conversion efficiency in the temperature range between 500-900°C while the mass conversion efficiency depended upon the temperature and decreased below 800°C. Sheth et al. [11] examined the effect of various parameters on the performance of the gasifier and syngas composition. They found a decrease in biomass consumption rate with an increase in moisture content and an increase with increase in air-flow rate. Syngas composition, calorific value and gas output ratio with respect to equivalence ratio were also reported. The optimal equivalence ratio was 0.20, beyond which a decrease in calorific value was observed. Sharma [12] proposed an equilibrium model for a downdraft gasifier which showed a decrease in CO with an increase in CO_2 and H_2 for feedstock with higher moisture content. In another study, Zainal et al. [13] reported an increase in CO_2 and H_2 for an increase in moisture content from 0% to 40% while noting a decrease in CO for the same moisture content variation.

Mass and energy analyses are very important since they serve as a validation of overall gasification process. These are the applications of mass conservation and the first law of thermodynamics. Carbon closure can be done to serve the purpose of the mass balance if the latter is not possible due to experimental reasons such as inability to measure ash. The ratio of input carbon from biomass to the sum of output carbon in various carbonaceous syngas

75

constituents is the measure of carbon closure. Total energy content in biomass can be measured by the knowledge of higher heating value and total mass used in the experiment. Energy output is the sum of chemical energy of the syngas output and the sensible energy gained in the gasification process. The ratio of output energy to input energy gives the energy ratio of the overall gasification process. While energy ratio can provide us the validity of the experiments, it is not sufficient to measure the "quality of energy" that can be obtained from the gasification process. Exergy is the amount of energy that can be used for useful work. Since exergy also accounts for the losses due to irreversibilities of the process, exergy ratio is usually lower than energy ratio [14].

This chapter reports syngas composition and its heating value from wood chips and other feedstocks such as pelleted wood, peanut hulls, sawdust, and poultry litter. Detail study was conducted to calculate the carbon closure, energy and exergy ratio for the commercial wood pellets due to their uniformity in size and moisture content. Low bulk density of many types of agricultural residues entails the need for a densification process such as pelletizing which increases the bulk density thereby improving the handling characteristics and significantly reducing the space required to store and transport biomass [15]. Furthermore, the effect of moisture content and biomass flow rate on composition and heating value of syngas obtained from wood chip gasification were studied.

The objectives of the present study are:

- To examine the syngas composition and heating value of syngas from selected feedstocks in a stratified downdraft gasifier, and

- To conduct mass, energy and exergy analyses of the overall downdraft gasification process

3.3   EXPERIMENTAL PROCEDURE

3.3.1   SYSTEM DESCRIPTION

Experiments were conducted in a mobile downdraft gasifier developed by the Community Power Corporation (Community Power Corporation (CPC), Littleton, CO).   A schematic of an overall system is depicted in Figure 3.1 and a photograph of the gasifier is presented in Figure 3.2. Figure 3.3 depicts the picture of the mobile gasifier. The interface between the controls and the gasifier were created using LABVIEW. Biomass was loaded into two bins (1 and 2) and passed through a sorting screen, which rejected biomass above 44.45 mm (1.75 inch) and below 6.35 mm (0.25 inch). An auger was used to feed biomass into the gasifier once it was sorted. The feeding rate was controlled based on a specified level of biomass inside the gasifier. A level sensor detected the level of biomass in the gasifier and turned the feeder (auger) once the biomass level fell below the set value. Air was used as an oxidizing agent for biomass gasification. Primary air in the gasifier was obtained from the open top of the gasifier (Figure 3.1). The gasifier had multiple secondary air injection nozzles where the secondary air was fed with the 248.67 W (1/3 HP) air blower. The secondary air supplied was meant to improve the combustion reaction and also to maintain uniformity in temperature along the region. The grate was shaken at an adjustable regular interval via grate-shaker mechanism to remove the ashes formed during the operation. The gasifier was also shaken at a regular interval to facilitate the smooth flow of biomass inside the gasifier and prevent "rat holes" and bridging, inside the gasifier. Charcoal left from the previous run (or fresh charcoal if the run was for the

77

first time) inside the gasifier was ignited with a cal rod (igniter/heater) before the fresh biomass

was fed inside the gasifier. The height and inside diameter of the gasifier reactor were 1200 mm

and 350 mm respectively.
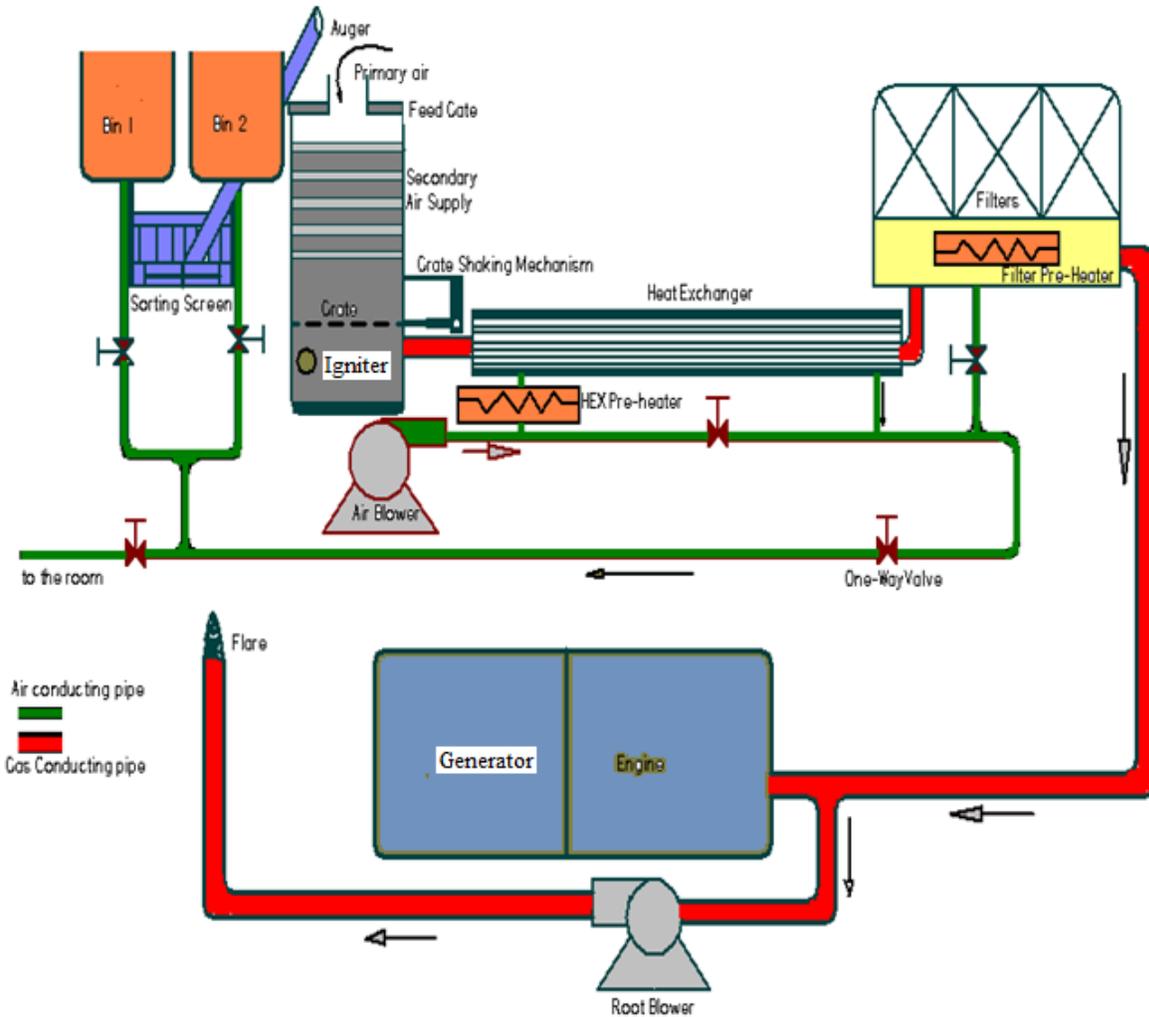
Figure 3.1 Schematic of the Auburn mobile downdraft gasifier designed by CPC
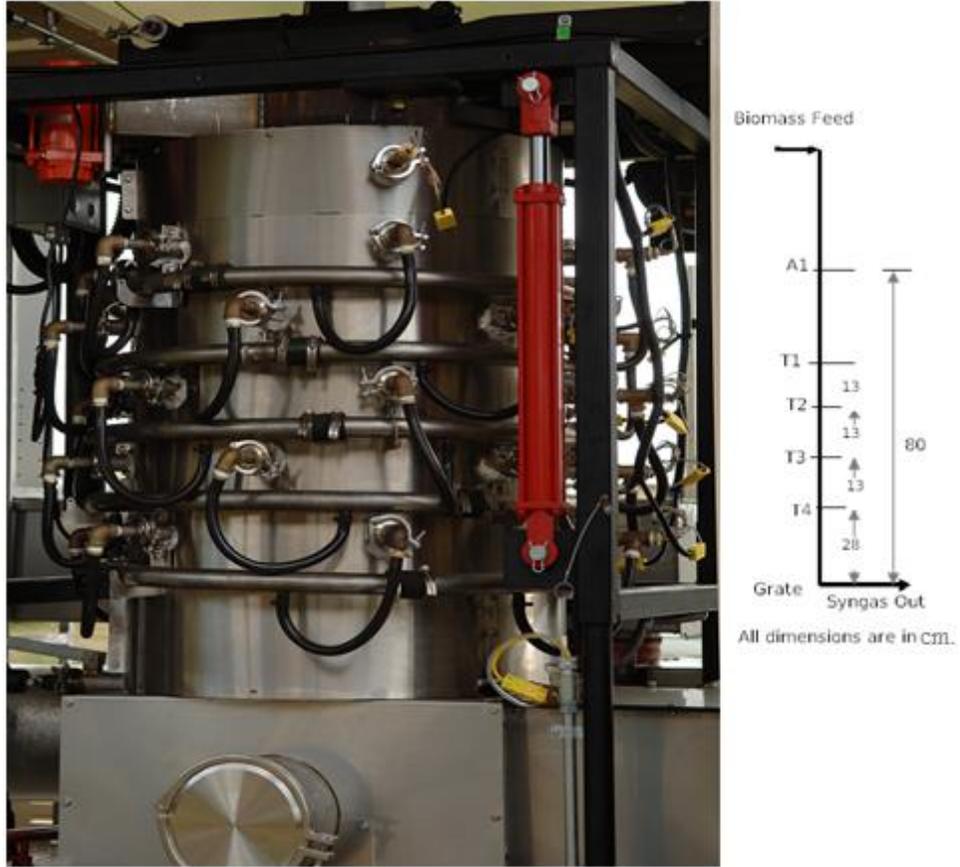
Figure 3.2 Photograph of the Auburn gasifier along with dimensional sketch of thermocouples

position (Measurements are not to scale; A1 and T1 to T4 represent the position of

thermocouples in the gasifier).

Figure 3.3 The Auburn mobile downdraft gasifier parked outside the capitol building in Montgomery, AL

3.3.2 SYSTEM OPERATION

A certain protocol was followed prior to starting the gasifier for beginning of each experiment, including conducting a pre-run check, involving checking leaks, various hose connections, motors and electrical devices associated with the system, charcoal level, complete flare raising etc. Heat exchangers and filters were preheated to 40˚C before igniting charcoal inside the gasifier to avoid any condensation during the process. The heat exchangers and filters were heated using electricity from the grid or using electricity generated from the generator (that runs on propane gas). Once the filters and heat-exchanger were heated to 40˚C, igniter located inside the gasifier was turned on. Igniter heats the charcoal inside the gasifier caused the temperature inside the gasifier to rise. Temperatures across various locations inside the gasifier were measured by thermocouples (K-type). Temperature data were automatically logged at 15

seconds intervals. Among many thermocouples in the system, only the location of various thermocouples of interest as measured from the grate is shown in Figure 3.2 schematically. Secondary air supplies, via a char-air blower, were injected for each level, as the temperatures, for the corresponding levels, reached 350°C. Feeding of wood chips started only when thermocouples measured above 800°C in any three locations inside the gasifier.

Hot syngas coming out from the gasifier was cooled using the heat exchanger (HEX). This results in the heating of air supplied by gas cooling blower and cooling of syngas. Char and particulates were then removed by passing the cooled syngas through the filters. Even though the cleaned syngas could be burned in an engine to produce power, the cleaned syngas was flared in this study since the focus on the study was on effect of biomass feedstocks and operating conditions on syngas composition. Syngas was sampled with online gas analysis system after passing through the filters, the details of which are discussed in the following section.

The steady state of the system was indicated by steady temperature across the various levels of the gasifier, most commonly 800°C at any three locations among T1-T4. The time required to attain steady-state generally varied from 30 minutes to one hour and was affected by biomass feedstock type, and operating conditions. Once the gasifier reached steady-state, parameters to be considered were the differential pressure in the HEX and the temperature of syngas out of the HEX. An increase in higher pressure differential in the HEX suggests clogging, which prevents smooth flow of syngas and reduces the effectiveness of the HEX. As the effectiveness of HEX decreases, syngas temperature after passing through it is a concern as high temperatures may ignite filter bags. Ideally, the amount of oxygen in the syngas has to be zero but the system used in this experiment was bigger than that used in lab-scale experiments, making this difficult. It was found that the oxygen level was between 0.5-2.0 (vol./vol.,% dry). If

the amount of oxygen in the syngas was more than 2 %, a leak inspection was carried out. A typical temperature profile of the gasifier is attached in Appendix D (Table D. 7 and Figure D.1-D.5).

After the experiment was completed, proper shut-down was carried out. During the shutdown process, syngas flow rate increases because of an increase in the roots-blower speed. This is pre-set to make sure that no gas remains inside after leaving the gasifier. More air is drawn to obtain higher combustion so that fresh wood chips inside the gasifier can be burned faster and are converted into charcoal for the next run. This also removes any smoke that may occur. The feeder is automatically turned off and temperature increases to rise near the upper level of the gasifier due to a higher combustion rate. The feed-gate and roots-blower will turn off once the upper level of the gasifier attains a certain temperature that is sufficient to sustain slow pyrolysis. This varies according to the operating conditions. The system is thus completely shut down. Most of the experiments were carried out for 4 to 5 hours except in the case of poultry litter where steady state conditions could not be supported for more than two hours.

3.3.3 DATA COLLECTION AND ANALYSIS

This study was conducted to examine the effect of various feedstocks on syngas composition. Five types of feedstock (pine wood chips, peanut hulls, poultry litter, saw dust pellets and commercial wood pellets) shown in Figure 3.4 were tested. Commercial wood pellets were obtained from American Wood Fiber, Columbia, MD. Furthermore, the effects of moisture content and biomass-flow rate in gas composition and its calorific value were analyzed for pine wood chips.

Carbon, energy and exergy analyses for the gasification tests were done only when commercial wood pellets was used as a feedstock. Wood pellets were fed into the gasifier by an external biomass feeder for an accurate measurement of the mass used in each experiment. Instead of analyzing syngas after filters, syngas was sampled immediately after the gasifier because of simultaneous measurement of tar content (Reported in Chapter 4) in syngas. Experiments with commercial wood pellets were run for almost 4 hours for all tests.

Since the design of this gasifier makes it difficult to control the biomass feed rate directly, an alternative approach is taken to achieve varying biomass feed rates. Since syngas output rate depends upon the biomass feed rate in the system, the syngas output rate (which can be easily computer controlled in this gasifier) was varied to control the biomass feed rate.

Peanut hulls pellets Poultry litter pellets Saw dust pellets Wood chips Commercial wood pellets

Figure 3.4 Image of various biomass feedstocks

Syngas composition was measured using a gas analyzer (Nova 7905AQN4, Niagara Falls, NY) on site and the gas composition was measured in a volumetric basis. The gas analyzer used has the capacity of measuring oxygen (O_2):0-25%, CO: 0-25%, CO_2: 0-20%, methane (CH_4) 0-10%, 0-20% H_2. It uses non-dispersive infrared (NDIR) detector for CO, CO_2 and CH_4 and temperature controlled thermal cell for H_2 and electrochemical sensor for O_2. The accuracy of this instrument is ±1% of full scale. The gas analyzer was calibrated with air for oxygen. For

other gases, a known mixture of gases with the following composition was used: CO 25.16%, CO_2 20.05%, CH_4 9.968%, H_2 20.04% and the balance was nitrogen.

Once the gasifier reached a steady state temperature, syngas data (CO, CO_2, H_2, CH_4 and O_2) were logged into a computer at 15 s intervals via the data logging software supplied with the gas analyzer. The remaining volumetric proportion was assumed to contain only nitrogen. Gasification temperature is not high enough to form nitrogen oxides (NO_X) and the nitrogen content in biomass is also fairly low except in the case of poultry litter. Therefore, NO_x measurement was not carried out in this study. Air-flow rate was calculated assuming that the source of nitrogen was from air only and thus atmospheric mass proportion of nitrogen was utilized for the calculation. The volumetric content of syngas constituents multiplied by their individual higher heating value (HHV) gave the overall higher heating HHV of the syngas as shown in Eqn. (1).

$$HHV_{syngas} = y_{H_2} HHV_{H_2} + y_{CO} HHV_{CO} + y_{CH_4} HHV_{CH_4} \qquad (1)$$

In above equation, HHV_{syngas} is the heating value of syngas while HHV_i and y_i are higher heating value and volumetric fraction of syngas constituents (i=H_2, CO, CH_4). The HHV of H_2, CO and CH_4 are 12.76 MJ/m^3, 12.6 MJ/m^3 and 39.8 MJ/m^3, respectively [16].

3.3.4 CHARACTERIZATION OF BIOMASS

Moisture content was measured following ASTM standard E871-82 where a representative sample of biomass feedstock used for the experiment was heated for 16 hr at 103°C to calculate the mass difference and hence the moisture content [17]. Bulk density of biomass feedstock was

measured by determining a known quantity in a standard container with volume of 946.35 mL (1 quart). Ash content was measured according to the ASTM standard E 1755-01. This involves heating of biomass sample (0.5 g-1 g) in a muffle furnace to $575 \pm 25^{\circ}C$ for three hours and finding the amount that remains in the container [18]. Biomass samples were sent to Midwest Microlab, LLC (Indianapolis, IN) for an ultimate analysis. Although the procedure for measuring elemental composition (ultimate analysis) varies from instrument to instrument, the basic principle for almost all is the combustion of small biomass sample in a pure oxygen environment and subsequent measurement of C, H, N and S in the output stream which can easily be found. HHV of the biomass was calculated by Dulong and Petit's Formula given in Eqn. (2) using results from ultimate analysis and also experimentally using an oxygen bomb calorimeter (IKA, model C200, Wilmington, NC) with reference to ASTM D 2015-96 for verification [16, 19]. Moisture content in biomass samples was determined by calculating the weight loss of samples by heating in an oven at $103\ ^{\circ}C$ for 16 hours using ASTM E 871 Standard [20]. Ash fusion temperatures were determined using ASTM D 1857 Standard in Alabama Power General Test laboratory (Birmingham, AL) and Hazen Research Inc. (Golden, CO) [21]. Results of ultimate and proximate analyses along with HHV are shown in Table 3.1.

$$\text{HHV} = 33823\ C + 144{,}249\left(H - \frac{O}{8}\right) + 9418\ S\ \text{kJ/kg} \qquad (2)$$

where C, H, O and S are the carbon, hydrogen, oxygen and sulfur content of biomass in dry basis.

Table 3.1: Characteristics of biomass feedstock used for gasification

(% mass) Ultimate Analysis‡, wt.%	Pellets				Wood Chips
	Poultry	Peanut hulls	Saw dust	Commercial wood*	
C	22.1	47.8	45.2	47.7	45.2
H	4.3	5.5	5.8	6.0	5.6
N	3.1	0.8	0.3	0.0	0.1
S	0.6	-	0.0	0.0	0.0
O†	31.3	43.1	46.3	45.8	47.7
Ash, wt.%	33.3	2.78	2.29	0.44	0.33
HHV$^\diamond$, MJ/kg	11.21 (10.34)	18.67 (15.91)	18.07 (15.48)	18.34 (16.51)	18.82 (15.05)
Bulk density, kg/m^3	680	790	725	750	210
M.C wt.%	8.5	5.1	4.7	2.5-5.3	17.6-25

*: Ultimate analysis done for dry pellets

‡ash free basis, †by difference, "-": Not detectable, $^\diamond$values within the parenthesis are calculated using Dulong and Petit's Formula.

3.4 RESULTS AND DISCUSSION

3.4.1 SYNGAS COMPOSITION FROM DIFFERENT FEEDSTOCKS

Syngas composition from selected feedstocks was evaluated at a constant syngas output flow rate and the average values are reported in Table 3.2. Although equal moisture content for all the feedstocks was not achieved as a proper moisture controlling set-up was not available, the results show comparison between syngas from various feedstocks. All other feedstocks except wood chips were tested as they were received. Wood chips were tested at the moisture content of 19.6 wt. %. Although syngas flow rate was set to 65 Nm^3/hr, mass flow rate varied from 26.5 kg/hr for wood chips to 31 kg/hr for peanut hulls pellets under same experimental conditions. As expected, pellets have slightly higher feed rate than wood chips due to better flow characteristics.

Syngas from peanut hulls pellets showed the largest fraction of CO as well as H_2 and thus had the highest HHV among all the feedstocks selected for this study. The carbon fraction of peanut hulls, as can be seen from the ultimate analysis, had the highest fraction of carbon amongst all the feedstocks under consideration for the current experiment. This could perhaps be the reason why gasification of peanut hulls showed the highest heating value of syngas. Other impacts could be due to the moisture variation and some difference in mass flow rate. Further, research with accurate control on moisture and other conditions are already initiated and the results will be reported in the future. The overall HHV as well as total volumetric combustibles (CO, CH_4 and H_2) were found to be the lowest for poultry litter due to its high level of ash content and low level of carbon content.

Table 3.2: Syngas Composition from different feedstocks[‡]

Feedstock[†]	vol. %					HHV(MJ/m^3)
	O_2	CO	CO_2	CH_4	H_2	
Peanut hulls (5.1)	$0.5^{\pm0.1}$	$22.8^{\pm0.7}$	$8.9^{\pm0.5}$	$2.7^{\pm0.3}$	$20.1^{\pm0.3}$	$6.1^{\pm0.2}$
Saw dust (4.7)	$1.1^{\pm0.3}$	$22.2^{\pm0.5}$	$8.3^{\pm0.3}$	$3.0^{\pm0.2}$	$19.4^{\pm0.3}$	$6.0^{\pm0.2}$
Poultry litter (8.5)	$0.8^{\pm0.1}$	$20.9^{\pm2.3}$	$8.8^{\pm1.6}$	$1.2^{\pm0.4}$	$16.2^{\pm2.0}$	$4.8^{\pm0.7}$
Commercial pellets (3.5)	$0.5^{\pm0.2}$	$22.1^{\pm0.8}$	$10.4^{\pm0.7}$	$1.9^{\pm0.2}$	$16.6^{\pm1.0}$	$6.1^{\pm0.2}$
Wood chips (19.6)	$0.7^{\pm0.1}$	$21.1^{\pm1.3}$	$12.2^{\pm0.9}$	$2.3^{\pm0.4}$	$20.4^{\pm0.5}$	$5.7^{\pm0.4}$

[‡]±sign followed by numerical values are standard deviation, [†]number given within the parentheses is the moisture content (wt.%) of the feedstock during gasification.

3.4.2 EFFECT OF MOISTURE CONTENT IN SYNGAS COMPOSITION

To examine the effect of moisture content, syngas flow rate was set to 65 Nm^3/hr thus adjusting almost equal mass flow rate for all experiment which was about 26.5-27.5 kg/hr. Table 3.3 depicts syngas composition at various moisture content with pine wood chips.

Table 3.3: Effect of moisture content in syngas composition[‡]

Moisture Content (% wet basis)	Dry Biomass Flow rate (kg/hr)	vol. %					HHV(MJ/m^3)
		O_2	CO	CO_2	CH_4	H_2	
19.6	21.3	$0.7^{\pm0.1}$	$21.1^{\pm1.3}$	$12.2^{\pm0.9}$	$2.3^{\pm0.4}$	$20.4^{\pm0.5}$	$5.7^{\pm0.4}$
23	20.9	$0.9^{\pm0.1}$	$18.1^{\pm1.1}$	$13.0^{\pm0.8}$	$2.5^{\pm0.5}$	$20.5^{\pm0.4}$	$5.5^{\pm0.4}$
25	20	$1.3^{\pm0.1}$	$16.4^{\pm0.4}$	$13.0^{\pm0.3}$	$2.5^{\pm0.2}$	$19.3^{\pm0.2}$	$5.2^{\pm0.2}$

[‡]±sign followed by numerical values are standard deviations

Although biomass gasification is a complex process, the following reactions typically can be used to represent the gasification process inside the gasifier [6, 22].

$$C + \frac{1}{2}O_2 \leftrightarrow CO + 110 \text{ MJ/kgmol} \tag{3}$$

$$C + O_2 \leftrightarrow CO_2 + 393 \text{ MJ/kgmol} \tag{4}$$

$$C + H_2O \leftrightarrow CO + H_2 - 132 \text{ MJ/kgmol} \tag{5}$$

$$C + CO_2 \leftrightarrow 2CO - 173 \text{ MJ/kgmol} \tag{6}$$

$$CH_4 + H_2O \leftrightarrow CO + 3H_2 - 206 \text{ MJ/kgmol} \qquad (7)$$

$$CO + H_2O \leftrightarrow CO_2 + H_2 + 42 \text{ MJ/kgmol} \qquad (8)$$

$$CH_4 + 2H_2O \leftrightarrow CO_2 + 4H_2 - 165 \text{ MJ/kgmol} \qquad (9)$$
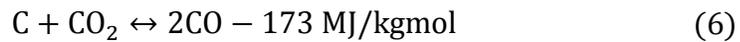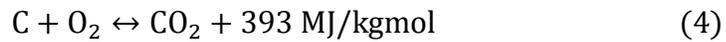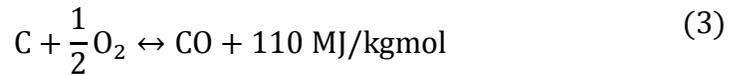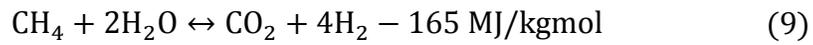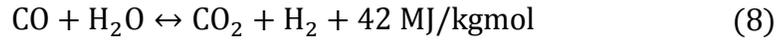
As can be seen from Eq. 7, an increase in moisture content decreases the amount of CO and produces CO_2 and H_2. As expected, a decrease in CO was observed in the experiments with an increase in moisture content but the increase/decrease in CO_2, H_2 and CH_4 were not significant. The gasifier used for current research was temperature-controlled which tries to adjust its pre-set temperature (usually set at $800^{\circ}C$) at various locations by increasing/decreasing the amount of secondary air through proportional valve opening. However, H_2 proportion in syngas is also a strong function of temperature. As can be seen from Eqns., (4), (6) and (7), reactions producing hydrogen are highly endothermic in nature so they demand high heat. The temperature distribution for various moisture content discussed in a later section shows a similar temperature profile. Due to this reason, there could be a small change in the hydrogen concentration.

3.4.3 EFFECT OF BIOMASS FEED RATE IN SYNGAS COMPOSITION

The moisture content of wood chips used to analyze the effect of biomass feed rate varied from 17.6 wt.% to 19.6 wt.%. Biomass feed rate was varied by setting the syngas flow rate which automatically adjusts the biomass flow. Three syngas flow rates selected were 65, 55 and 45 Nm^3/hr, which changed the biomass feed rate. The CO and H_2 were found to increase slightly with an increase in biomass feed while oxygen decreased. The effect of biomass feed rate upon CH_4 did not show any significant pattern. Syngas composition from different biomass feed rate is shown in Table 3.4.

Table 3.4 Effect of biomass feed rate in syngas composition[‡]

Biomass flow rate (kg/hr, wet basis)	Moisture content (% wet basis)	vol. %					HHV MJ/m^3
		O_2	CO	CO_2	CH_4	H_2	
16.4	17.7	$1.8^{\pm0.4}$	$15.6^{\pm1.7}$	$11.4^{\pm1.1}$	$2.2^{\pm0.6}$	$19.4^{\pm0.8}$	$4.9^{\pm0.5}$
21.5	17.6	$1.1^{\pm0.3}$	$20.9^{\pm2.2}$	$11.4^{\pm1.4}$	$2.6^{\pm0.7}$	$20.2^{\pm0.8}$	$5.8^{\pm0.6}$
26.5	19.6	$0.7^{\pm0.1}$	$21.1^{\pm1.3}$	$12.2^{\pm0.9}$	$2.3^{\pm0.4}$	$20.4^{\pm0.5}$	$5.7^{\pm0.4}$

[‡]±sign followed by numerical values are standard

3.4.4 TEMPERATURE VARIATION IN GASIFIER

Moisture content reduces the reactor temperature of the gasifier due to heat absorption for its evaporation. However as seen in Figure 3.5, deviation in temperature at various heights inside the gasifier was found to be less than $30^{\circ}C$ even at a 5.4 wt % increase in moisture content. This was probably due to automatic adjustments in the gasifier which tries to maintain the pre-set temperature at different zones by increasing the amount of secondary air flow hence promoting

combustion around that region. Thus, Equivalence ratio was higher biomass with higher moisture content. The equivalence ratio for various moisture contents is shown in Table 3.5.
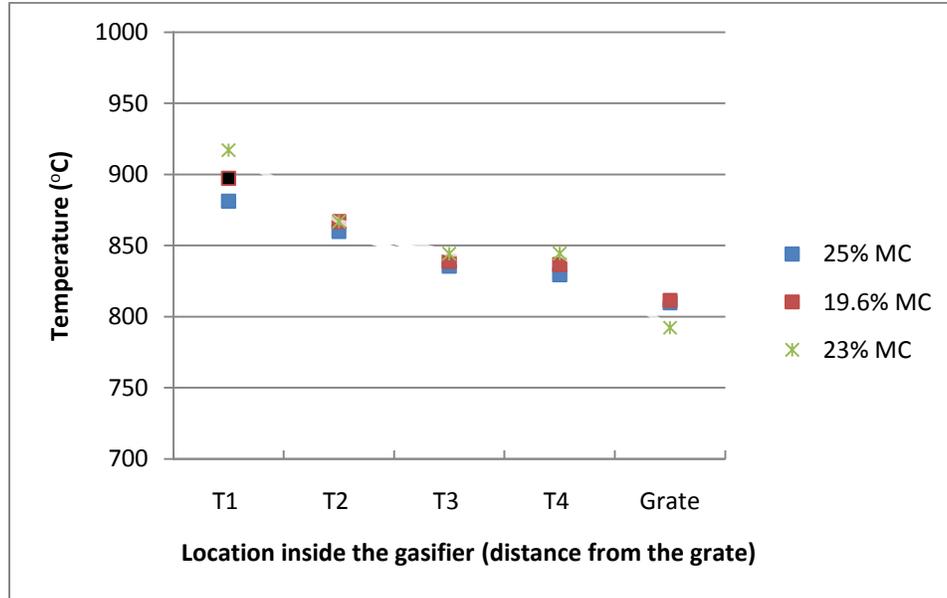
Figure 3.5 Effect of moisture content in gasifier temperature

(Data for this plot in Appendix D: Table D.8)

Table 3.5 Equivalence ratio at various moisture contents

Moisture Content (% wet basis)	Wet biomass flow rate (kg/hr)	Equivalence ratio (ER)
19.6	26.5	0.48
23	27.1	0.51
25	26.6	0.52

The temperature variation for various feedstocks in the gasifier is shown in Figure 3.6. The moisture content and biomass flow rate corresponding to different biomass in Figure 3.6 is shown in Table 3.6. While the temperature along the gasifier height was approximately equal for saw dust and wood chips, a lower temperature distribution was found for the gasification of

91

peanut hulls. On the other hand, the temperature distribution for poultry litter gasification had a different profile than the rest of the feedstocks with a sudden increase from T1 to T2. This sudden increase in temperature was due to ash fusion around the vicinity of initial start-up ignition and thus heat localization at one point which resulted in high temperatures. Since this fused ash had high thermal resistance, no heat diffuses to the upper part of the gasifier.

Table 3.6 Moisture content and biomass flow rate for different feedstocks

Feedstock	Moisture content (% wet basis)	Wet biomass flow rate (kg/hr)
Peanut hulls	5.7	31.8
Saw dust pellets	4.7	29.9
Poultry litter pellets	8.5	-*
Commercial wood pellets	3.5	28.8
Wood chips	25	26.6

-* could not measure due to operational problem
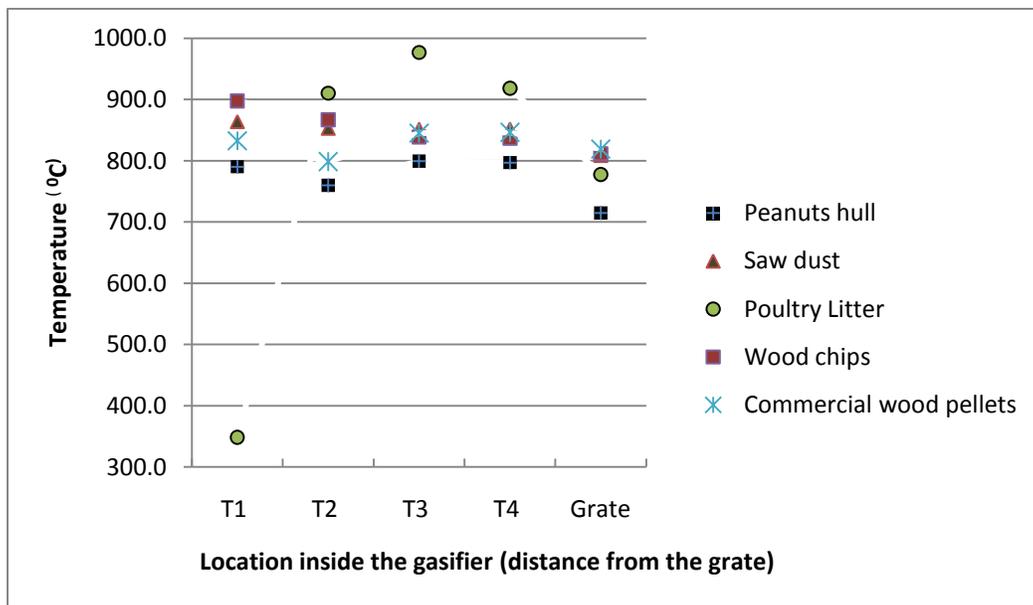
Figure 3.6 Effect of feedstock in gasifier temperature

(Data for this plot in Appendix D: Table D.9)
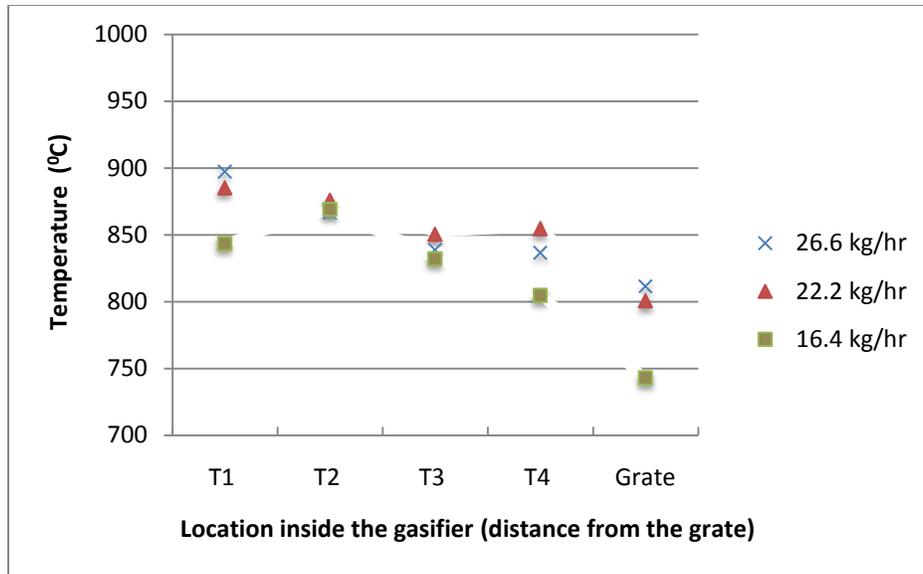
Figure 3.7 Effect of biomass flow rate in gasifier temperature

(Data for this plot in Appendix D: Table D.10)

Decreasing the biomass flow rate into the gasifier increases the grate temperature. The moisture content of woodchips (% wet basis) is 19.2% to19.7% for the three biomass flow rate shown in Figure 3.7. Lower feed rate increases the residence time of the biomass inside the gasifier, and hence promotes efficient reduction reactions inside the gasifier. These reactions are endothermic, hence the reduction in temperature with decrease in mass flow rate.

3.4.5   GASIFICATION ISSUES WITH PELLETS AND POULTRY LITTER

Due to good flow characteristics of pellets and a higher density than wood chips, the residence time was increased from experience. Setting the same residence time resulted in incomplete combustion of pellets and also a high pressure differential inside the gasifier in many cases. The increase in residence time was achieved mainly by adjusting the interval of the grate-shaker and of the gasifier vibrator itself. Normally when running the experiment with pellets, the

frequency of the grate shaker was decreased by a factor of four and gasifier vibration frequency by 1.3 compared to the settings used for wood chips. Despite the modifications made, problems were encountered with the gasification of poultry litter. It has been reported that agglomeration could occur in the gasification of the feedstock with moisture greater than 5 wt.% of ash-content [22]. Poultry litter test runs could not be sustained for more than two hours without significant agglomeration. The low-melting mixture created blockage inside the gasifier and thus further gasification was not possible. The snapshot shown in Figure 8 shows one of the clinkers removed after poultry litter gasification.

Figure 3.8 Ash agglomeration in the grate of gasifier after the gasification of poultry litter

Formation of ash clinker was assumed to be due to the low ash fusion temperature of the minerals inherent in poultry litter. Abelha et al., reported the ash fusion temperature to be $660^{\circ}C$ for poultry litter [23]. Gasification of poultry litter in a downdraft gasifier may also be greatly affected by the temperature inside the gasifier. The temperature should thus be such that it can sustain the gasification but at the same time be lower than the ash-fusion temperature of the poultry litter. Surprisingly, the results in the current study reported in Table 3.7, showed that the ash fusion temperature for poultry litter was significantly higher than the numbers reported in the literature [16]. Analyses were performed in two different laboratories to validate the results and

94

they were within 5% variation. Further, ash-fusion temperature of peanut hulls and poultry litters do not differ significantly although, no problem was noticed while gasifying peanut hulls. Therefore, the proper reason for ash agglomeration is unknown.

Table 3.7 Ash fusion temperature for various feedstocks[‡]

Feedstock	Reducing Atmosphere, ^{o}C			
	Initial Temp.	Softening Temp.	Hemispherical Temp.	Fluid Temp.
Pine wood	1538	1538	1538	1538
Saw dust	1301	1450	1454	1463
Peanut hulls	1253	1309	1325	1348
Poultry Litter[‡]	1235 (1293)	1293 (1323)	1312(1330)	1385(1337)

[ǂ]Results obtained from Alabama Power General Test laboratory, [‡]Numbers in the parenthesis are obtained from Hazen Research Inc.

3.4.6 CARBON, ENERGY AND EXERGY ANALYSES WITH COMMERCIAL WOOD PELLETS

Since the source of carbon input is only from pellets, amount of carbon fed into the gasifier is calculated from pellets-flow rate and ultimate analysis. The amount of carbon output was measured from the flow rate of individual carbonaceous syngas constituents.

The following assumptions were made in calculating the energy and exergy of biomass and individual gases:

-Negligible pressure variations inside the gasifier

95

-Ideal gas consideration for the syngas and its constituent gases

The gasifier used in the experiment is operated at atmospheric pressure and the pressure drop across the gasifier is not significant. Gases can be treated as ideal gases at low pressure and high temperature. Thus, the assumptions stated above are valid and introduce a negligible amount of error in the calculation.

The following formulas are used to calculate energy and exergy of individual gases in syngas [24].

$$E_i = E_{0i} + \int_{T_d}^{T} C_p dT \tag{10}$$

$$Ex_i = Ex_{0i} + \int_{T_d}^{T} \left[C_p \left(1 - \frac{T_d}{T} \right) \right] dT \tag{11}$$

E_i and Ex_i are the energy and exergy of the gas in MJ/kg at the temperature T in kelvin while E_{0i} and Ex_{0i} represents energy and exergy of the gases at the reference or dead state (T_d) taken to be at $25^{\circ}C$ or 298 K, respectively. The chemical energy (also known as the enthalpy of formation) is taken from the corresponding reference [25]. The specific heat capacity, C_p is in kJ/kg-K at constant pressure and is expressed by the following equation.

$$C_p = c_0 + c_1 \theta + c_2 \theta^2 + c_3 \theta^3 \quad (\theta = T(K)/1000) \tag{12}$$

The values for the coefficients for Eqn. (12) are listed in the corresponding reference and are shown in Table 3.8 [24].

Table 3.8 Coefficients for the specific heat capacity of various gases

Gases	c_0	c_1	c_2	c_3
CO	1.1	-0.46	1	-0.454
CO_2	0.45	1.67	-1.27	0.39
CH_4	1.2	3.25	0.75	-0.71
N_2	1.11	-0.48	0.96	-0.42
O_2	0.88	-0.0001	0.54	-0.33
H_2	13.46	4.6	-6.85	3.79

Exergy of dry ash-free biomass without any sulfur is found using Eqn. (13) and (14) [14].

$$E_{x0} = \beta(LHV_{org}) \tag{13}$$

$$\beta = \frac{1.044 + 0.016(H/C) - 0.3493O/C[1 + 0.0531H/C] + 0.0493N/C}{1 - 0.4124O/C} \tag{14}$$

In Eqn. (13) and (14), β is the ratio of chemical exergy of the biomass to the lower heating value of the organic fraction of biomass (LHV_{org}). H, C, O, N denotes the hydrogen, carbon, oxygen and nitrogen fraction by weight in biomass. Lower heating value of feedstock was found using Eqn. (15) [16].

$$LHV_{org} = \frac{HHV - 22,604H}{1000} MJ/kg \tag{15}$$

The tests were run at different biomass flow rate dictated by the syngas flow rate set for the experiment. Carbon, energy and exergy analyses were done for each test and are reported in

97

Table 3.9. Ideally, carbon closure is expected to be unity since input should be equal to output. However, carbon closure was found greater than one for some experiments which might be due to some instrumental errors as well as the residual biomass inside the gasifier, which could not be measured due to operational difficulties. Also, the size of the gasifier contributed to these discrepancies in carbon closures because of the higher probability that significant amount of biomass that can remain in the gasifier after the completion of experiment. Wander et al. [10] reported the similar carbon closure in their experiments with downdraft gasifier with the biomass flow rate capacity of 12 kg/hr. Carbon closure obtained in all experiments were higher than 0.89, comparable to those reported in the literature [10, 26-27].Detailed calculation procedure on carbon, energy and exergy analyses is presented in Appendix E.

Table 3.9 Carbon, energy and exergy analyses of commercial wood pellets

Wet biomass flow rate (kg/hr)	Moisture content (% w.b)	SF	F_s	Carbon Closure	E_{out} (MJ/kg)	E_{in} (MJ/kg)	E_{out}/E_{in}	Ex_{out} (MJ/kg)	Ex_{in} (MJ/kg)	Ex_{out}/Ex_{in}
17.6	3.4	45	45.0	1.08	311.5	310.4	1.00	224.0	337.0	0.66
18.0	3.8	45	45.8	1.04	318.7	316.6	1.01	223.5	343.8	0.65
18.6	4.5	45	45.0	0.98	306.9	325.4	0.94	215.1	353.3	0.61
18.7	4.1	45	44.3	0.99	299.9	327.6	0.92	210.9	355.7	0.59
19.0	2.7	45	47.4	1.02	335.8	337.4	1.00	239.0	366.4	0.65
19.8	3.4	55	55.0	1.15	382.1	349.1	1.09	274.2	379.0	0.72
20.6	5.3	55	54.9	1.15	390.3	356.6	1.09	279.5	387.2	0.72
23.1	3.8	55	50.0	0.91	358.4	405.4	0.88	258.7	440.1	0.59
24.6	2.7	65	59.9	0.98	424.4	437.9	0.97	299.3	475.4	0.63
24.9	5.3	65	65.0	1.13	465.9	430.7	1.08	332.2	467.7	0.71
26.5	3.7	65	57.6	0.89	403.0	465.4	0.87	285.5	505.3	0.57
27.0	3.8	65	62.6	0.96	442.7	475.6	0.93	317.5	516.3	0.61
28.8	3.5	65	65.0	0.90	445.0	508.9	0.87	319.1	552.5	0.58

SF: Syngas flow rate set for the experiment (Nm^3/hr), F_s: Actual flow rate of syngas (Nm^3/hr), Δ: in wet basis,

E_{in}, E_{out}, Ex_{in}, Ex_{out} are input energy, output energy, input exergy and output exergy, respectively.

High energy ratios observed in all of the gasification tests reported in Table 3.9 shows that the heat losses from the gasification system is minimal, and almost all of the energy present in biomass is retained in the syngas. An Exergy ratio varies from 0.57 to 0.72 which is similar to those reported in literature. Rao et al. [25] reported exergy ratios from 64% to 66% for different biomass in updraft gasifier.

The moisture content of the pellets was measured after each experiment and moisture content of the pellets used in the experiment was found to be in the range of 2.5-5.3% (wet basis). Figure 3.9 shows the volumetric fraction of individual gases with respect to biomass flow rate.
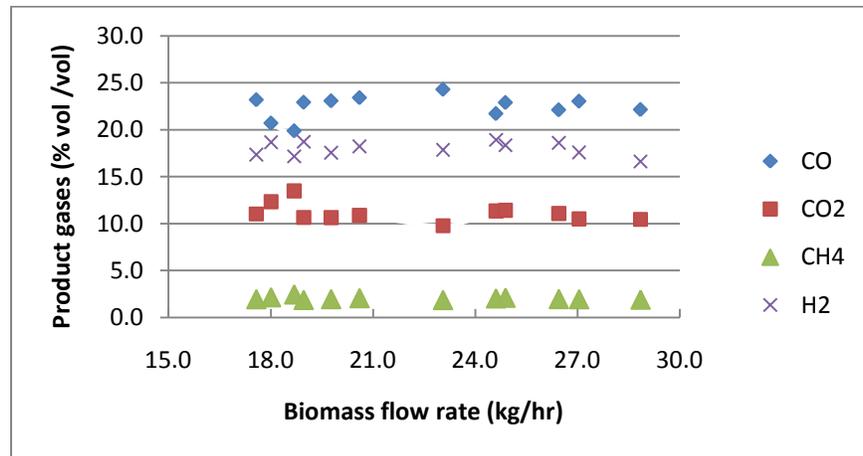
Figure 3.9 Biomass flow rate versus product gases for wood pellets

(Data for this plot in Appendix D: Table D.11)

Syngas composition from wood pellets do not show any specific pattern change with change in biomass feed rate inside the gasifier. The automatic adjustment of the gasifier, which is difficult to control manually, tries to pre-set the temperature pre-set so that the effect of

100

biomass flow rate alone cannot be seen at constant syngas output. Thus, the temperature tries to remain consistent as seen from the Figure 3.10 in spite of the change in biomass flow rate.
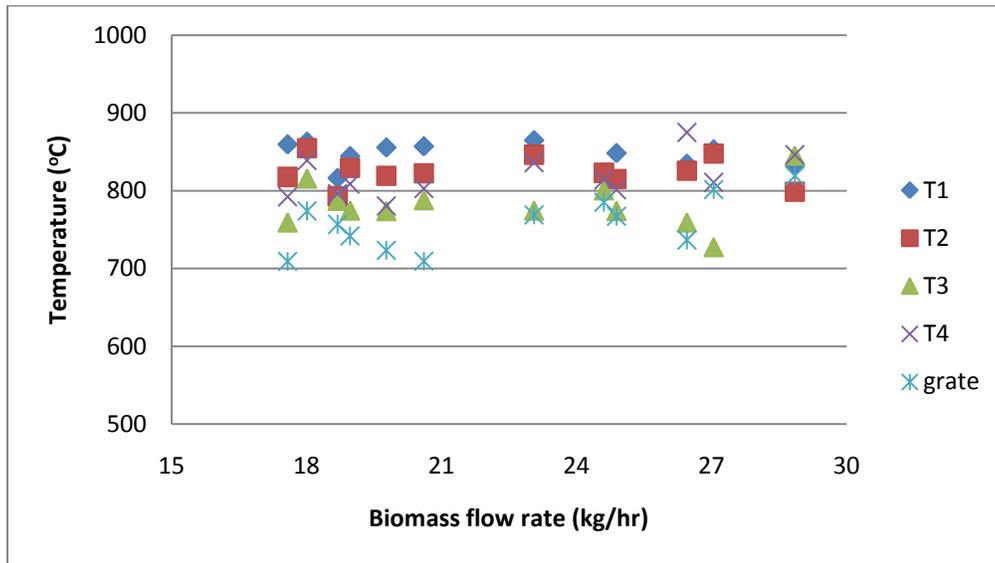
Figure 3.10 Effect of biomass flow rate upon temperature

(Data for this plot in Appendix D: Table D.12)

Figure 3.11 shows the effect of biomass flow rate on HHV of the syngas. For all the experiments conducted with wood pellets, HHV lies between 5.7-6.1 MJ/m^3.
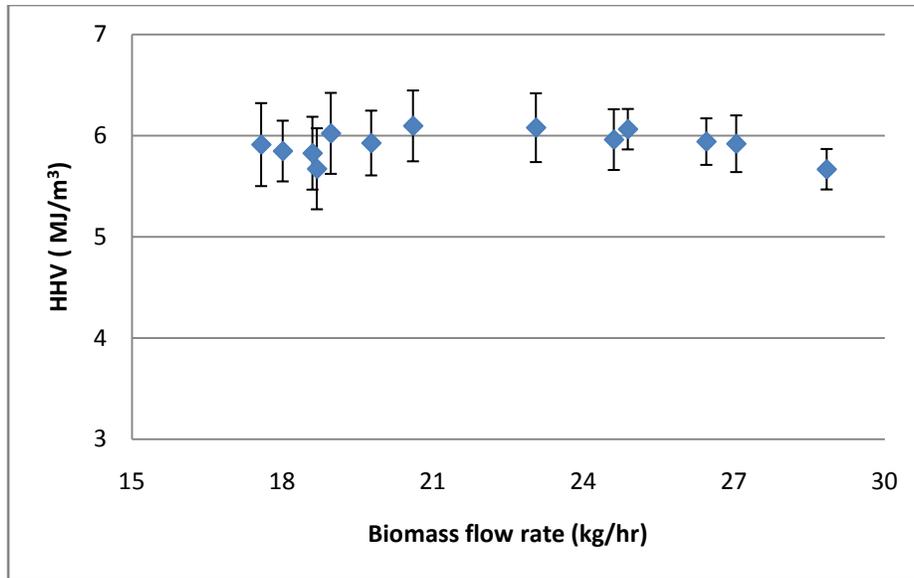
Figure 3.11 Effect of biomass flow rate on HHV

3.5   CONCLUSION AND FINAL REMARKS

Results based on biomass gasification using selected feedstocks in the Auburn mobile commercial gasifier were presented along with the extended study of the effect of biomass flow rate on syngas composition for commercial wood pellets. Syngas obtained from the gasifier was found to have appreciable HHV for atmospheric air gasification. This particular gasifier was found to maintain almost a constant pre-set temperature over a wide range of moisture contents investigated in this study while decreasing temperatures were observed as the biomass feed rate decreased. Pellets of various agricultural residues showed excellent gasification possibilities. Difficulties encountered during the gasification of poultry litter warrants further research on finding the suitable operating parameters as well as feedstock treatment. Carbon closures were greater than 0.89 for all of the experiments conducted with commercial wood pellets suggesting high carbon conversion efficiency of the gasifier. High energy ratios were obtained which indicates negligible amount of heat losses from the gasifier. Exergy ratio of the gasifier was from 0.63 to 0.78 indicating significant amount of useful energy that can be recovered from syngas.

3.6   REFERENCES

[1] A.A.C.M. Beenackers, Biomass gasification in moving beds, a review of European technologies, Renewable Energy, 16 (1998) 1180-1186.

[2] I. Olofsson, A. Nordin, U. Söderlind, Initial Review and Evaluation of Process Technologies and Systems Suitable for Cost-Efficient Medium-Scale Gasification for Biomass to Liquid Fuels., in: ETPC Report, 2005.

[3] Annual energy outlook 2009 in: D.o.E. Energy information adminstration (Ed.), Washington, DC, 2009.

[4] A. Milbrandt, A geographic perspective on the current biomass resource availability in the United States, in, National renewable energy laboratory, Golden, Colorado, 2005.

[5] Z.A. Zainal, A. Rifau, G.A. Quadir, K.N. Seetharamu, Experimental investigation of a downdraft gasifier, Biomass and Bioenergy, 23 (2002) 283-289.

[6] V. Skoulou, A. Zabaniotou, G. Stavropoulos, G. Sakelaropoulos, Syngas production from olive tree cuttings and olive kernels in a downdraft fixed-bed gasifier, International Journal of Hydrogen Energy, 33 (2008) 1185-1194.

[7] T.H. Jayah, L. Aye, R.J. Fuller, D.F. Stewart, Computer simulation of a downdraft wood gasifier for tea drying, Biomass and Bioenergy, 25 (2003) 459-469

[8] P. García-Bacaicoa, J.F. Mastral, J. Ceamanos, C. Berrueco, S. Serrano, Gasification of biomass/high density polyethylene mixtures in a downdraft gasifier, Bioresource Technology, 99 (2008) 5485-5491.

[9] K.S. Lin, H.P. Wang, C.J. Lin, C.-I. Juch, A process development for gasification of rice husk, Fuel Processing Technology, 55 (1998) 185-192.

[10] P.R. Wander, C.R. Altafini, R.M. Barreto, Assessment of a small sawdust gasification unit, Biomass and Bioenergy, 27 (2004) 467-476.

[11] P.N. Sheth, B.V. Babu, Experimental studies on producer gas generation from wood waste in a downdraft biomass gasifier, Bioresource Technology, 100 (2009) 3127-3133.

[12] A.K. Sharma, Equilibrium modeling of global reduction reactions for a downdraft (biomass) gasifier, Energy Conversion and Management, 49 (2008) 832-842.

[13] Z.A. Zainal, R. Ali, C.H. Lean, K.N. Seetharamu, Prediction of performance of a downdraft gasifier using equilibrium modeling for different biomass materials, Energy Conversion and Management, 42 (2001) 1499-1515.

[14] K.J. Ptasinski, M.J. Prins, A. Pierik, Exergetic evaluation of biomass gasification, Energy, 32 (2007) 568-574.

[15] J. Werther, M. Saenger, E.U. Hartge, T. Ogada, Z. Siagi, Combustion of agricultural residues, Progress in Energy and Combustion Science, 26 (2000) 1-27.

[16] P. Basu, Combustion and gasification in fluidized beds, Taylor and Francis Group, LLC, Boca Raton, FL, 2006.

[17] ASTM, ASTM Standards E 871-82-standard test method for moisture analysis of particulate wood fuels, in, PA, USA, 2006.

[18] ASTM, ASTM Standards E 1755-01.standard test method for ash in biomass, in, PA, USA, 2007.

[19] ASTM, ASTM Standards D 2015-96—Standard test method for gross calorific value of coal and coke by the adiabatic bomb calorimeter., in, PA, USA, 1998.

[20] ASTM, ASTM Standards E 871 - 82. Standard test method for ash in biomass, in, PA, USA, 2006.

[21] ASTM, ASTM Standards D 1857-04. Standard Test Method for Fusibility of Coal and Coke Ash, in, PA, USA, 2006.

[22] P. McKendry, Energy production from biomass (part 3): gasification technologies, Bioresource Technology, 83 (2002) 55-63.

[23] P. Abelha, I. Gulyurtlu, D. Boavida, J. Seabra Barros, I. Cabrita, J. Leahy, B. Kelleher, M. Leahy, Combustion of poultry litter in a fluidised bed combustor[small star, filled], Fuel, 82 (2003) 687-692.

[24] R.E. Sonntag, C. Borgnakke, G.J.V. Wylen, Fundamentals of thermodynamics, Sixth ed., John Wiley & Sons, Inc., 2003.

[25] M.S. Rao, S.P. Singh, M.S. Sodha, A.K. Dubey, M. Shyam, Stoichiometric, mass, energy and exergy balance analysis of countercurrent fixed-bed gasification of post-consumer residues, Biomass and Bioenergy, 27 (2004) 155-171.

[26] M. Dogru, C.R. Howarth, G. Akay, B. Keskinler, A.A. Malik, Gasification of hazelnut shells in a downdraft gasifier, Energy, 27 (2002) 415-427.

[27] M. Dogru, A. Midilli, C.R. Howarth, Gasification of sewage sludge using a throated downdraft gasifier and uncertainty analysis, Fuel Processing Technology, 75 (2002) 55-82.

CHAPTER 4

TAR CONCENTRATION IN SYNGAS FROM STRATIFIED DOWNDRAFT GASIFIER

4.1   ABSTRACT

A study was conducted to see the different tar compounds and the effect of biomass flow rate on tar concentration in a stratified downdraft gasifier. Tertiary condensed tar products such as toluene, o/p-xylene, naphthalene, phenol, styrene and indene were observed in significant amount. Tar concentration in the syngas was found to be in the range of 0.34-0.68 g/Nm^3 lower than those reported for conventional downdraft gasifiers.

KEYWORDS: biomass, downdraft, gasifier, naphthalene, syngas, tar, toluene, xylene

4.2   INTRODUCTION

Milne and Evans [1] defined tar from the gasification process as a material in the syngas which condense inside the gasifier or in the equipment used for handling the product stream to its end use. Tar compounds are largely aromatic in nature. They further classify the tar obtained due to thermal-cracking into four groups which is shown in Table 4.1.

Table 4.1 Classification of tar from thermal cracking of biomass

Classification	Tar compounds
Primary	cellulose-derived products such as levoglucosan, hydroxyacetaldehyde, and furfurals and similar hemicellulose and lignin-derived products
Secondary	phenolics and olefins
Alkyl tertiary	methyl derivatives of aromatics
Condensed tertiary	benzene, naphthalene,acenaphthylene, anthracene/phenanthrene, pyrene

Among the type of products in the tar classified above, condensed tertiary products are formed as a result of consecutive conversion of primary tar at high temperature, and thus these two types, condensed tertiary and primary tar products are not usually found in the syngas at the same time [1].

The maximum limit of tar concentration in syngas varies depending upon its end use. The tolerable limit of tar concentration in syngas is 50-500 mg/Nm^3, 50-100 mg/Nm^3, less than 0.5 mg/Nm^3 and less than 5 mg/Nm^3 for compressors, internal combustion engines, methanol synthesis and gas turbines, respectively [1]. Tar production in a downdraft gasifier is much lower than in both updraft and fluidized bed gasifiers although it may not meet the requirements needed to be used directly without prior treatment in power generation applications and liquid fuel synthesis processes [2]. While liquid fuel syntheses from syngas requires purity in the reacting gases and thus tar removal, the major problem with tar, when used in power generation, is condensation at low temperature which creates blocking as well as fouling in power plant equipment [3]. Hence, subsequent treatment is usually warranted depending upon the end use of the syngas. Also the nature of tar from gasifier varies according to its design. Downdraft gasifiers produce tertiary tar while tar from updraft gasifiers contain mostly primary tar due to

lower possibility of tar cracking inside the gasifier [1]. Syngas from fluidized bed gasifiers contain tar which is the mixture of secondary and tertiary tar [1]. Tar content in a downdraft gasifier is usually in the range of 0.01-6 g/Nm^3 while updraft and fluidized bed gasifiers usually have the tar content about 50 g/Nm^3 and 6-12 g/Nm^3 in average, respectively [1]. The residence time and temperature in the gasification and reduction zones is the most important factor that determining the level of tar in a downdraft gasifier [4]. With increase in temperature, tar content in the syngas decreases due to thermal cracking [5]. Li et al., have reported that with increase in temperature from about $700^{\circ}C$ to $820^{\circ}C$, tar content decreases significantly from 15 to 0.54 g/Nm^3 in a circulating fluidized bed [6]. Figure 4.1 shows the relationship between gasifier reaction temperature and tar yield [7]. It can be observed from the figure that increase in temperature significantly reduces the fraction of liquid, and hence the tar from the gasification process. Increase in equivalence ratio also decreases tar content at the expense of higher level of combustion inside the gasifier and results in a higher concentration of CO_2, which is an undesirable product [8]. Although tar concentration in syngas from a downdraft gasifier is usually lower, these tars are also more stable and might be difficult to crack and remove depending upon the end-need [9]. For use in an internal combustion engine, concentration of tar should be less than 100 mg/Nm^3 for successful long-term operation [1, 10].
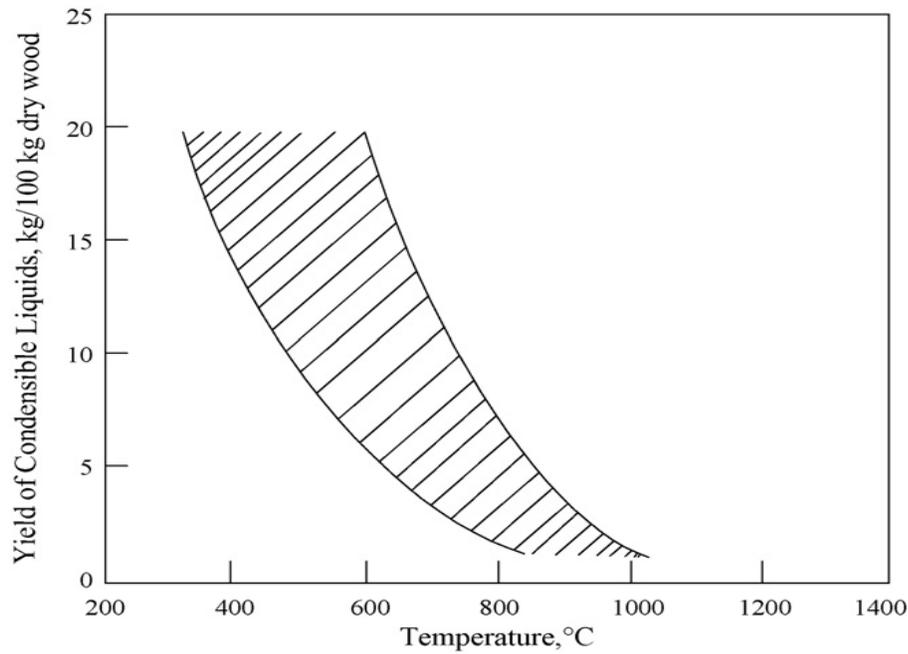
Figure 4.1 Effect of maximum reactor temperature on tar production (Baker et.al [7])

Milne and Evans have discussed the tar reduction procedure as any one of physical, thermal and catalytic techniques [1]. Han and Kim [5] have classified tar reduction methods into five groups which are: mechanism method, self-modification, thermal-cracking, catalytic cracking and plasma method. The mechanism method can effectively remove tar from 40-99% in syngas but the useful energy that can be achieved from tar conversion is lost. In other methods, tar is converted into other gases which increase the heating value of the syngas thus increasing the energetic efficiency of the process. Devi et al. [3] suggest three methods for tar removal which are adjustments of the operational parameters, addition of bed additives/catalysts and gasifier modification. One-lump model, as shown in Figure 4.2 by Li and Suzuki [11], considers all tar compounds lumped together as "tar" which disappears after simultaneous application of various cracking and reforming processes and finally appears as secondary gases.
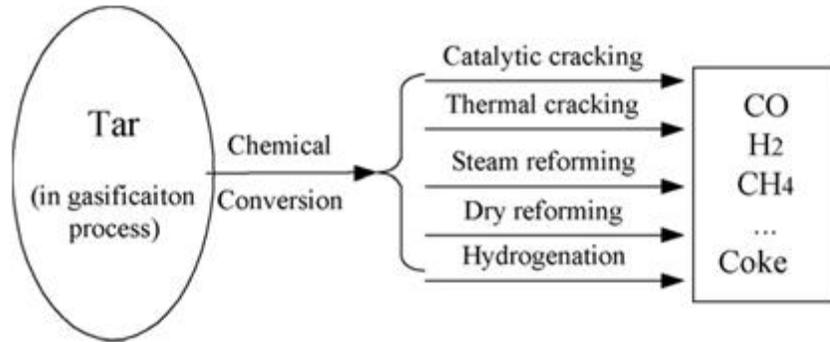
Figure 4.2 One-lump model for tar reduction (Li and Suzuki [11])

This chapter quantifies different tar compounds present in "tar" from stratified downdraft gasifier. Also reported is the tar concentration from the gasification of wood pellets as a function of various biomass flow rate.

4.3   EXPERIMENTAL SET-UP AND METHODOLOGY

Experiments to quantify the tar concentration in syngas were done with wood pellets from the commercial source as the feedstock. The ultimate and proximate analysis of wood pellets used for these experiments is shown in Table 4.2.

Table 4.2 Ultimate and proximate analysis of wood pellets

Sample	Wood pellets
Ultimate analysis (w/w%, dry basis)	
Carbon	47.7
Hydrogen	6.0
Nitrogen	0.04
Sulfur	not detected
Oxygen*	45.8
Proximate Analysis (w/w%)	
Ash content	0.33
Higher heating value (MJ/kg)	18.34
*: Calculated by difference	

Figure 4.3 shows the schematic diagram of the experimental set-up used to measure tar concentration in a syngas sample from the gasification of wood pellets in a stratified downdraft gasifier. Syngas is sampled from the port immediately after the downdraft gasifier and passed through impinger bottles each containing 50 mL of isopropyl alcohol. The first impinger bottle is kept at ambient conditions while the other two are kept in an ice-bath in order to maintain the temperature around the freezing point of water. The tar present in the syngas condenses under these conditions in the impinger bottles and later can be quantified. The water absorber after the impinger bottles attracts all the moisture present in the syngas stream after condensation and the syngas leaves dry after passing through the water-absorber. A flow-meter placed after the water-absorber measures the syngas flow rate which is required to find the tar concentration per standard volume.

The tar components were analyzed with an Agilent 7890 GC/5975MS using DB-1701 column (30 m; 0.25 mm i.d.; 0.25 mm film thickness). Thirty-one compounds were selected for quantification and five data points were generated in such a way that concentration of tar compounds fell within those five points. The tar which was already dissolved in isopropyl alcohol was further diluted 5 times with dichloromethane. A dilute tar sample was injected into the column and each sample was injected twice. Splitless injection was selected. The injector and the GC/MS interface were kept at constant temperature of $280^{o}C$ and $250^{o}C$, respectively. The initial temperature of the column, $40^{o}C$, was maintained for 2 min and the temperature was subsequently increased to $250^{o}C$ at $5^{o}C$/min and the final temperature was held for 8 min. Helium of ultra high purity (99.99%) supplied from Airgas Inc. (Charlotte, NC) was used as a carrier gas and flowed at 1.25 mL/min. Compounds were ionized at 69.9 eV electron impact conditions and analyzed over a mass per change (m/z) range of 50 − 550. Tar compounds were identified by comparing the mass spectra with the NIST (National Institute of Standards and Technology) mass spectral library and were reported as mg/Nm^3 of syngas flow rate.
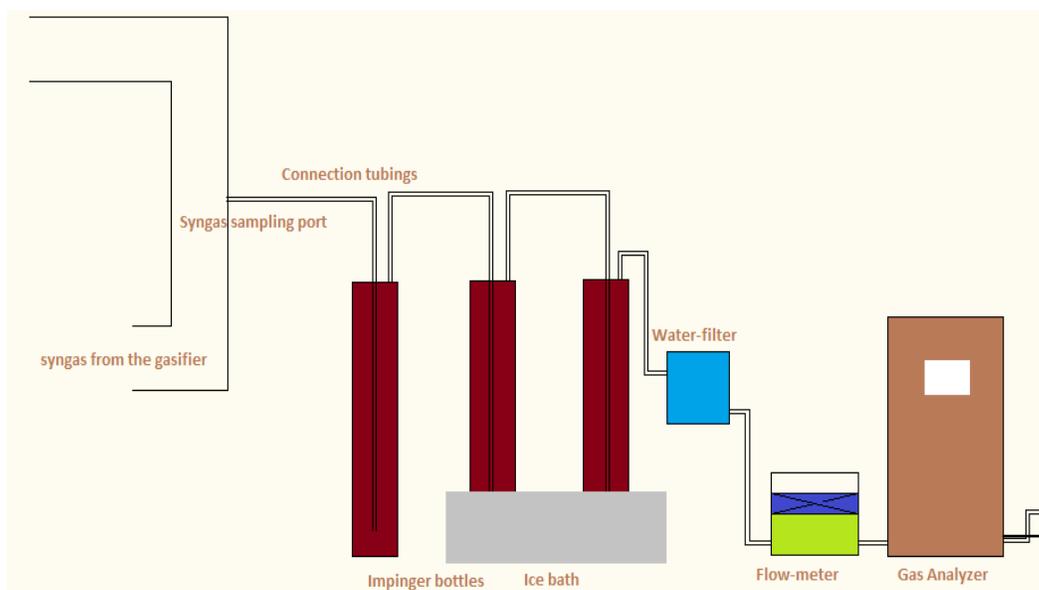
Figure 4.3 Experimental set-up for tar quantification

112

4.4   RESULTS AND DISCUSSIONS

Table 4.3 shows the various tar compounds along with the amount obtained from the test runs from the gasifier. Individual concentration of tar compounds from each run of the experiment is attached in Appendix F (Table F.1 and F.2). The major constituents observed in tar are similar to those observed by other similar studies. Bari et.al [12] reported toluene, ethylbenzene, styrene and p-xylene as a major tar constituents in the syngas obtained from the gasification of feedstocks such as almond shells and oak in a downdraft gasifier using air as a gasifying medium. Similar results was reported by Yamazaki et al. [13] on the experimental investigation of the effect of superficial velocity on tar concentration in downdraft gasifier using fir wood chips as a feedstock. As expected, the majority of tar compounds observed in higher proportions are tertiary condensed tar products due to thermal cracking inside the gasifier. Figure 4.4 shows the fraction of various compounds in a typical gasification run.
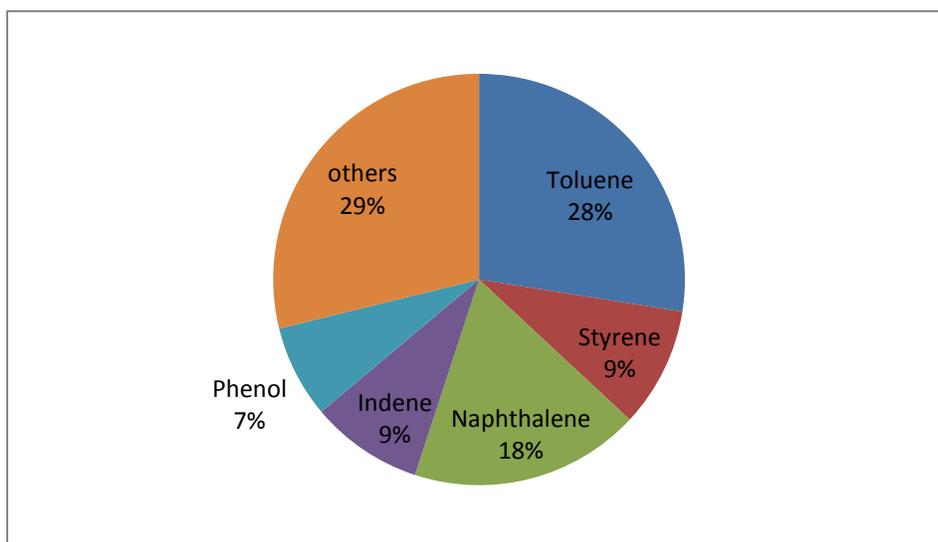
Figure 4.4 Tar compounds in syngas for a typical gasification run

Table 4.3 Quantification of tar constituents in syngas from experiments

Tar Compounds	Concentration (mg/Nm^3)
Toluene	76.8-198.3
o/p-Xylene	9.3-111.6
Naphthalene	62.3-126.1
Phenol	6.9-67.2
Styrene	21.0-65.1
Indene	15.7-55.8
Ethylbenzene	2.5-25.0
Phenol, 3-methyl-	1.3-25.4
Benzofuran	8.5-24.9
Biphenylene	7.1-22.2
Benzofuran, 2-methyl-	0-23.8
Benzene, 1-ethenyl-3-methyl-; (m-Methylstyrene)	6.6-18.8
Naphthalene, 2-methyl-	5.1-16.2
Naphthalene, 1-methyl-	5.9-14.6
Biphenyl	2.6-10.1
Phenol, 2-methyl-	0.5-8.9
Naphthalene, 2-ethenyl-; (2-Vinylnaphthalene)	0.4-6.7
Furfural	0-4.0
Naphthalene, 1,8-dimethyl-	0.6-3.6
Naphthalene, 1,5-dimethyl-	0-3.6
Dibenzofuran	0.4-3.4
.alpha.-Methylstyrene	1.5-3.1
Benzene, 1-ethyl-2-methyl-; (2-Ethyltoluene)	0.6-3.0
Benzene, 1,2,3-trimethyl-	1.4-2.4
Phenol, 2,4-dimethyl-	0-2.4
Acenaphthene	0.3-2.1
Phenol, 3,5-dimethyl-	0-1.9
Naphthalene, 2,3-dimethyl-	0-1.4
Phenol, 3-ethyl-	0-1.3
Phenol, 4-ethyl-	0-1.0
Naphthalene, 1,8-dimethyl-	0-0.8
Total	**340-680**

(Data for each experiment is attached in Appendix F)

Tar concentration in syngas from this stratified downdraft gasifier was found to be 0.34-0.68 g/Nm^3. Dogru et.al [14] and Phuphukrat et.al [15] reported tar concentration of 6.37-8.38 g/Nm^3 for throated and throat-less downdraft gasifier respectively while using sewage sludge as a feedstock. In another study conducted in the similar type of downdraft gasifier used for these current experiments, Wei [16] reported the tar concentration of 0.054 mg/Nm^3 when using wood chips as a feedstock. This might be due to the difference in a bulk density of wood pellets and wood chips. Since wood pellets are more than three times denser than wood chips, temperature at the core of wood pellets might be lower than that in the surface and thus, producing higher tar concentration.

Figure 4.5 shows the effect of biomass flow rate upon tar concentration in stratified downdraft gasifier. Tar concentration shows the increase with increase in biomass flow rate from 17.6 kg/hr and it is observed to be highest at the biomass flow rate of 23.1 kg/hr. After an increase in biomass flow rate from 17.6 kg/hr, tar concentration decreases with increase in biomass flow and again increases after the biomass flow rate reaches to 26.5 kg/hr.
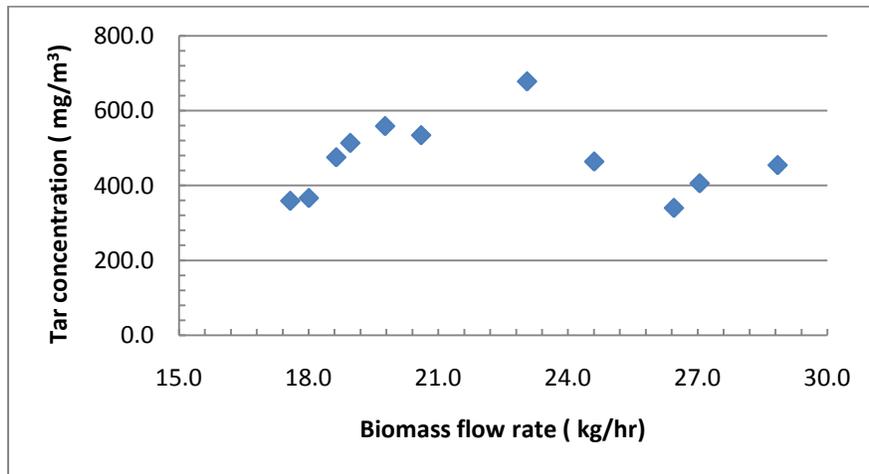
Figure 4.5 Effect of biomass flow rate upon tar concentration

From Figure 4.5, it can be seen that biomass flow rate affects tar concentration in syngas from a downdraft gasifier. However in this case, automatic temperature adjustment done by the gasifier (already described in Chapter 3) injecting secondary air makes it difficult to analyze the above tar concentration pattern due to the sole effect of biomass flow rate.

4.5   CONCLUSION AND FINAL REMARKS

Tar concentration from the stratified downdraft gasifier was mostly condensed tertiary products with significant amount of toluene (76.8-198.3 mg/Nm^3), o/p-xylene (9.3-11.6 mg/Nm^3), naphthalene (62.3-126.1 mg/Nm^3), phenol (6.9-67.2 mg/Nm^3), styrene (21-65.1 mg/Nm^3), and Indene (15.7-55.8 mg/Nm^3). This shows that the primary and secondary tar cracking is very efficient in the current configuration of the downdraft gasifier. Tar concentration was also significantly lower than those reported by other in similar studies in conventional downdraft gasifiers. Also, the tar concentration from the gasification of pellets was found to be significantly higher than those with the gasification wood chips in similar type of gasifier due to higher bulk density. The low tar concentration present in syngas from the downdraft gasifier used for experiment makes it suitable for many synthesis process and power generation with minimal cleaning requirement.

4.6   REFERENCES

[1] T.A. Milne, R.J. Evan, Biomass gasification "tars"; their nature, formation and conversion, in, NREL, Golden, 1998.

[2] R. Warnecke, Gasification of biomass: comparison of fixed bed and fluidized bed gasifier, Biomass and Bioenergy, 18 (2000) 489-497.

[3] L. Devi, K.J. Ptasinski, F.J.J.G. Janssen, A review of the primary measures for tar elimination in biomass gasification processes, Biomass and Bioenergy, 24 (2003) 125-140.

[4] S. Monteiro Nunes, N. Paterson, D.R. Dugwell, R. Kandiyoti, Tar formation and destruction in a simulated downdraft, fixed-bed gasifier: reactor design and initial results, Energy & Fuels, 21 (2007) 3028-3035.

[5] J. Han, H. Kim, The reduction and control technology of tar during biomass gasification/pyrolysis: An overview, Renewable and Sustainable Energy Reviews, 12 (2008) 397-416.

[6] X.T. Li, J.R. Grace, C.J. Lim, A.P. Watkinson, H.P. Chen, J.R. Kim, Biomass gasification in a circulating fluidized bed, Biomass and Bioenergy, 26 (2004) 171-193.

[7] E.G. Baker, M.D. Brown, D.C. Elliott, L.K. Mudge, Characterization and treatment of tars from biomass gasifiers, in: Summer National Meeting, AIChE, Denver CO, 1988, pp. 1–11.

[8] P.M. Lv, Z.H. Xiong, J. Chang, C.Z. Wu, Y. Chen, J.X. Zhu, An experimental study on biomass air-steam gasification in a fluidized bed, Bioresource Technology, 95 (2004) 95-101.

[9] A.A.C.M. Beenackers, Biomass gasification in moving beds, a review of European technologies, Renewable Energy, 16 (1998) 1180-1186.

[10] P. Hasler, T. Nussbaumer, Gas cleaning for IC engine applications from fixed bed biomass gasification, Biomass and Bioenergy, 16 (1999) 385-395.

[11] C. Li, K. Suzuki, Tar property, analysis, reforming mechanism and model for biomass gasification--An overview, Renewable and Sustainable Energy Reviews, 13 (2009) 594-604.

[12] I. De Bari, D. Barisano, M. Cardinale, D. Matera, F. Nanna, D. Viggiano, Air gasification of biomass in a downdraft fixed bed: a comparative study of the inorganic and organic products distribution, Energy & Fuels, 14 (2000) 889-898.

[13] T. Yamazaki, H. Kozu, S. Yamagata, N. Murao, S. Ohta, S. Shiya, T. Ohba, Effect of superficial velocity on tar from downdraft gasification of biomass, Energy & Fuels, 19 (2005) 1186-1191.

[14] M. Dogru, A. Midilli, C.R. Howarth, Gasification of sewage sludge using a throated downdraft gasifier and uncertainty analysis, Fuel Processing Technology, 75 (2002) 55-82.

[15] T. Phuphuakrat, N. Nipattummakul, T. Namioka, S. Kerdsuwan, K. Yoshikawa, Characterization of tar content in the syngas produced in a downdraft type fixed bed gasification system from dried sewage sludge, Fuel, 89 (2010) 2278-2284.

[16] L. Wei, Experimental study on the effects of operational parameters of a downdraft gasifier, in: Department of Agricultural and Biological Engineering, Mississippi State University, Mississippi, 2005.

CHAPTER 5

SUMMARY AND FUTURE WORK

5.1   CONCLUDING REMARKS

This thesis describes a theoretical study on equilibrium modeling, its application in predicting syngas composition depending upon the change in various operating parameters. The linear equations derived to predict syngas composition based on knowledge of ultimate analysis and moisture content of biomass is a significant achievement that can be applied to the gasification process to find the upper limit of syngas production from an existing plant. The effect of moisture content and temperature is also studied through the equilibrium model, which serves as an improvement tool in the field of gasifier design.

Additionally, experimental studies were successfully conducted to find the effect of syngas composition as a function of biomass flow rate in a commercial-scale stratified downdraft gasifier. The results obtained, however are impacted significantly by the automatic factory pre-set condition of the gasifier. Though clear effect of one parameter alone could not be seen from the results, valuable information is provided about the syngas composition and temperature distribution inside the gasifier under variable operating conditions. The final chapter which discusses the tar content in syngas stream from the stratified downdraft gasifier is important

when it comes to the utilization of syngas for power generation and liquid-fuel synthesis from syngas.

5.2   RECOMMENDATIONS FOR FUTURE WORK

Future work can be done to develop a model that can accurately predict the syngas composition depending on the configuration setting of the gasifier. Steady-state modeling of the gasification process can be very useful for this purpose and can be used to predict the syngas composition from the gasifier which cannot be predicted through the equilibrium model. With a steady-state model, the effect of secondary air which is automatically injected inside the gasifier can be more closely examined and validated. The steady state model can be also used to study the effect of external gas addition in greater detail and accuracy.

The experimental results obtained also shows some inconsistencies in temperature profile of the gasifier. The temperature inside the gasifier, currently measured by the thermocouples around the wall of the gasifier might not represent the true gasification temperature. Additional temperature probes can be used to measure the temperature in the center of the reactor which will give the better picture of temperature distribution inside the gasifier. Lack of temperature uniformity has always remained one of the major problems of fixed bed gasification which can be more closely studied with the addition of temperature measurement devices in the center of the reactor.

One of the problems encountered during the operation of current gasifier used was the limitations imposed by the automatic gasifier control system. Thus, effect of single parameter on the downdraft gasification process could not be studied in detail. The modification of this current configuration to accommodate the study of individual parameter or the design and fabrication of

new gasifier with the possibility of manual adjustments of various parameters will be immensely

helpful.

APPENDIX A

MATLAB CODE FOR SYNGAS EQUILIBRIUM MODELING FOR ADIABATIC CONDITIONS

A.1   MAIN FUNCTION FILE

```matlab
%THIS PROGRAM IS SET TO GIVE SYNGAS COMPOSITION IN DRY SYNGAS BASIS. IF FOR
%SOME REASON YOU WANT TO CHANGE, PLEASE MODIFY IN LINE 113 AND 114.
function[final_frac_comp]=eq_comp_model_gen(g_temp,ele_comp)
format short
tol=0.0001;
maxit=100;
%disp('elemental composition should be of the form [C, H, O, N, Ash]');
%ele_comp=input('Enter elemental composition of biomass: ');
%disp('Initial guess is of the form [H2 CO CO2 H2O CH4 3.76N2] ')
xx0=[0.1,0.1,0.1,0.1,0.1,0.1]';
%%%%%%%%%%%%%%%%%%%%%%%%%%%%%%%%%%%%%%%%%%%%%%%%%%%%%%%%%%%%%%%%%%%%%%%%%%%%
% Heat of formation of different compounds at 25 C, kJ/kmol
H_f_H2O_g=-241818;H_f_H2O_l=-285830;H_f_CO2=-393509;H_f_CO=-110525;
H_f_CH4=-74520;H_f_H2=0;H_f_O2=0;H_f_N2=0;
%%%%%%%%%%%%%%%%%%%%%%%%%%%%%%%%%%%%%%%%%%%%%%%%%%%%%%%%%%%%%%%%%%%%%%%%%%%%
%Function for finding sensible heat for various gases
%constants
C_p_H2O=[32.24 0.1923e-2 1.055e-5 -3.595e-9];
C_p_H2=[29.11 -0.1916e-2 0.4003e-5 -0.8704e-9];
C_p_CO=[28.16 0.1675e-2 0.5372e-5 -2.222e-9];
C_p_CO2=[22.26 5.981e-2 -3.501e-5 -7.469e-9];
C_p_CH4=[19.89 5.204e-2 1.269e-5 -11.01e-9];
C_p_N2=[28.90 -0.1571e-2 0.8081e-5 -2.873e-9];
%%%%%%%%%%%%%%%%%%%%%%%%%%%%%%%%%%%%%%%%%%%%%%%%%%%%%%%%%%%%%%%%%%%%%%%%%%%%
%finding general equations for calculating k1 and k2
%%%%%%%%%%%%%%%%%%%%%%%%%%%%%%%%%%%%%%%%%%%%%%%%%%%%%%%%%%%%%%%%%%%%%%%%%%%%
G_CO=[3.376 0.557e-3 0 -0.031e5 -110525 -137169];
G_CO2=[5.457 1.045e-3 0 -1.157e5 -393509 -394359];
G_H2O=[3.470 1.450e-3 0 0.121e5 -241818 -228572];
G_H2=[3.249 0.422e-3 0 0.083e5 0 0];
G_C=[1.771 0.771e-3 0 -0.867e5 0 0];
G_CH4=[1.702 9.081e-3 -2.164e-6 0 -74520 -50460];
delta_ws_final=[];
delta_meth_final=[];
for iii=1:6
    delta_ws=G_H2(iii)+G_CO2(iii)-G_CO(iii)-G_H2O(iii);
    delta_meth=G_CH4(iii)-G_C(iii)-2*G_H2(iii);
    delta_ws_final=[delta_ws_final delta_ws];
```

122

```matlab
        delta_meth_final=[delta_meth_final delta_meth];
    end
T_0=298;
k1=exp(-((delta_meth_final(6)-
delta_meth_final(5))/(8.314*298.15)+(delta_meth_final(5)/(8.314*g_temp))...
    +(int_eq_sp2(delta_meth_final,g_temp)/g_temp)-
int_eq_sp1(delta_meth_final,g_temp)));
k2=exp(-((delta_ws_final(6)-
delta_ws_final(5))/(8.314*298.15)+(delta_ws_final(5)/(8.314*g_temp))...
    +(int_eq_sp2(delta_ws_final,g_temp)/g_temp)-
int_eq_sp1(delta_ws_final,g_temp)));
%%%%%%%%%%%%%%%%%%%%%%%%%%%%Continued below%%%%%%%%%%%%%%%%%%%%%%%%%%%%%%%%

%%%%%%%%%%%%%%%%%%%%%%%%%%%%%%%%%%%%%%%%%%%%%%%%%%%%%%%%%%%%%%%%%%%%%%%%%%%%%
%function for calculating int_eq_sp
    function int_for_gibbs_difff1= int_eq_sp1(difff,g_temp)
        tau=g_temp/298.15;
        int_for_gibbs_difff1=difff(1).*log(tau)+((difff(2).*T_0+...
            ((difff(3)*T_0^2+(difff(4)/(tau^2.*T_0^2)))*((tau+1)/2)))*(tau-
1));
    end
    function int_for_gibbs_difff2= int_eq_sp2(var_sp,g_temp)
        tau=g_temp/298.15;
        int_for_gibbs_difff2=var_sp(1).*T_0*(tau-1)+...
            var_sp(2)*0.5*T_0^2*(tau^2-1)+var_sp(3)*T_0^3*(tau^3-1)/3+...
            var_sp(4)*(tau-1)/(tau*T_0);
    end
%%%%%%%%%%%%%%%%%%%%%%%%%%%%%%%%%%%%%%%%%%%%%%%%%%%%%%%%%%%%%%%%%%%%%%%%%%%%%
%%%%%%%%%%%%%%%%%%%%%%%%%%%%%%%%%%%%%%%%%%%%%%%%%%%%%%%%%%%%%%%%%%%%%%%%%%%%%
%%%%finding lambda and gamma for below calculation%%%%%%%%%%%%%%%%%%%%%%%%%%
norm_1_C=ele_comp(1)/(12);
norm_1_H=ele_comp(2)/(1.008);
norm_1_O=ele_comp(3)/(16);
norm_1_N=ele_comp(4)/(14.007);
lambda=norm_1_H/norm_1_C;
gamma=norm_1_O/norm_1_C;
beta=norm_1_N/norm_1_C;
%%%%%%%%%%%%%%%%%%%%%%%%%%%%%%%%%%%%%%%%%%%%%%%%%%%%%%%%%%%%%%%%%%%%%%%%%%%%%
x0=xx0;
iter=1;
iter_m=1;
sol_final=[];
%w=M_fs*Moisture_Content/(18*(1-Moisture_Content));
w=linspace(0,1,15);
%w=0;
Moisture_Content=[];
M_fs=12+lambda*1.008+gamma*16;
for N=1:length(w)
    Moisture_Content=[Moisture_Content 18*100*w(N)/(M_fs+18*w(N))];
end
Moisture_Content
%%%%%%%%%%%%%%%%%%%%%%%%%%%%%%%%%%%%%%%%%%%%%%%%%%%%%%%%%%%%%%%%%%%%%%%%%%%%%
%Main Loop for solving the equations of interests
%%%%%%%%%%%%%%%%%%%%%%%%%%%%%%%%%%%%%%%%%%%%%%%%%%%%%%%%%%%%%%%%%%%%%%%%%%%%%
for iter_m=1:length(w)
    while(iter<=maxit)
        y=-df1(x0)\f1(x0);
```

```matlab
        xn=x0+y;
        err=max(abs(xn-x0));
        if(err<=tol)
            x=xn;
        else
            x0=xn;
        end
        iter=iter+1;
    end
    iter=1;
    sol_temp=x;
%%%%%%%%%%%%%%%%%Continued below%%%%%%%%%%%%%%%%%%%%%%%%%%%%%%%%%%%%%%%


    sol_final=[sol_final sol_temp];
    iter_m=iter_m+1;
end
%%%%%%%%%%%%%%%%%%%%%%%%%%%%%%%%%%%%%%%%%%%%%%%%%%%%%%%%%%%%%%%%%%%%%%%%%
%%%%%%%%%%%%%%%%%%%%%%%%%%%%%%%%%%%%%%%%%%%%%%%%%%%%%%%%%%%%%%%%%%%%%%%%%
%Multiplying m with 3.76 to get correct N2 mols
p=length(w);
frac_N2=[];
for l=1:p
    frac_N2=[frac_N2 sol_final(6,l)*3.76];
end
final_comp=[sol_final(1:5,1:p);frac_N2]
%%%%%%%%%%%%%%%%%%%%%%%%%%%%%%%%%%%%%%%%%%%%%%%%%%%%%%%%%%%%%%%%%%%%%%%%%
%fin_rep=input('Do you want to find syngas composition in dry syngas
basis(y/n): ','s');
fin_rep='y';
if fin_rep=='n';

%%%%%%%%%%%%%%%%%%%%%%%%%%%%%%%%%%%%%%%%%%%%%%%%%%%%%%%%%%%%%%%%%%%%%%%%%
    %finding total amount of product gas for each moisture content
    total_frac_m=[];
    for n=1:p
        total_frac_m=[total_frac_m sum(final_comp(1:6,n))];
    end
    total_frac_m; %sum of all product gases
else

%%%%%%%%%%%%%%%%%%%%%%%%%%%%%%%%%%%%%%%%%%%%%%%%%%%%%%%%%%%%%%%%%%%%%%%%%
    %finding total amount of product gas on dry basis for each moisture
    %content
    dry_final_comp=final_comp;
    dry_final_comp(4,:)=[];
    total_frac_m=[];
    for n=1:p
        total_frac_m=[total_frac_m sum(dry_final_comp(1:5,n))];
    end
    total_frac_m;
    final_comp=dry_final_comp;
end
%%%%%%%%%%%%%%%%%%%%%%%%%%%%%%%%%%%%%%%%%%%%%%%%%%%%%%%%%%%%%%%%%%%%%%%%%
%expressing all the components in molar fraction or volumetric fraction
final_frac_comp=[];
for MM=1:length(total_frac_m)
```

```matlab
        final_frac_m=[];
        if fin_rep=='y'
            l_in=length(xx0)-1;
        else
            l_in=length(xx0);
        end
        for NN=1:l_in
            final_frac_m=[final_frac_m;final_comp(NN,MM)/total_frac_m(MM)];
        end
        final_frac_comp=[final_frac_comp final_frac_m];
end
%%%%%%%%%%%%%%%%%%Continued below%%%%%%%%%%%%%%%%%%%%%%%%%%%%%%%%%%%%%%%%%%%


%%%%%%%%%%%%%%%%%%%%%%%%%%%%%%%%%%%%%%%%%%%%%%%%%%%%%%%%%%%%%%%%%%%%%%%%%%%%%
function f=f1(X)
x_1=X(1); x_2=X(2); x_3=X(3);x_4=X(4);x_5=X(5);m=X(6);
val_1=x_2+x_3+x_5-1;
val_2=x_1+x_4+2*x_5-w(iter_m)-(lambda/2);
val_3=x_2+2*x_3+x_4-2*m-gamma-w(iter_m);
val_4=-k1*x_1^2+(x_5*(x_1+x_2+x_3+x_4+x_5+3.76*m));
val_5=x_2*x_4*k2-x_1*x_3;
val_6=x_1*t_en_gas(H_f_H2, C_p_H2, g_temp)+...
    x_2*t_en_gas(H_f_CO, C_p_CO, g_temp)+...
    x_3*t_en_gas(H_f_CO2, C_p_CO2,g_temp)+...
    x_4*t_en_gas(H_f_H2O_g, C_p_H2O, g_temp)+...
    x_5*t_en_gas(H_f_CH4, C_p_CH4, g_temp)+...
    3.76*m*t_en_gas(H_f_N2, C_p_N2, g_temp)-...
    heat_bio(ele_comp)-w(iter_m)*(H_f_H2O_l+1000);
f=[val_1; val_2;val_3;val_4;val_5;val_6];
end
%%%%%%%%%%%%%%%%%%%%%%%%%%%%%%%%%%%%%%%%%%%%%%%%%%%%%%%%%%%%%%%%%%%%%%%%%%%%%
function df=df1(X);
x_1=X(1); x_2=X(2); x_3=X(3);x_4=X(4);x_5=X(5);m=X(6);
df=[0,1,1,0,1,0;1 0 0 1 2 0; 0 1 2 1 0 -2;-
2*x_1*k1+x_5,x_5,x_5,x_5,2*x_5+(x_1+x_2+x_3+x_4+3.76*m),3.76*x_5; -x_3
k2*x_4...
    -x_1 k2*x_2 0 0; t_en_gas(H_f_H2, C_p_H2, g_temp)...
    t_en_gas(H_f_CO, C_p_CO, g_temp) t_en_gas(H_f_CO2, C_p_CO2, g_temp)...
    t_en_gas(H_f_H2O_g, C_p_H2O, g_temp) t_en_gas(H_f_CH4, C_p_CH4,
g_temp)...
    3.76*t_en_gas(H_f_N2, C_p_N2, g_temp)];
end
%%%%%%%%%%%%%%%%%%%%%%%%%%%%%%%%%%%%%%%%%%%%%%%%%%%%%%%%%%%%%%%%%%%%%%%%%%%%%
    function dh_comp=t_en_gas(H_for, sp_heat, temp)
    heat_coeff=sp_heat;
    dh_comp=H_for+quad(@sensible,298,temp);
        function sens_heat=sensible(t)

sens_heat=heat_coeff(1)+heat_coeff(2).*t+heat_coeff(3).*t.^2+heat_coeff(4).*t
.^3;
        end
    end
%%%%%%%%%%%%%%%%%%%%%%%%%%%%%%%%%%%%%%%%%%%%%%%%%%%%%%%%%%%%%%%%%%%%%%%%%%%%%
%Standard heat of formation of various biomass
%H_f_XX is the heat of formation of XX compound, units in kJ/kmol
%LHV is lower heating value of biomass, kJ/kg
```

```matlab
%LHV_mol is the lower heating value of biomass, kJ/kmol
%%%%%%%%%%%%%%%%%%%%%%%%%%%%%%%%%%%%%%%%%%%%%%%%%%%%%%%%%%%%%%%%%%%%%%%%%
%%%%%%%%%%%%%%%%%%%%%%%%%%%%%%%%%%%%%%%%%%%%%%%%%%%%%%%%%%%%%%%%%%%%%%%%%
    function H_f_bio= heat_bio(comp)
    LHV=4.187*(81*comp(1)+300*comp(2)-26*comp(3)-54*comp(2));
    LHV_mol=LHV*(12+lambda*1.008+gamma*16);
    H_f_bio=(lambda/2)*H_f_H2O_l+H_f_CO2+LHV_mol;
    end
%%%%%%%%%%%%%%%%%%%%%%%%%%%%%%%%%%%%%%%%%%%%%%%%%%%%%%%%%%%%%%%%%%%%%%%%%
end
```

A.2   FUNCTION FILE FOR FINDING EQUILIBRIUM CONSTANTS

```matlab
%Program for finding equilibrium constant for various reaction
%Rxn-1: CO+H_2O=CO_2+H_2
%Rxn-2: C+2H_2=CH4
function[k]=Delta_G(T)
%%%%%%%%%%%%%%%%%%%%%%%%%%%%%%%%%%%%%%%%%%%%%%%%%%%%%%%%%%%%%%%%%%%%%%%%%
%finding general equations for calculating k1 and k2
%%%%%%%%%%%%%%%%%%%%%%%%%%%%%%%%%%%%%%%%%%%%%%%%%%%%%%%%%%%%%%%%%%%%%%%%%
G_CO=[3.376 0.557e-3 0 -0.031e5 -110525 -137169];
G_CO2=[5.457 1.045e-3 0 -1.157e5 -393509 -394359];
G_H2O=[3.470 1.450e-3 0 0.121e5 -241818 -228572];
G_H2=[3.249 0.422e-3 0 0.083e5 0 0];
G_C=[1.771 0.771e-3 0 -0.867e5 0 0];
G_CH4=[1.702 9.081e-3 -2.164e-6 0 -74520 -50460];
delta_ws_final=[];
delta_meth_final=[];
for iii=1:6
    delta_ws=G_H2(iii)+G_CO2(iii)-G_CO(iii)-G_H2O(iii);
    delta_meth=G_CH4(iii)-G_C(iii)-2*G_H2(iii);
    delta_ws_final=[delta_ws_final delta_ws];
    delta_meth_final=[delta_meth_final delta_meth];
end
T_0=298;
k1=exp(-((delta_meth_final(6)-
delta_meth_final(5))/(8.314*298.15)+(delta_meth_final(5)/(8.314*T))...
    +(int_eq_sp2(delta_meth_final,T)/T)-int_eq_sp1(delta_meth_final,T)))
k2=exp(-((delta_ws_final(6)-
delta_ws_final(5))/(8.314*298.15)+(delta_ws_final(5)/(8.314*T))...
    +(int_eq_sp2(delta_ws_final,T)/T)-int_eq_sp1(delta_ws_final,T)))
k=[k1,k2];
%%%%%%%%%%%%%%%%%%%%%%%%%%%%%%%%%%%%%%%%%%%%%%%%%%%%%%%%%%%%%%%%%%%%%%%%%
%function for calculating int_eq_sp
    function int_for_gibbs_difff1= int_eq_sp1(difff,T)
        tau=T/298.15;
        int_for_gibbs_difff1=difff(1).*log(tau)+((difff(2).*T_0+...
            ((difff(3)*T_0^2+(difff(4)/(tau^2.*T_0^2)))*((tau+1)/2)))*(tau-
1));
    end
    function int_for_gibbs_difff2= int_eq_sp2(var_sp,T)
        tau=T/298.15;
        int_for_gibbs_difff2=var_sp(1).*T_0*(tau-1)+...
```

126

```
                var_sp(2)*0.5*T_0^2*(tau^2-1)+var_sp(3)*T_0^3*(tau^3-1)/3+...
                var_sp(4)*(tau-1)/(tau*T_0);
        end
end
%%%%%%%%%%%%%%%%%%%%%%%%%%%%%%%%%%%%%%%%%%%%%%%%%%%%%%%%%%%%%%%%%%%%%%%%%%%%%%%%
%%%%%%%%%%%%%%%%%%%%%%%%%%%%%%%%%%%%%%%%%%%%%%%%%%%%%%%%%%%%%%%%%%%%%%%%%%%%%%%%
```

A.3   FUNCTION FILE FOR FINDING THE ENTHALPY CHANGE IN GASES

```
%calculates the total enthalpy change with reference to 298 K of different
%chemical elements in kJ/kg
%%%%%%%%%%%%%%%%%%%%%%%%%%%%%%%%%%%%%%%%%%%%%%%%%%%%%%%%%%%%%%%%%%%%%%%%%%%%
function H_Tot=En_Ch(T,S)
switch (S)
    case('CO2')
        M_Wt=44.0095;HoF=-393.51;
        C_p=[22.26 5.981e-2 -3.501e-5 -7.469e-9];
    case ('CO')
        M_Wt=28.0101; HoF=-110.53;
        C_p=[28.16 0.1675e-2 0.5372e-5 -2.222e-9];
    case ('CH4')
        M_Wt=16.0425; HoF=-74.87;
        C_p=[19.89 5.204e-2 1.269e-5 -11.01e-9];
    case ('H2O')
        M_Wt=18.0153; HoF=-241.83;
        C_p=[32.24 0.1923e-2 1.055e-5 -3.595e-9];
    case ('N2')
        M_Wt=28.01348;
        C_p=[28.90 -0.1571e-2 0.8081e-5 -2.873e-9];
    case ('O2')
        M_Wt=31.9988;
end
H_Tot=(1000/M_Wt)*HoF+quad(@sensible,298,T);
    function sens_heat=sensible(T)
    sens_heat=C_p(1)+C_p(2).*T+C_p(3).*T.^2+C_p(4).*T.^3;
    end
end
%EOF, En_Ch.m
```

APPENDIX B

FUNCTION FILE FOR FINDING SYNGAS COMPOSITION AT CONSTANT

EQUIVALENCE RATIO

The functions used for calculating the enthalpy change and equilibrium constants are same as that for adiabatic condition which is already mentioned in appendix A. However, the main function file is different which is as follows.

```matlab
%THIS PROGRAM IS SET TO GIVE SYNGAS COMPOSITION IN DRY SYNGAS BASIS. IF FOR
%SOME REASON YOU WANT TO CHANGE, PLEASE MODIFY IN LINE 113 AND 114.
function[final_comp]=eq_model_const(g_temp,ele_comp,m)
format short
tol=0.00001;
maxit=100;
%disp('elemental composition should be of the form [C, H, O, N, Ash]');
%ele_comp=input('Enter elemental composition of biomass: ');
%disp('Initial guess is of the form [H2 CO CO2 H2O CH4] ')
xx0=[0.1,0.1,0.1,0.1,0.1]';
%%%%%%%%%%%%%%%%%%%%%%%%%%%%%%%%%%%%%%%%%%%%%%%%%%%%%%%%%%%%%%%%%%%%%%%%%%%%
% Heat of formation of different compounds at 25 C, kJ/kmol
H_f_H2O_g=-241818;H_f_H2O_l=-285830;H_f_CO2=-393509;H_f_CO=-110525;
H_f_CH4=-74520;H_f_H2=0;H_f_O2=0;H_f_N2=0;
%%%%%%%%%%%%%%%%%%%%%%%%%%%%%%%%%%%%%%%%%%%%%%%%%%%%%%%%%%%%%%%%%%%%%%%%%%%%
%Function for finding sensible heat for various gases
%constants
C_p_H2O=[32.24 0.1923e-2 1.055e-5 -3.595e-9];
C_p_H2=[29.11 -0.1916e-2 0.4003e-5 -0.8704e-9];
C_p_CO=[28.16 0.1675e-2 0.5372e-5 -2.222e-9];
C_p_CO2=[22.26 5.981e-2 -3.501e-5 -7.469e-9];
C_p_CH4=[19.89 5.204e-2 1.269e-5 -11.01e-9];
C_p_N2=[28.90 -0.1571e-2 0.8081e-5 -2.873e-9];
%%%%%%%%%%%%%%%%%%%%%%%%%%%%%%%%%%%%%%%%%%%%%%%%%%%%%%%%%%%%%%%%%%%%%%%%%%%%
%finding general equations for calculating k1 and k2
%%%%%%%%%%%%%%%%%%%%%%%%%%%%%%%%%%%%%%%%%%%%%%%%%%%%%%%%%%%%%%%%%%%%%%%%%%%%
G_CO=[3.376 0.557e-3 0 -0.031e5 -110525 -137169];
G_CO2=[5.457 1.045e-3 0 -1.157e5 -393509 -394359];
G_H2O=[3.470 1.450e-3 0 0.121e5 -241818 -228572];
G_H2=[3.249 0.422e-3 0 0.083e5 0 0];
G_C=[1.771 0.771e-3 0 -0.867e5 0 0];
G_CH4=[1.702 9.081e-3 -2.164e-6 0 -74520 -50460];
delta_ws_final=[];
```

```matlab
delta_meth_final=[];
for iii=1:6
    delta_ws=G_H2(iii)+G_CO2(iii)-G_CO(iii)-G_H2O(iii);
    delta_meth=G_CH4(iii)-G_C(iii)-2*G_H2(iii);
    delta_ws_final=[delta_ws_final delta_ws];
    delta_meth_final=[delta_meth_final delta_meth];
end
T_0=298.15;


%%%%%%%%%%%%%%%%%%%%%%%Continued below%%%%%%%%%%%%%%%%%%%%%%%%%%%%%%%%%%%
%%%%%%%%%%%%%%%%%%%%%%%%%%%%%%%%%%%%%%%%%%%%%%%%%%%%%%%%%%%%%%%%%%%%%%%%%%%
k1=exp(-((delta_meth_final(6)-
delta_meth_final(5))/(8.314*298.15)+(delta_meth_final(5)/(8.314*g_temp))...
    +(int_eq_sp2(delta_meth_final,g_temp)/g_temp)-
int_eq_sp1(delta_meth_final,g_temp)));
k2=exp(-((delta_ws_final(6)-
delta_ws_final(5))/(8.314*298.15)+(delta_ws_final(5)/(8.314*g_temp))...
    +(int_eq_sp2(delta_ws_final,g_temp)/g_temp)-
int_eq_sp1(delta_ws_final,g_temp)));
%%%%%%%%%%%%%%%%%%%%%%%%%%%%%%%%%%%%%%%%%%%%%%%%%%%%%%%%%%%%%%%%%%%%%%%%%%%
%function for calculating int_eq_sp
    function int_for_gibbs_difff1= int_eq_sp1(difff,g_temp)
        tau=g_temp/298.15;
        int_for_gibbs_difff1=difff(1).*log(tau)+((difff(2).*T_0+...
            ((difff(3)*T_0^2+(difff(4)/(tau^2.*T_0^2)))*((tau+1)/2)))*(tau-
1));
    end
    function int_for_gibbs_difff2= int_eq_sp2(var_sp,g_temp)
        tau=g_temp/298.15;
        int_for_gibbs_difff2=var_sp(1).*T_0*(tau-1)+...
            var_sp(2)*0.5*T_0^2*(tau^2-1)+var_sp(3)*T_0^3*(tau^3-1)/3+...
            var_sp(4)*(tau-1)/(tau*T_0);
    end

%k1=9.72e-02;k2=1.4561;
%%%%%%%%%%%%%%%%%%%%%%%%%%%%%%%%%%%%%%%%%%%%%%%%%%%%%%%%%%%%%%%%%%%%%%%%%%%
%%%%%%%%%%%%%%%%%%%%%%%%%%%%%%%%%%%%%%%%%%%%%%%%%%%%%%%%%%%%%%%%%%%%%%%%%%%
%%%%finding lambda and gamma for below calculation%%%%%%%%%%%%%%%%%%%%%%%%
norm_1_C=ele_comp(1)/(12);
norm_1_H=ele_comp(2)/(1.008);
norm_1_O=ele_comp(3)/(16);
norm_1_N=ele_comp(4)/(14.007);
lambda=norm_1_H/norm_1_C;
gamma=norm_1_O/norm_1_C;
beta=norm_1_N/norm_1_C;
%%%%%%%%%%%%%%%%%%%%%%%%%%%%%%%%%%%%%%%%%%%%%%%%%%%%%%%%%%%%%%%%%%%%%%%%%%%
x0=xx0;
iter=1;
iter_m=1;
sol_final=[];
w=0;
Moisture_Content=[];
for N=1:length(w)
    Moisture_Content=[Moisture_Content 18*100*w(N)/(24+18*w(N))];
end
Moisture_Content;
```

```matlab
%%%%%%%%%%%%%%%%%%%%%%%%%%%%%%%%%%%%%%%%%%%%%%%%%%%%%%%%%%%%%%%%%%%%%%%%%%%
%Main Loop for solving the equations of interests
%%%%%%%%%%%%%%%%%%%%%%%%%%%%%%%%%%%%%%%%%%%%%%%%%%%%%%%%%%%%%%%%%%%%%%%%%%%
for iter_m=1:length(w)
    while(iter<=maxit)
        y=-df1(x0)\f1(x0);
        xn=x0+y;
        err=max(abs(xn-x0));
        if(err<=tol)
            x=xn;
        else
%%%%%%%%%%%%%%%%%%%%%%%%%Continued below%%%%%%%%%%%%%%%%%%%%%%%%%%%%%%%%%%%

            x0=xn;
        end
        iter=iter+1;
    end
    iter=1;
    sol_temp=x;
    sol_final=[sol_final sol_temp];
    iter_m=iter_m+1;
end
%%%%%%%%%%%%%%%%%%%%%%%%%%%%%%%%%%%%%%%%%%%%%%%%%%%%%%%%%%%%%%%%%%%%%%%%%%%
%%%%%%%%%%%%%%%%%%%%%%%%%%%%%%%%%%%%%%%%%%%%%%%%%%%%%%%%%%%%%%%%%%%%%%%%%%%
%Multiplying m with 3.76 to get correct N2 mols
p=length(w);
frac_N2=[];
for l=1:p
    frac_N2=[frac_N2 m*3.76];
end
final_comp=[sol_final(1:5,1:p);frac_N2];
%%%%%%%%%%%%%%%%%%%%%%%%%%%%%%%%%%%%%%%%%%%%%%%%%%%%%%%%%%%%%%%%%%%%%%%%%%%
%fin_rep=input('Do you want to find syngas composition in dry syngas
basis(y/n): ','s');
fin_rep='n';
if fin_rep=='n';

%%%%%%%%%%%%%%%%%%%%%%%%%%%%%%%%%%%%%%%%%%%%%%%%%%%%%%%%%%%%%%%%%%%%%%%%%%%
    %finding total amount of product gas for each moisture content
    total_frac_m=[];
    for n=1:p
        total_frac_m=[total_frac_m sum(final_comp(1:6,n))];
    end
    total_frac_m; %sum of all product gases
else

%%%%%%%%%%%%%%%%%%%%%%%%%%%%%%%%%%%%%%%%%%%%%%%%%%%%%%%%%%%%%%%%%%%%%%%%%%%
    %finding total amount of product gas on dry basis for each moisture
    %content
    dry_final_comp=final_comp;
    dry_final_comp(4,:)=[];
    total_frac_m=[];
    for n=1:p
        total_frac_m=[total_frac_m sum(dry_final_comp(1:5,n))];
    end
    total_frac_m;
    final_comp=dry_final_comp;
```
130

```matlab
end
%%%%%%%%%%%%%%%%%%%%%%%%%%%%%%%%%%%%%%%%%%%%%%%%%%%%%%%%%%%%%%%%%%%%%%%%%%%%%%
%expressing all the components in molar fraction or volumetric fraction
final_frac_comp=[];
for MM=1:length(total_frac_m)
    final_frac_m=[];
    if fin_rep=='y'
        l_in=length(xx0);
    else
        l_in=length(xx0)+1;
    end
%%%%%%%%%%%%%%%%%%%%%%%%%Continued below%%%%%%%%%%%%%%%%%%%%%%%%%%%%%%%%%%%%%

    for NN=1:l_in
        final_frac_m=[final_frac_m;final_comp(NN,MM)/total_frac_m(MM)];
    end
    final_frac_comp=[final_frac_comp final_frac_m];
end
%%%%%%%%%%%%%%%%%%%%%%%%%%%%%%%%%%%%%%%%%%%%%%%%%%%%%%%%%%%%%%%%%%%%%%%%%%%%%%
%%%%%%%%%%%%%%%%%%%%%%%%%%%%%%%%%%%%%%%%%%%%%%%%%%%%%%%%%%%%%%%%%%%%%%%%%%%%%%
function f=f1(X)
x_1=X(1); x_2=X(2); x_3=X(3);x_4=X(4);x_5=X(5);
val_1=x_2+x_3+x_5-1;
val_2=x_1+x_4+2*x_5-w(iter_m)-(lambda/2);
val_3=x_2+2*x_3+x_4-2*m-gamma-w(iter_m);
val_4=-k1*x_1^2+(x_5*(x_1+x_2+x_3+x_4+x_5+3.76*m));
val_5=x_2*x_4*k2-x_1*x_3;
f=[val_1; val_2;val_3;val_4;val_5];
end
%%%%%%%%%%%%%%%%%%%%%%%%%%%%%%%%%%%%%%%%%%%%%%%%%%%%%%%%%%%%%%%%%%%%%%%%%%%%%%
function df=df1(X)
x_1=X(1); x_2=X(2); x_3=X(3);x_4=X(4);x_5=X(5);
df=[0,1,1,0,1;1 0 0 1 2; 0 1 2 1 0;-
2*x_1*k1+x_5,x_5,x_5,x_5,2*x_5+(x_1+x_2+x_3+x_4+3.76*m); -x_3 k2*x_4...
    -x_1 k2*x_2 0];
end
end
```

APPENDIX C

SYNGAS COMPOSITION FROM MATLAB SIMULATION USED FOR GENERAL

FORMULA DERIVATION

Table C.1 Syngas composition from MATLAB model

Moisture-free elemental composition					Dry syngas composition			
C	H	O	N	Ash	CO	CO_2	CH_4	H_2
50.0	6.0	44.0	0.0	0.0	20.3	7.1	0.2	20.3
38.5	5.7	39.8	0.5	15.5	15.3	12.6	0.1	15.3
43.4	5.8	44.3	0.3	6.0	18.4	10.4	0.1	18.4
47.6	6.0	32.9	1.2	12.0	15.4	9.1	0.1	15.4
47.2	6.0	38.2	2.7	5.3	18.1	8.3	0.1	18.1
44.9	5.5	41.8	0.4	7.0	16.9	10.0	0.1	16.9
38.8	4.8	35.5	0.5	20.3	11.9	13.2	0.1	11.9
38.2	5.2	36.3	0.9	18.7	13.1	13.0	0.1	13.1
46.7	5.8	37.4	0.8	9.0	16.5	9.3	0.1	16.5
48.6	5.9	42.8	0.2	2.4	19.1	8.0	0.2	19.1
49.9	5.9	41.8	0.6	1.7	19.3	7.3	0.2	19.3
50.2	6.1	40.4	0.6	2.7	19.1	7.2	0.2	19.1
49.3	6.0	40.6	0.8	3.3	18.8	7.6	0.2	18.8
47.5	6.0	39.2	1.1	6.1	17.9	8.5	0.1	17.9
50.2	6.3	41.2	0.7	1.4	20.1	7.0	0.2	20.1
52.8	6.7	38.3	0.5	1.7	20.2	6.0	0.2	20.2
46.3	5.4	34.5	0.6	13.1	14.2	10.0	0.1	14.2
41.5	4.8	31.9	0.9	20.4	11.4	12.2	0.1	11.4
51.2	6.0	42.1	0.1	0.4	19.7	6.7	0.2	19.7
48.0	6.6	36.8	0.1	8.3	18.0	8.5	0.1	18.0
39.3	5.8	27.2	0.8	26.1	11.1	12.4	0.1	11.1
47.3	5.8	45.0	0.8	1.1	19.9	8.3	0.2	19.9
48.6	6.4	46.3	0.0	0.0	22.1	7.4	0.2	22.1
35.1	7.6	57.0	0.0	0.0	27.0	13.0	0.3	27.0
27.1	4.3	26.3	3.1	38.5	7.2	16.0	0.0	7.2
46.3	5.5	42.6	0.8	3.4	17.8	9.2	0.1	17.8
46.3	5.6	47.3	0.1	0.4	19.9	9.0	0.2	19.9
47.9	5.5	41.0	0.5	4.8	17.4	8.6	0.1	17.4
30.8	1.0	21.5	1.1	44.2	1.7	20.0	0.0	1.7
37.8	6.2	53.6	0.7	1.5	22.8	12.8	0.2	22.8

Continued in the next page…

Moisture-free elemental composition					Dry syngas composition			
C	H	O	N	Ash	CO	CO_2	CH_4	H_2
49.5	6.0	40.6	0.5	3.5	18.7	7.6	0.2	18.7
49.7	5.8	41.5	0.7	2.3	18.9	7.4	0.2	18.9
50.6	6.1	41.6	0.5	1.3	19.7	6.9	0.2	19.7
50.0	6.2	41.1	0.5	2.2	19.7	7.2	0.2	19.7
49.9	5.7	42.3	0.1	2.1	18.7	7.5	0.2	18.7
49.9	5.9	43.5	0.1	0.7	19.7	7.3	0.2	19.7
49.5	6.3	42.0	0.5	1.8	20.1	7.3	0.2	20.1
51.7	4.5	35.1	0.2	8.5	13.4	8.0	0.1	13.4
49.4	5.8	42.3	0.2	2.4	18.8	7.7	0.2	18.8
49.9	6.0	41.2	0.2	2.7	19.1	7.4	0.2	19.1
50.0	6.2	39.6	0.2	4.1	18.7	7.5	0.2	18.7
50.7	6.4	41.8	0.3	1.0	20.4	6.8	0.2	20.4
49.5	6.2	41.7	0.2	2.4	19.7	7.5	0.2	19.7
49.7	6.2	43.8	0.3	0.1	20.6	7.1	0.2	20.6
49.8	5.7	39.8	0.3	4.4	17.7	7.8	0.1	17.7
49.4	6.1	43.0	0.2	1.3	20.0	7.4	0.2	20.0
48.4	6.0	41.6	0.2	3.8	18.9	8.1	0.2	18.9
49.0	5.5	39.2	0.2	6.2	16.7	8.4	0.1	16.7
48.5	5.8	41.2	0.2	4.3	18.3	8.2	0.1	18.3
48.2	5.7	41.6	0.2	4.3	18.0	8.4	0.1	18.0
46.0	5.9	41.4	0.9	5.9	18.1	9.2	0.1	18.1
47.0	5.5	41.1	0.7	5.7	17.2	9.0	0.1	17.2
46.5	5.8	40.4	0.6	6.7	17.6	9.1	0.1	17.6
46.0	5.4	39.2	0.6	8.7	16.1	9.7	0.1	16.1
46.7	5.5	40.6	0.6	6.5	17.0	9.2	0.1	17.0
44.8	5.5	37.7	0.7	11.3	15.5	10.2	0.1	15.5
47.0	5.7	40.7	0.6	6.0	17.6	8.9	0.1	17.6
46.5	6.1	40.1	0.7	6.5	18.3	8.9	0.1	18.3
46.3	5.6	41.0	0.7	6.5	17.2	9.3	0.1	17.2
47.1	5.8	37.5	0.7	8.9	16.5	9.1	0.1	16.5
48.0	5.8	37.0	0.7	8.5	16.6	8.7	0.1	16.6
46.8	5.5	38.4	0.7	8.7	16.1	9.4	0.1	16.1
47.0	5.7	41.4	0.7	5.3	17.8	8.9	0.1	17.8
48.8	5.5	42.3	1.0	2.4	18.4	7.8	0.2	18.4
49.4	5.2	39.5	1.1	4.8	16.6	8.0	0.1	16.6
49.4	5.8	39.6	1.3	4.0	18.2	7.6	0.1	18.2
46.5	5.6	41.9	1.2	4.9	17.9	9.0	0.1	17.9
49.5	5.6	37.4	1.1	6.5	16.7	8.0	0.1	16.7
49.3	5.9	42.8	0.7	1.3	19.6	7.4	0.2	19.6

Continued in the next page…

Moisture-free elemental composition					Dry syngas composition			
C	H	O	N	Ash	CO	CO_2	CH_4	H_2
50.3	5.6	40.9	0.7	2.6	18.1	7.3	0.1	18.1
49.7	5.6	42.6	0.6	1.6	18.7	7.4	0.2	18.7
50.7	5.5	35.4	0.8	7.7	15.8	7.9	0.1	15.8
50.4	5.9	38.1	0.9	4.7	17.8	7.4	0.1	17.8
49.5	5.7	36.0	0.8	8.0	16.2	8.2	0.1	16.2
49.6	5.5	42.3	0.7	2.0	18.4	7.5	0.2	18.4
47.3	5.3	41.6	0.5	5.3	17.0	9.0	0.1	17.0
47.3	5.6	41.1	0.7	5.3	17.6	8.8	0.1	17.6
47.6	5.6	40.2	0.6	6.0	17.3	8.7	0.1	17.3
47.8	5.6	39.2	0.7	6.7	17.0	8.7	0.1	17.0
48.0	5.7	40.0	0.7	5.6	17.6	8.5	0.1	17.6
48.0	5.6	39.0	0.5	6.9	16.8	8.7	0.1	16.8
48.5	5.5	38.2	0.6	7.1	16.5	8.6	0.1	16.5
46.7	5.6	41.5	0.4	5.8	17.6	9.1	0.1	17.6
46.7	5.7	42.1	0.6	4.9	18.1	8.9	0.1	18.1
46.9	5.5	42.0	0.6	5.0	17.7	9.0	0.1	17.7
46.6	5.6	41.2	0.6	6.0	17.5	9.1	0.1	17.5
47.0	5.4	41.1	0.6	5.9	17.0	9.1	0.1	17.0
46.7	5.6	41.0	0.5	6.3	17.3	9.2	0.1	17.3
46.6	5.7	41.5	0.6	5.7	17.8	9.1	0.1	17.8
47.6	5.6	41.4	0.2	5.3	17.7	8.8	0.1	17.7
49.7	5.9	41.9	0.1	2.5	18.9	7.6	0.2	18.9
50.3	6.0	42.1	0.0	1.6	19.4	7.2	0.2	19.4
43.9	5.3	38.8	0.6	11.5	15.1	10.7	0.1	15.1
45.4	5.4	31.0	1.0	15.9	12.9	10.5	0.1	12.9
35.0	4.4	21.3	2.8	35.4	7.2	14.2	0.0	7.2
45.4	5.9	35.9	0.9	11.4	15.9	9.8	0.1	15.9
39.7	5.8	27.2	0.8	26.1	11.1	12.3	0.1	11.1
49.8	5.5	42.4	0.5	1.8	18.5	7.5	0.2	18.5
50.4	5.7	40.6	0.5	2.8	18.3	7.3	0.2	18.3

APPENDIX D

SUPPLEMENTAL DATA FOR SELECTED FIGURES

The data used for figures in different chapters is reported in this appendix. Data in each table corresponds to the figure mentioned alongside.

Table D.1 Data for Figs. 2.1-2.2

Moisture Content (% wet basis)	H_2 (% vol.)	CO (% vol.)	CO_2 (% vol.)	CH_4 (%vol.)	N_2 (%vol.)	HHV (MJ/m^3)	Eq. ratio
0.0	16.9	23.2	9.4	0.1	50.2	5.1	0.40
5.1	17.3	21.5	10.6	0.1	50.4	5.0	0.41
9.7	17.6	19.9	11.6	0.1	50.7	4.8	0.41
13.8	17.8	18.5	12.5	0.1	51.0	4.7	0.42
17.6	17.9	17.2	13.3	0.1	51.4	4.5	0.43
21.1	17.9	16.1	14.0	0.1	51.8	4.4	0.44
24.3	17.9	15.0	14.7	0.1	52.3	4.2	0.45
27.3	17.8	14.0	15.3	0.1	52.8	4.1	0.47
30.0	17.7	13.1	15.8	0.1	53.3	4.0	0.48
32.5	17.5	12.2	16.3	0.1	53.8	3.8	0.49
34.9	17.3	11.5	16.7	0.1	54.4	3.7	0.50
37.1	17.1	10.7	17.1	0.1	54.9	3.6	0.51
39.1	16.8	10.1	17.5	0.1	55.5	3.5	0.52
41.1	16.5	9.4	17.8	0.1	56.1	3.3	0.53
42.9	16.2	8.9	18.1	0.1	56.7	3.2	0.54

Table D.2 Data for Figure 2.3

Temperature	H_2 (% vol.)	CO (%vol.)	CO_2 (% vol.)	CH_4 (% vol.)	N_2 (% vol.)	HHV(MJ/m^3)
650.0	19.20	23.87	9.86	0.838	46.24	5.8
677.5	18.93	23.78	9.73	0.581	46.99	5.6
705.0	18.56	23.67	9.63	0.406	47.73	5.5
732.5	18.14	23.56	9.56	0.286	48.46	5.4
760.0	17.67	23.44	9.50	0.204	49.18	5.3
787.5	17.18	23.31	9.46	0.146	49.91	5.2
815.0	16.67	23.16	9.43	0.106	50.63	5.1
842.5	16.15	23.01	9.42	0.078	51.35	5.0
870.0	15.62	22.84	9.42	0.057	52.07	4.9
897.5	15.09	22.66	9.43	0.043	52.79	4.8
925.0	14.56	22.46	9.44	0.032	53.50	4.7
952.5	14.03	22.25	9.47	0.024	54.22	4.6
980.0	13.51	22.03	9.51	0.018	54.94	4.5
1007.5	12.98	21.79	9.56	0.014	55.65	4.4
1035.0	12.47	21.54	9.62	0.011	56.36	4.3
1062.5	11.96	21.28	9.69	0.008	57.07	4.2
1090.0	11.46	21.00	9.76	0.006	57.77	4.1
1117.5	10.96	20.71	9.85	0.005	58.47	4.0
1145.0	10.47	20.40	9.95	0.004	59.17	3.9
1172.5	9.99	20.09	10.06	0.003	59.86	3.8
1200.0	9.52	19.76	10.17	0.002	60.54	3.7

Table D.3 Data for Figure 2.4

Temperature	H_2 (mol)	CO (mol)	CO_2 (mol)	H_2O (mol)	CH_4 (mol)	N_2 (mol)
650.0	0.56	0.69	0.29	0.11	0.0242	1.34
677.5	0.56	0.70	0.29	0.12	0.0170	1.38
705.0	0.55	0.70	0.29	0.14	0.0120	1.42
732.5	0.54	0.71	0.29	0.15	0.0086	1.45
760.0	0.53	0.71	0.29	0.17	0.0061	1.48
787.5	0.52	0.71	0.29	0.18	0.0044	1.52
815.0	0.51	0.71	0.29	0.20	0.0032	1.55
842.5	0.50	0.71	0.29	0.21	0.0024	1.58
870.0	0.48	0.71	0.29	0.23	0.0018	1.61
897.5	0.47	0.71	0.29	0.24	0.0013	1.64
925.0	0.46	0.70	0.30	0.26	0.0010	1.68
952.5	0.44	0.70	0.30	0.27	0.0008	1.71
980.0	0.43	0.70	0.30	0.29	0.0006	1.74
1007.5	0.41	0.69	0.30	0.30	0.0004	1.77
1035.0	0.40	0.69	0.31	0.31	0.0003	1.81
1062.5	0.39	0.69	0.31	0.33	0.0003	1.84
1090.0	0.37	0.68	0.32	0.34	0.0002	1.88
1117.5	0.36	0.68	0.32	0.36	0.0002	1.91
1145.0	0.34	0.67	0.33	0.37	0.0001	1.95
1172.5	0.33	0.67	0.33	0.38	0.0001	1.99
1200.0	0.32	0.66	0.34	0.40	0.0001	2.02

Table D.4 Data for Figure 2.5

Temperature ($^{\circ}$C)	Equivalence ratio (ER)
650.0	0.35
677.5	0.35
705.0	0.37
732.5	0.38
760.0	0.38
787.5	0.39
815.0	0.40
842.5	0.41
870.0	0.42
897.5	0.43
925.0	0.43
952.5	0.43
980.0	0.44
1007.5	0.45
1035.0	0.47
1062.5	0.48
1090.0	0.49
1117.5	0.50
1145.0	0.50
1172.5	0.51
1200.0	0.52

Table D.5 Data for Figure 2.6

Temperature	H_2 (% vol.)	CO (% vol.)	CO_2 (% vol.)	CH_4 (% vol.)	N_2 (% vol.)	HHV(MJ/m^3)
650.0	17.31	20.50	11.50	0.7	50.01	5.1
677.5	17.38	21.16	11.00	0.5	49.97	5.1
705.0	17.36	21.73	10.58	0.4	49.99	5.1
732.5	17.28	22.22	10.21	0.3	50.04	5.1
760.0	17.16	22.67	9.87	0.2	50.11	5.1
787.5	17.02	23.07	9.58	0.1	50.19	5.1
815.0	16.86	23.44	9.30	0.1	50.29	5.2
842.5	16.70	23.79	9.05	0.1	50.38	5.2
870.0	16.53	24.11	8.81	0.1	50.48	5.2
897.5	16.37	24.41	8.59	0.1	50.58	5.2
925.0	16.21	24.69	8.38	0.0	50.68	5.2
952.5	16.05	24.96	8.18	0.0	50.78	5.2
980.0	15.90	25.21	8.00	0.0	50.87	5.2
1007.5	15.75	25.45	7.82	0.0	50.96	5.2
1035.0	15.61	25.67	7.66	0.0	51.04	5.2
1062.5	15.47	25.89	7.50	0.0	51.13	5.2
1090.0	15.34	26.09	7.35	0.0	51.20	5.3
1117.5	15.22	26.29	7.20	0.0	51.28	5.3
1145.0	15.10	26.47	7.07	0.0	51.35	5.3
1172.5	14.98	26.65	6.94	0.0	51.42	5.3
1200.0	14.87	26.81	6.82	0.0	51.49	5.3

Table D.6 Data for Figure 2.7

Temperature (°C)	H_2 (mol)	CO (mol)	CO_2 (mol)	H_2O (mol)	CH_4 (mol)	N_2 (mol)
650.0	0.53	0.63	0.35	0.14	0.0207	1.53
677.5	0.53	0.65	0.34	0.15	0.0149	1.53
705.0	0.53	0.67	0.32	0.16	0.0108	1.53
732.5	0.53	0.68	0.31	0.17	0.0079	1.53
760.0	0.52	0.69	0.30	0.18	0.0059	1.53
787.5	0.52	0.70	0.29	0.19	0.0044	1.53
815.0	0.51	0.71	0.28	0.19	0.0033	1.53
842.5	0.51	0.72	0.27	0.20	0.0025	1.53
870.0	0.50	0.73	0.27	0.21	0.0020	1.53
897.5	0.50	0.74	0.26	0.22	0.0015	1.53
925.0	0.49	0.75	0.25	0.22	0.0012	1.53
952.5	0.48	0.75	0.25	0.23	0.0010	1.53
980.0	0.48	0.76	0.24	0.23	0.0008	1.53
1007.5	0.47	0.76	0.23	0.24	0.0006	1.53
1035.0	0.47	0.77	0.23	0.25	0.0005	1.53
1062.5	0.46	0.78	0.22	0.25	0.0004	1.53
1090.0	0.46	0.78	0.22	0.25	0.0003	1.53
1117.5	0.45	0.78	0.22	0.26	0.0003	1.53
1145.0	0.45	0.79	0.21	0.26	0.0002	1.53
1172.5	0.45	0.79	0.21	0.27	0.0002	1.53
1200.0	0.44	0.80	0.20	0.27	0.0002	1.53

Table D.7 Snapshot of temperature of one typical run in the gasifier

(Time A.M)	T1 ($^{\circ}$C)	T2 ($^{\circ}$C)	T3 ($^{\circ}$C)	T4 ($^{\circ}$C)	Grate ($^{\circ}$C)
9:53	861.5	816.7	769.6	745.8	685.5
9:53	862.2	816.8	769.8	745.8	686.3
9:53	862.8	816.9	770.1	745.8	686.4
9:53	863.3	818	770.3	745.8	685.3
9:53	863.9	819.4	770.4	745.8	684.6
9:54	864.6	820.8	770.7	745.7	685.4
9:54	865.1	821.8	770.8	745.8	686.1
9:54	865.7	822.6	771	745.7	685.4
9:54	866.1	823.4	771.1	745.8	685.6
9:54	866.5	823.9	771.2	745.8	684.9
9:54	866.8	824.4	771.4	745.8	683.4
9:55	867.2	824.9	771.5	745.8	682.9
9:55	867.6	825.2	771.7	745.9	683.8
9:55	868	825.5	771.8	745.9	684.4
9:55	868.4	825.8	772	745.9	683.3
9:55	868.9	826.1	772.1	746	682.1
9:56	869.4	826.4	772.4	746	682.7
9:56	869.8	826.5	772.5	746.1	684
9:56	870.2	826.8	772.8	746.1	683.4
9:56	870.6	827	773	746.2	682.2
9:56	870.9	827.2	773.2	746.3	682.9
9:56	871.3	827.4	773.4	746.3	683.9
9:57	871.4	827.5	773.5	746.4	684.1
9:57	871.7	827.6	773.7	746.4	682.6
9:57	871.8	827.8	773.9	746.5	681.8
9:57	872	827.9	774	746.6	682.5

Figure D.1 to D.5 represents the temperature variations inside the gasifier from the initial start-up to the steady state at which temperature almost remains constant.
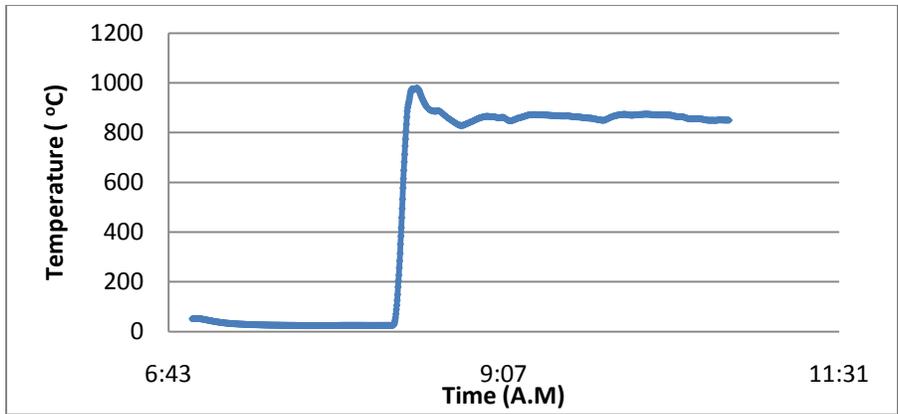
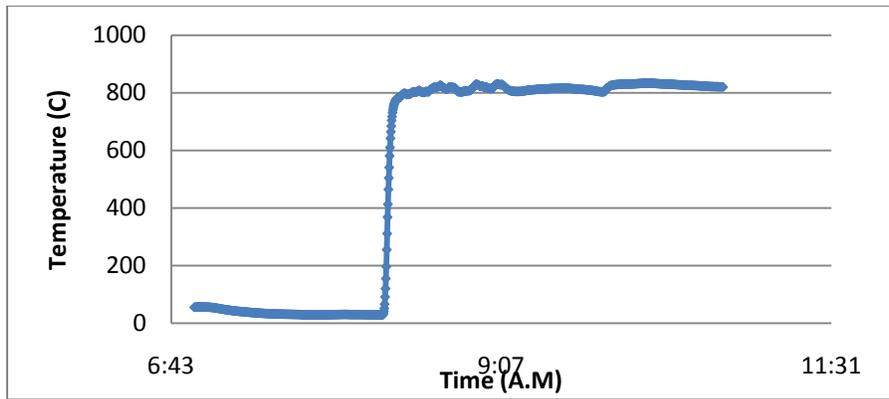Figure D.1 Temperature recorded by thermocouple at T1 from its start-up to steady state

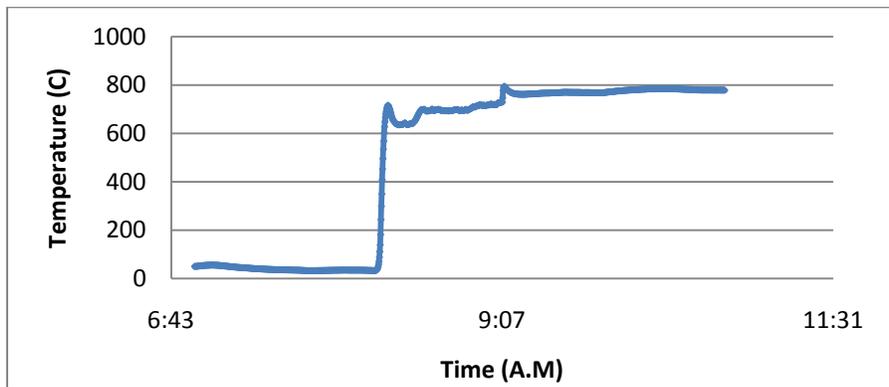Figure D.2 Temperature recorded by thermocouple at T2 from its start-up to steady state

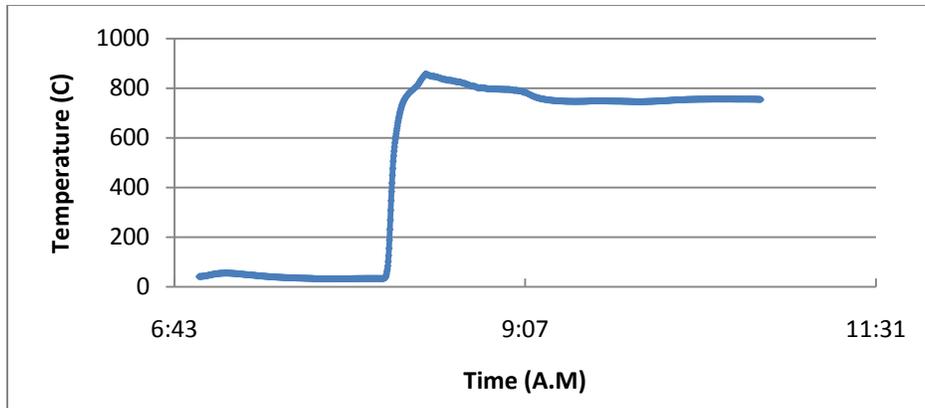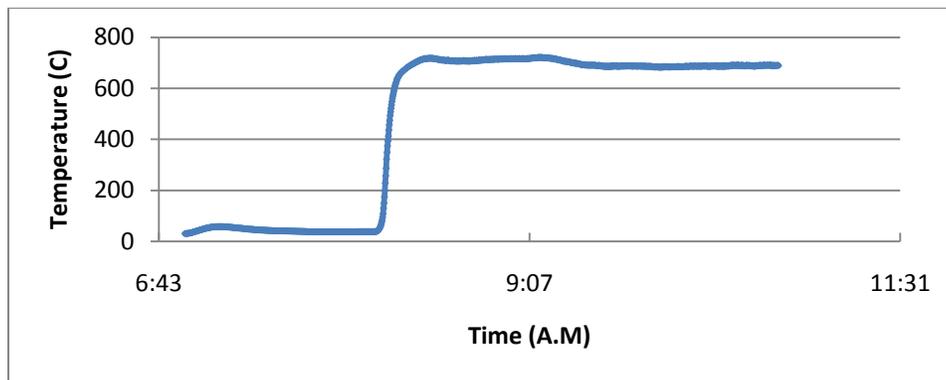Figure D.3 Temperature recorded by thermocouple at T3 from its start-up to steady state

142

Figure D.4 Temperature recorded by thermocouple at T4 from its start-up to steady state

Figure D.5 Temperature recorded by thermocouple at T1 from its start-up to steady state

Table D.8 Data for Figure 3.5

Moisture Content (% wet basis)	T1($^{\circ}$C)	T2($^{\circ}$C)	T3($^{\circ}$C)	T4($^{\circ}$C)	Grate($^{\circ}$C)
19.6	$897^{\pm46}$	$867^{\pm39}$	$839^{\pm34}$	$837^{\pm10}$	$811^{\pm8}$
23	$917^{\pm39}$	$867^{\pm27}$	$844^{\pm29}$	$844^{\pm14}$	$792^{\pm8}$
25	$881^{\pm49}$	$860^{\pm20}$	$836^{\pm19}$	$829^{\pm19}$	$810^{\pm2}$

Table D.9 Data for Figure 3.6

Feedstock	T1($^\circ$C)	T2($^\circ$C)	T3($^\circ$C)	T4($^\circ$C)	Grate($^\circ$C)
Peanut hull pellets	$790^{\pm48}$	$760^{\pm37}$	$799^{\pm29}$	$797^{\pm17}$	$715^{\pm5}$
Saw dust pellets	$864^{\pm32}$	$853^{\pm27}$	$851^{\pm10}$	$852^{\pm9}$	$808^{\pm2}$
Poultry litter	$348^{\pm59}$	$910^{\pm53}$	$977^{\pm60}$	$918^{\pm40}$	$777^{\pm19}$
Wood chips	$897^{\pm46}$	$867^{\pm39}$	$839^{\pm34}$	$837^{\pm10}$	$811^{\pm8}$
Commercial wood pellets	$832^{\pm8}$	$799^{\pm13}$	$845^{\pm18}$	$846^{\pm18}$	$819^{\pm14}$

Table D.10 Data for Figure 3.7

Mass flow rate (kg/hr)	T1($^\circ$C)	T2($^\circ$C)	T3($^\circ$C)	T4($^\circ$C)	Grate($^\circ$C)
16.4	$844^{\pm48}$	$869^{\pm33}$	$832^{\pm29}$	$805^{\pm17}$	$743^{\pm20}$
22.2	$885^{\pm43}$	$876^{\pm61}$	$850^{\pm50}$	$855^{\pm30}$	$801^{\pm17}$
26.6	$897^{\pm46}$	$867^{\pm39}$	$839^{\pm34}$	$837^{\pm10}$	$811^{\pm8}$

Table D.11 Data for Figure 3.9

Feedstock Mass Flow Rate (kg/hr)	CO (% vol.)	CO_2(% vol.)	CH_4(% vol.)	H_2(%. vol.)
17.6	$23.2^{\pm2.1}$	$11.0^{\pm1.8}$	$1.9^{\pm0.6}$	$17.3^{\pm2.3}$
18.0	$20.7^{\pm1.9}$	$12.3^{\pm1.9}$	$2.1^{\pm0.7}$	$18.7^{\pm2.7}$
18.7	$19.9^{\pm2.3}$	$13.5^{\pm2.0}$	$2.4^{\pm0.5}$	$17.2^{\pm2.9}$
19.0	$22.9^{\pm2.1}$	$10.6^{\pm1.7}$	$1.9^{\pm0.7}$	$18.7^{\pm1.8}$
19.8	$23.1^{\pm2.0}$	$10.6^{\pm1.7}$	$1.9^{\pm0.3}$	$17.6^{\pm2.1}$
20.6	$23.4^{\pm2.3}$	$10.9^{\pm1.6}$	$2.0^{\pm0.4}$	$18.2^{\pm1.9}$
23.1	$24.3^{\pm1.8}$	$9.8^{\pm1.2}$	$1.8^{\pm0.5}$	$17.8^{\pm1.9}$
24.6	$21.7^{\pm1.3}$	$11.3^{\pm0.7}$	$2.0^{\pm0.2}$	$18.9^{\pm1.0}$
24.9	$22.9^{\pm1.3}$	$11.4^{\pm1.0}$	$2.1^{\pm0.4}$	$18.3^{\pm0.9}$
26.5	$22.1^{\pm1.0}$	$11.1^{\pm0.6}$	$2.0^{\pm0.3}$	$18.6^{\pm0.9}$
27.0	$23.0^{\pm1.1}$	$10.5^{\pm0.8}$	$1.9^{\pm0.2}$	$17.6^{\pm1.3}$
28.8	$22.1^{\pm1.3}$	$10.4^{\pm0.9}$	$1.9^{\pm0.4}$	$16.6^{\pm0.5}$

Table D.12 Data for Figure 3.10

Biomass flow rate (kg/hr)	T1($^{\circ}$C)	T2($^{\circ}$C)	T3($^{\circ}$C)	T4($^{\circ}$C)	Grate($^{\circ}$C)
17.6	$860^{\pm53}$	$818^{\pm51}$	$759^{\pm49}$	$792^{\pm3}$	$709^{\pm5}$
18.0	$863^{\pm50}$	$855^{\pm50}$	$816^{\pm34}$	$839^{\pm7}$	$774^{\pm9}$
18.7	$816^{\pm46}$	$793^{\pm53}$	$787^{\pm49}$	$796^{\pm1}$	$757^{\pm4}$
19.0	$844^{\pm9}$	$829^{\pm9}$	$774^{\pm31}$	$809^{\pm50}$	$742^{\pm14}$
19.8	$856^{\pm44}$	$819^{\pm7}$	$774^{\pm4}$	$780^{\pm1}$	$723^{\pm1}$
20.6	$857^{\pm35}$	$822^{\pm41}$	$788^{\pm39}$	$803^{\pm10}$	$710^{\pm6}$
23.1	$865^{\pm30}$	$846^{\pm22}$	$774^{\pm17}$	$836^{\pm12}$	$769^{\pm1}$
24.9	$848^{\pm37}$	$815^{\pm26}$	$774^{\pm20}$	$801^{\pm39}$	$767^{\pm10}$
24.6	$823^{\pm20}$	$823^{\pm20}$	$800^{\pm40}$	$814^{\pm38}$	$785^{\pm16}$
26.5	$835^{\pm7}$	$826^{\pm18}$	$759^{\pm12}$	$875^{\pm19}$	$737^{\pm10}$
27.0	$853^{\pm23}$	$848^{\pm15}$	$727^{\pm9}$	$811^{\pm16}$	$801^{\pm4}$
28.8	$832^{\pm8}$	$799^{\pm13}$	$845^{\pm18}$	$846^{\pm18}$	$819^{\pm14}$

APPENDIX E

SAMPLE CALCULATIONS

E.1 SAMPLE CALCULATIONS FOR EQUILIBRIUM MODELING

The input for the program is elemental composition of the feedstock and reaction temperature. Program automatically calculates the molecular formula for the biomass in the form of $CH_xO_yN_z$.

$$C^* = C/12, H^* = H/1.008, O^* = O/16, N^* = N/16$$

$$C_N = \frac{C^*}{C^*} = 1, H_N = H^*/C^*, O_N = O^*/C^*, N_N = N^*/C^*$$

The system of equations mentioned in Chapter 2 is solved using Newton's Jacobi method using these stoichiometric numbers and accessing various function files for finding equilibrium constants and other thermodynamic properties of various gases involved in the gasification process.

Solving these equations, the number of moles of H_2O, CO, CO_2, CH_4 and N_2 required for the gasification process is obtained. The fraction of gases can be either expressed as wet syngas composition or dry syngas composition by calculating fractions excluding or including moisture content. Table below shows the typical data when the program was run with elemental composition of 50%-C, 6%-H, 44%-O and completely dry biomass.

Table E.1 Calculation of syngas composition from MATLAB

Gases	Number of moles of Output	Syngas constituents (% wet basis)	Syngas constituents (% dry basis)
H_2	0.516	16.0	16.9
CO	0.708	21.9	23.2
CO_2	0.288	8.9	9.4
H_2O	0.190	5.9	-
CH_4	0.004	0.1	0.1
N_2	1.531	47.3	50.2

The syngas constituent is one of the representatives of Figure 2.1 in Chapter 2.

The calculation procedure for other tables in Chapter 2 are very similar to that explained above and is not reported.

E.2   CARBON, ENERGY AND EXERGY ANALYSES

Table E.2 shows the syngas composition at different biomass flow rates along with the moisture content, grate temperature and actual syngas flow rate upon the gasification of commercial wood pellets. This is also the supplemental data from the experiments with commercial wood pellets, part of which is reported in Table 3.9.

Table E.2 Syngas composition at different biomass flow rate for commercial wood pellets

Wet biomass rate (kg/hr)	Moisture content (% wet basis)	Grate Temperature (^0C)	Syngas constituents fraction (% vol, dry basis)				AF Syngas flow rate (m^3/hr)
			CO	CO_2	CH_4	H_2	
24.6	2.65	785.1	21.7	11.3	2.0	18.9	59.9
19.0	2.67	741.7	22.9	10.6	1.9	18.7	47.4
26.5	3.74	736.6	22.1	11.1	2.0	18.6	57.6
18.0	3.8	773.9	20.7	12.3	2.1	18.7	45.8
18.7	4.1	756.7	19.9	13.5	2.4	17.2	44.3
27.0	3.8	801.4	23.0	10.5	1.9	17.6	62.6
23.1	3.8	768.7	24.3	9.8	1.8	17.8	50.0
18.6	4.5	698.0	20.7	11.7	2.1	18.7	45.0
28.8	3.5	819.1	22.1	10.4	1.9	16.6	65.0
24.9	5.3	767.2	22.9	11.4	2.1	18.3	65.0
20.6	5.3	709.6	23.4	10.9	2.0	18.2	54.9
17.6	3.4	709.2	23.2	11.0	1.9	17.3	45.0
19.8	3.4	723.4	23.1	10.6	1.9	17.6	55.0

The experiment done with a biomass flow rate of 28.8 kg/hr is selected for sample calculation purpose (highlighted above). Sample calculations of carbon closure, energy ratio and exergy ratio are shown in the following sections.

E.2.1 CARBON CLOSURE

Carbon closure for the experiment taken for sample calculation is 0.90 from Table 3.9 for the experiment highlighted in Table E.2.

The dry biomass flow rate (m_{dry}) is calculated by subtracting the amount of moisture present which is:

$$m_{dry} = m - m_w$$

where, m_{dry}, m and m_w are mass of dry biomass flow rate, wet biomass flow rate and amount of moisture present in biomass per hour, respectively.

$$m_{dry} = 28.8 - \left(\frac{3.5}{100}\right) \times 28.8 = 27.8 \text{ kg/hr}$$

The amount of carbon present in the biomass can be found by multiplying the dry biomass flow rate with its carbon content which is 47.7% (Reported in Chapter 3-Table 3.1).

Carbon flow rate per hour (C_{in}) = $27.8 \times 0.477 = 13.3$ kg/hr

The following relation gives the carbon content in syngas.

$$C_{out} = (y_{CO} + y_{CO_2} + y_{CH_4}) \cdot \rho_{mol} \cdot M_c \cdot F_s \tag{1}$$

where $y_{CO}, y_{CO_2}, y_{CH_4}, \rho_{mol}, M_c$ and F_s is the volumetric or molar fraction of CO, CO_2, CH_4, molar density of ideal gas, molecular weight of carbon in kg/mol, and syngas flow rate (m^3/hr),

respectively. For ideal gas condition, molar density at standard temperature and pressure (STP) is 44.615 mol/m^3.

Substituting the respective values in Eqn. (1) gives the following result.

$$C_{out} = (0.221 + 0.109 + 0.019) \times 44.615 \times \frac{12}{1000} \times 65 = 12 \text{ kg/hr}$$

Carbon closure is the ratio of C_{out} to $C_{in.}$

$$C_c = \frac{C_{out}}{C_{in}} = \frac{12}{13.3} = 0.90$$

E.2.2   ENERGY RATIO

Energy ratio for the experiment taken for sample calculation is 0.87 is taken from Table 3.9 for the experiment highlighted in Table E.2.

The specific density ρ_i of selected gases $i = CO, CO_2, CH_4, H_2$ and N_2 at STP is given in Table E.3.

Table E.3 Properties of syngas constituents

Gases	gas constant, R (kJ/(kg-K))	molecular mass (g/mol)	ρ at STP (kg/m^3)	E_{s0} (MJ/kg)	Ex_0 (MJ/kg)
N_2	0.2970	28.0	1.249	0	0
CO	0.2968	28.01	1.2498	10.1	9.9
CO_2	0.1889	44.01	1.9637	0	0
CH_4	0.5183	16.043	0.7157	55.5	39.8
H_2	4.1243	2.016	0.0899	142.4	68.9

The energy content in biomass can be found using Eqn. (2). Higher heating value (HHV) of biomass is reported in Chapter 3 in Table 3.1.

$$E_{in} = HHV \times m_{dry} \qquad (2)$$

$E_{in} = 18.3 \times 27.8 = 508.9 \text{ MJ/hr}$

The volumetric flow rate of CO, CH_4 and H_2 is expressed in the form of mass flow rate as following (m_i as a mass flow rate of i constituent of syngas).

$m_{CO} = y_{CO} \times \rho_{CO} \times F_s = 18 \text{ kg/hr}$

$m_{CH_4} = y_{CH_4} \times \rho_{CH_4} \times F_s = 0.9 \text{ kg/hr}$

$m_{H_2} = y_{H_2} \times \rho_{H_2} \times F_s = 1 \text{ kg/hr}$

$$m_{CO_2} = y_{CO_2} \times \rho_{CO_2} \times F_s = 13.3 \text{ kg/hr}$$

$$m_{N_2} = y_{N_2} \times \rho_{N_2} \times F_s = 39.7 \text{ kg/hr}$$

y_{N_2} is obtained by difference as follows.

$$y_{N_2} = 1 - \sum_{y=CO,CO_2,CH_4,H_2} y_i$$

As mentioned in Chapter 3-Eqn. (10), the total energy of a gas is given by Eqn. (3).

$$E_i = E_{0i} + \int_{T_d}^{T} C_p dT \tag{3}$$

where E_i and E_{0i} ($i = CO, CO_2, CH_4, H_2$ and N_2) are the total energy and chemical energy at dead state temperature (T_d) taken as $25^{\circ}C$, respectively. C_p is the specific heat capacity (kJ/kg-K) of syngas while T is the syngas temperature (taken as grate temperature) in Kelvin as highlighted Table E.2.

The specific heat capacity for given temperature can be calculated from Eqn. (4) where $\theta = T/1000$.

$$C_p = a + b\theta + c\theta^2 + d\theta^3 \tag{4}$$

In above equation, a, b, c and d are the coefficients of specific heat capacity which is reported in Chapter 3 -Table 3.8.

Integrating Eqn. (3) gives the specific energy of an individual gas. Then, multiplying the specific energy of biomass at given temperature with biomass flow rate will give the total energy of syngas as follows.

$$E_i' = E_i \times m_i$$

E_i' denotes the energy of gas i in MJ/hr.

$$E'_{CO} = 197.7 \text{ MJ/hr}$$

$$E'_{CO_2} = 11.7 \text{ MJ/hr}$$

$$E'_{CH_4} = 51.2 \text{ MJ/hr}$$

$$E'_{H_2} = 149.6 \text{ MJ/hr}$$

$$E'_{N_2} = 34.8 \text{ MJ/hr}$$

By adding the enthalpy of individual gases, we can find E_{out}, the total energy of the output gas.

$$E_{out} = 445.0 \text{ MJ/hr}$$

Thus, the required ratio is calculated as following.

$$E_{out}/E_{in} = \frac{445.0}{508.9} = 0.87$$

E.2.3 EXERGY RATIO

Exergy ratio for the experiment taken for sample calculation is 0.58 from Table 3.9.

The chemical exergy associated with biomass can be found from Eqn. (5).

$$Ex_{in} = \beta. LHV. y_{biomass} \tag{5}$$

$$\beta = \frac{1.044 + 0.016H/C - 0.3493O/C[1 + 0.0531H/C] + 0.0493N/C}{1 - 0.4124O/C} \tag{6}$$

Ex_{in} is the chemical exergy of biomass. LHV and $y_{biomass}$ are the lower heating value (MJ/kg) and ash free fraction of biomass, respectively. H, C, O and N represent the fraction of hydrogen, carbon, oxygen and nitrogen present in the biomass respectively. H/C, N/C and O/C are calculated from the ultimate analysis of the feedstock which is 47.7% C, 6.0% H, 45.8% O and 0.04% N as reported in Chapter 3-Table 3.1.

$$H/C = 0.156, O/C = 0.96, N/C = 0.0008$$

Substitution of these values in above equation gives:

$$\beta = 1.17$$

LHV was calculated according to the Eqn. (7) where HHV should be expressed as (kJ/kg).

$$LHV_{org} = \frac{HHV - 22,604\,H}{1000} \text{ (MJ/kg)} \tag{7}$$

$$LHV_{org} = 16.98 \text{ MJ/kg}$$

$$y_{biomass} = 1 - y_{ash} = 0.996$$

y_{ash} is the fraction of ash in the feedstock which was found to be 0.44% in the commercial wood pellets, as can be seen in Table 3.1. Now, Ex_{in} can be calculated from above relations.

$$Ex_{in} = \beta. LHV. y_{biomass} = 1.17 \times 0.996 \times 16.98 = 552.5 \text{ MJ/kg}$$

$$Ex_i = Ex_{0i} + \int_{T_d}^{T} \left[C_p \left(1 - \frac{T_d}{T} \right) \right] dT \tag{8}$$

where Ex_{0i} and Ex_i (i = CO, CO$_2$, CH$_4$, H$_2$ and N$_2$) are the chemical exergy and total exergy of the individual gases. The chemical exergy of selected gases is given in Table E.2.

Integrating Eqn. (8) gives the specific exergy of an individual gas.

Multiplying the specific exergy of biomass at given temperature with biomass flow rate will give the total energy of syngas as follows.

$$Ex'_i = Ex_i \times m_i \tag{9}$$

Ex'_i denotes the energy of gas i in MJ/hr.

The following exergy of individual gases can be obtained by substituting the value of specific exergy of each gas from Eqn. (8) to Eqn. (9).

$$E'x_{CO} = 185.7 \text{ MJ/hr}$$

$$E'x_{CO_2} = 6.2 \text{ MJ/hr}$$

$$E'x_{CH_4} = 36.3 \text{ MJ/hr}$$

$$E'x_{H_2} = 72.8 \text{ MJ/hr}$$

$$E'x_{N_2} = 18.1 \text{ MJ/hr}$$

The addition of above exergy of individual gases gives the total exergy output per hour

155

$Ex_{out} = 319.1 \text{ MJ/hr}$

Exergy ration is the ratio of Ex_{in} to Ex_{out} can be now calculated.

$$Ex_{out}/Ex_{in} = \frac{319.1}{552.5} = 0.58$$

APPENDIX F

CONCENTRATION OF SELECTED COMPOUNDS IN TAR

Table F.1 and F.2 shows the concentration of various tar constituents in syngas from the gasification of commercial wood pellets in a downdraft gasifier for eleven experiments. The experiments were conducted at different biomass flow rate which reported along with its moisture content feedstock in the following tables.

Table F.1 Concentration of tar constituents in syngas (Supplemental data-A)

Tar compounds	Concentration in syngas (mg/Nm^3)				
Moisture content (% wet basis)	2.65	3.8	2.65	3.5	2.4
Wet biomass flow rate (kg/hr)	19	18	24.6	26.5	28.8
Toluene	92.2	87.2	81.6	77	198.3
Ethylbenzene	25	2.5	23.1	19.4	4.7
o/p-Xylene	111.6	9.9	96	74.2	10.3
Styrene	42.9	29.8	31.4	40.6	55.4
Furfural	0	0	0	0	0
Benzene, 1-ethyl-2-methyl-; (2-Ethyltoluene)	1.4	0.6	0.7	1.5	0.9
.alpha.-Methylstyrene	2.2	1.5	1.5	2	1.7
Benzene, 1,2,3-trimethyl-	2.4	1.4	1.8	2.4	1.4
Benzene, 1-ethenyl-3-methyl-; (m-Methylstyrene)	9.7	7.3	6.6	8.1	8.7
Benzofuran	11.5	8.5	9.4	7.8	11.8
Indene	29.7	26.2	25.2	15.7	33.5
Benzofuran, 2-methyl-	10.5	6.6	8.4	0	6
Phenol	14.6	7	13	6.9	13.7
Phenol, 2-methyl-	1.2	0.5	0.6	0.6	0.7
Naphthalene	97.3	123.4	109.3	62.3	78.8
Phenol, 3-methyl-	4.4	1.3	2.6	1.5	3.3
Phenol, 3-ethyl-	0.2	0	0.1	0	0
Phenol, 2,4-dimethyl-	0.2	0	0.1	0	0.1
Phenol, 3,5-dimethyl-	0.2	0	0.1	0	0.1
Naphthalene, 1-methyl-	13.1	12.8	11.8	5.9	6.6
Naphthalene, 2-methyl-	10.3	10.8	10.1	5.1	5.8
Biphenyl	7	7.2	7.1	2.6	3
Naphthalene, 1,5-dimethyl-	0.8	0.6	0.6	0.2	0
Naphthalene, 1,8-dimethyl-	1.7	1.4	1.5	0.6	0.6
Naphthalene, 2,3-dimethyl-	0.7	0.5	0.6	0.2	0
Naphthalene, 1,8-dimethyl-	0.7	0.1	0.3	0.1	0
Naphthalene, 2-ethenyl-; (2-Vinylnaphthalene)	2.8	1.8	1.3	0.4	0.6
Biphenylene	15.4	15.1	15.5	3.9	7.1
Acenaphthene	1.1	1	1.1	0.4	0.3
Dibenzofuran	2.4	1.4	2.5	0.4	0.5

Table F.2 Concentration of tar constituents in syngas (Supplemental data-B)

Tar compounds	Concentration in syngas (mg/Nm3)					
Moisture content (% wet basis)	5.3	3.4	3.4	3.8	3.8	4.5
Wet biomass flow rate (kg/hr)	20.6	17.6	19.8	23.1	27	18.6
Toluene	129.5	76.8	90.1	158	136.2	149.7
Ethylbenzene	9.1	5.6	6.6	6.3	5.2	8.4
o/p-Xylene	16.7	9.3	11.4	18.2	14.6	15.8
Styrene	60.9	33.5	49.7	65.1	47.2	47
Furfural	2.2	1.5	4	1.9	0	0
Benzene, 1-ethyl-2-methyl-; (2-Ethyltoluene)	3	1.8	2.1	2.7	1.5	2.6
.alpha.-Methylstyrene	3.1	1.7	2.7	3.1	2	1.9
Benzene, 1,2,3-trimethyl-	2.3	1.3	2	3.3	2.6	2
Benzene, 1-ethenyl-3-methyl-; (m-Methylstyrene)	14.1	7.6	11.4	18.8	10.7	9.9
Benzofuran	23.4	14.6	24.9	24.6	12	14.2
Indene	43.2	25.2	48.7	55.8	24.1	26.3
Benzofuran, 2-methyl-	17.8	11.1	20.7	23.8	10.5	11.8
Phenol	49.8	33.9	67.2	49.7	18.2	27.2
Phenol, 2-methyl-	5	3	8.9	6.1	1.5	1.8
Naphthalene	81.5	80.6	103.3	126.1	79.1	101.5
Phenol, 3-methyl-	17.8	11	25.4	19.5	5.5	7.6
Phenol, 4-ethyl-	0.6	0.4	1	0.7	0	0.2
Phenol, 3-ethyl-	0.8	0.5	1.3	1.2	0.2	0.3
Phenol, 2,4-dimethyl-	1.3	0.8	2.4	1.9	0.4	0.6
Phenol, 3,5-dimethyl-	1.2	0.7	1.9	1.8	0.3	0.5
Naphthalene, 1-methyl-	10.9	8.7	14.6	22.1	9.2	11.2
Naphthalene, 2-methyl-	8.9	7.2	12.5	16.2	7	9.2
Biphenyl	5.4	4.8	7.8	10.1	4.4	6.4
Naphthalene, 1,5-dimethyl-	0.8	0.5	1	1.7	0.5	0.6
Naphthalene, 1,8-dimethyl-	1.9	1.1	2.6	3.6	1.2	1.5
Naphthalene, 2,3-dimethyl-	0.7	0.4	1	1.4	0.4	0.5
Naphthalene, 1,8-dimethyl-	0.5	0.2	0.6	0.8	0.2	0.4
Naphthalene, 2-ethenyl-; (2-Vinylnaphthalene)	3.2	1.7	5.1	6.7	1.6	1.8
Biphenylene	14.7	9.8	22.2	21.7	7.2	10.9
Acenaphthene	1.3	1.4	2.1	1.7	0.6	1.7
Dibenzofuran	2.4	1.8	3.4	3.3	1.3	1.4

APPENDIX G

UNCERTAINTY ANALYSIS

Uncertainty analysis was conducted as described by Doebelin [1]. The quantity to be computed is expressed as a function of other known variables. Suppose, Y is the function of n number of independent parameters, $X_1, X_2, X_3 \ldots X_n$. Y can be thus expressed as the function of these independent parameters.

$$Y = f(X_1, X_2, X_3, \ldots X_n) \tag{1}$$

A Taylor series expansion can be used to find the infinitesimal change in Y due to the corresponding changes in $X_1, X_2, X_3 \ldots X_n$. Taylor expansion of Eqn.1 gives the following expression.

$$\Delta Y \approx \frac{\partial f}{\partial X_1} . \Delta X_1 + \frac{\partial f}{\partial X_2} . \Delta X_2 + \frac{\partial f}{\partial X_3} . \Delta X_3 + \cdots + \frac{\partial f}{\partial X_3} . \Delta X_n \tag{2}$$

If we consider ΔX's as the uncertainties in the measured value u_{xi}, the total uncertainty associated with U_Y can be expressed as the root-sum-square which is shown in the following equation.

160

$$U_Y = \sqrt{\left(\frac{\partial f}{\partial X_1} \cdot u_{X1}\right)^2 + \left(\frac{\partial f}{\partial X_2} \cdot u_{X2}\right)^2 + \left(\frac{\partial f}{\partial X_3} \cdot u_{X4}\right)^2 \ldots + \left(\frac{\partial f}{\partial X_n} \cdot u_{Xn}\right)^2} \qquad (3)$$

The above expression is used for calculating the uncertainty associated with finding mass, energy and exergy balance for the experiments described in Chapter 3.

G.1   UNCERTAINTY ASSOCIATED WITH CARBON CLOSURE

The following equation was implemented to calculate the mass closure σ_M in the gasifier which can be obtained by combining c_{in} and c_{out} from carbon closure sample calculation.

$$\sigma_M = \frac{F_s\left(y_{CO} + y_{CO_2} + y_{CH_4}\right) \cdot \rho_{mol} M_c}{m - m_w}$$

y_{CO} = Fraction of carbonaceous gas $i = CO, CO_2, CH_4$ in syngas

F_s = Total syngas flow-rate from the gasifier

m = Mass of the wet biomass

m_w = Mass of moisture in biomass

m_{ash} = Mass of ash in biomass

Following are the uncertainties associated with each parameter in above equation.

$\Delta y_i = \pm 2\%$ of a scale reading, $\Delta F_{syngas} = \pm 1 \, m^3/hr$ of a scale reading, $\Delta m = \pm 10^{-2}$ kg of a scale

reading, $\Delta m_w = \pm 10^{-6}$ kg of a scale reading, $\Delta m_{ash} = \pm 10^{-9}$ kg of a scale reading.

The following data was taken for uncertainty analysis:

$$F_s = 65 \, m^3/hr, \quad y_{CO} = 0.221, y_{CO_2} = 0.104,$$

$$y_{CH_4} = 0.019, \quad m = 28.8 \, kg/hr, \quad m_w = 1.1 \, kg/hr, M_{ash} = 0.127 \, kg/hr$$

$$\rho_{CO} = 1.245 \, kg/m^3, \rho_{CO_2} = 1.934 \, kg/m^3, \rho_{CH_4} = 0.716 \, kg/hr$$

It can easily be shown that:

$$\frac{\partial(\sigma_M)}{\partial F_s} = \frac{(y_{CO} + y_{CO_2} + y_{CH_4})M_c\rho_{mol}}{m - m_w} = 0.0066$$

$$\frac{\partial\sigma_M}{\partial y_{CO}} = \frac{F_s\rho_{mol}M_c}{m - m_w} = 1.2545$$

$$\frac{\partial\sigma_M}{\partial y_{CO_2}} = \frac{F_s\rho_{mol}M_c}{m - m_w} = 1.2545$$

$$\frac{\partial\sigma_M}{\partial y_{CH_4}} = \frac{\rho_{mol}M_cF_s}{m - m_w} = 1.2545$$

$$\frac{\partial\sigma_M}{\partial m} = \frac{-F_s\rho_{mol}M_c}{(m - m_w)^2} = -0.0452$$

$$\frac{\partial\sigma_M}{\partial m_w} = \frac{\rho_{mol}M_cF_s}{(m - m_w)^2} = 0.0452$$

Thus the absolute uncertainty associated with the mass closure is given by the following relation.

$$U_{\sigma_m} = \sqrt{\begin{array}{c}\left(\frac{\partial \sigma_m}{\partial F_s}.u_{Fs}\right)^2 + \left(\frac{\partial \sigma_m}{\partial y_{CO}}.u_{y_{CO}}\right)^2 + \left(\frac{\partial \sigma_m}{\partial y_{CO_2}}.u_{y_{CO_2}}\right)^2 + \left(\frac{\partial \sigma_m}{\partial y_{CH_4}}.u_{y_{CH_4}}\right)^2 \\ + \left(\frac{\partial \sigma_m}{\partial m}.u_m\right)^2 + \left(\frac{\partial \sigma_m}{\partial m_w}.u_{m_w}\right)^2\end{array}}$$

$$U_{\sigma_m} = 0.009$$

Substituting the values found above, the uncertainty associated with mass closure was found to be 0.009.

G.2   UNCERTAINTY ASSOCIATED WITH ENERGY RATIO

Enthalpy from biomass can be found using the following relation.

$$E_{in} = HHV \times (m - m_w)$$

HHV is the higher heating value of biomass (commercial wood pellets) which is expressed in the units of MJ/kg.

Specific energy of individual gas is given by following relation.

$$E_i = E_{0_i} + \int_{T_d}^{T} C_p dT$$

This specific energy can be converted into hourly flow rate as following.

$$E_i' = E_i \times m_i = E_i \cdot \rho_i \cdot y_i \cdot F_s$$

The following is the sum of total energy in the syngas from the gasification process.

$$E_{out} = \sum_{i=H_2,CO,CO_2,CH_4,N_2,H_2O} \rho_i y_i F_s \left(E_{0_i} + \int_{T_d}^{T} C_p dT \right)$$

where, ρ_i= Density of carbonaceous gas $i = CO, CO_2, CH_4$ in syngas.

Substituting $C_p = c_0^i + c_1^i T + c_2^i T^2 + c_3^i T^3$ in above equation where

$c_0^i = c_0, c_1^i = \frac{c_1}{1000}, c_2^i = \frac{c_2}{1000^2}, c_3^i = \frac{c_3}{1000^3}$, the following expression can be used to replace the

above equation which is already defined in Chapter 3- Eqn. (12). The uncertainty associated with

temperature (ΔT) is $\pm 0.1^{\circ}C$.

$$E_{out} = \sum_{i=H_2,CO,CO_2,CH_4,N_2,H_2O} \rho_i y_i F_s \left(E_{s0_i} + c_0^i(T - T_d) + c_1^i \left(\frac{T^2}{2} - \frac{T_d^2}{2} \right) + c_2^i \left(\frac{T^3}{3} - \frac{T_d^3}{3} \right) \right.$$
$$\left. + c_3^i \left(\frac{T^4}{4} - \frac{T_d^4}{4} \right) \right)$$

The following notation is used:

$$\delta_{T_i} = E_{s0_i} + c_0^i(T - T_d) + c_1^i \left(\frac{T^2}{2} - \frac{T_d^2}{2} \right) + c_2^i \left(\frac{T^3}{3} - \frac{T_d^3}{3} \right) + c_3^i \left(\frac{T^4}{4} - \frac{T_d^4}{4} \right)$$

$$E_{out} = \sum_{i=H_2,CO,CO_2,CH_4,N_2,H_2O} \rho_i y_i F_s \delta_{T_i}$$

Ratio of input enthalpy to output enthalpy is $\sigma_E = E_{out}/E_{in}$.

Thus, it can be seen from above discussion that: $\sigma_E = f(m, m_w, y_i, F_s, T)$

The following expressions can be easily computed.

$$\frac{\partial \sigma_E}{\partial(y_i)} = \frac{\rho_i F_s \delta_{T_i}}{HHV \times (m - m_w)}$$

$$= 1.754, 0.222, 5.332, 1.769, 0.140 \text{ for } CO, CO_2, CH_4, H_2 \text{ and } N_2 \text{ respectively}$$

$$\frac{\partial \sigma_E}{\partial(F_s)} = \frac{\sum_{(i=H_2,CO,CO_2,CH_4,N_2,H_2O)}(\rho_i y_i \delta_{T_i})}{HHV \times (m - m_w)} = 0.013$$

$$\frac{\partial \sigma_E}{\partial(T)} = \frac{\sum_{all\ gases} \rho_i F_s y_i (c_0^i + c_1^i T + c_2^i T^2 + c_3^i T^3)_1}{HHV \times (m - m_w)} = 0.205$$

$$\frac{\partial \sigma_E}{\partial(m)} = -\frac{\sum_{all\ gases} y_i \rho_i F_s \delta_{T_i}}{HHV \times (m - m_w)^2} = -0.206$$

$$\frac{\partial \sigma_E}{\partial(m_w)} = \frac{\sum_{all\ gases} y_i \rho_i F_s \delta_{T_i}}{HHV \times (m - m_w)^2} = 0.206$$

Finally, the uncertainty in enthalpy balance can be calculated using the following relation:

$$U_{\sigma_E} = \sqrt{\begin{array}{c}\left(\frac{\partial \sigma_E}{\partial F_s} \cdot u_{FS}\right)^2 + \sum_{all\ gases}\left(\frac{\partial \sigma_E}{\partial y_i} \cdot u_{y_i}\right)^2 + \left(\frac{\partial \sigma_E}{\partial T} \cdot u_T\right)^2 \\ + \left(\frac{\partial \sigma_E}{\partial m} \cdot u_m\right)^2 + \left(\frac{\partial \sigma_E}{\partial m_w} \cdot u_{mw}\right)^2\end{array}}$$

$$U_{\sigma_E} = 0.0266$$

Thus the uncertainty associated with energy balance is 0.00266.

G.3   UNCERTAINTY ASSOCIATED WITH EXERGY RATIO

Exergy of the input mass in a gasifier can be found by following relation assuming zero exergy for ash present in the biomass [2].

$$Ex_{in} = \beta. LHV \times (m - m_w)$$

Output exergy can be found as follows:

$$Ex_{out} = \sum_{i=CO,CO_2...all\ gases} \rho_i y_i F_s \left(Ex_{0i} + \int_{T_d}^{T} (C_{pi} \left(1 - \frac{T_d}{T}\right) dT \right)$$

Substituting $C_p = c_0^i + c_1^i T + c_2^i T^2 + c_3^i T^3$ in above equation where $c_0^i = c_0, c_1^i = \frac{c_1}{1000}, c_2^i = \frac{c_2}{1000^2}, c_3^i = \frac{c_3}{1000^3}$, and with integration and some simplification, the following expression can be used to replace the above equation.

$$Ex_{out} = \sum_{i=CO,CO_2...all\ gases} \rho_i y_i F_s \left(Ex_{s0_i} + a(T - T_d) + b(\ln T - \ln T_d) + c(T^2 - T_d^2) \right)$$

$$+ d(T^3 - T_d^3) + e(T^4 - T_d^4)$$

$$a = c_0^i - c_1^i T_d$$

$$b = -c_0^i T_d$$

$$c = \frac{(c_1^i - c_2^i T_d)}{2}$$

$$d = \frac{c_2^i - c_3^i T_d}{3}$$

$$e = c_3^i$$

The ratio of output exergy to input exergy is $\sigma_{Ex} = Ex_{out}/Ex_{in}$.

Thus, it can be seen from above discussion that: $\sigma_E = f(m, m_w, m_{ash}, y_i, \rho_i, F_s, T)$

The following notation is used here.

$$\gamma_{T_i} = \left(Ex_{0i} + a(T - T_d) + b(\ln T - \ln T_d) + c(T^2 - T_d^2) + d(T^3 - T_d^3) + e(T^4 - T_d^4)\right)$$

The above formula thus reduces to:

$$Ex_{out} = \sum_{i=CO,CO_2...all\ gases} \rho_i y_i F_s \gamma_{T_i}$$

The following expressions can be easily computed.

$$\frac{\partial \sigma_{Ex}}{\partial(y_i)} = \frac{\rho_i F_s \gamma_{T_i}}{\beta.\,LHV \times (m - m_w)}$$

$$= 1.615, 0.204, 4.910, 1.769, 0.139 \text{ for } CO, CO_2, CH_4, H_2, N_2 \text{ respectively}$$

$$\frac{\partial \sigma_{Ex}}{\partial(F_s)} = \frac{\sum_{(i=H_2,CO,CO_2,CH_4,N_2,H_2O)}(\rho_i y_i \gamma_{T_i})}{\beta.\,LHV \times (m - m_w)} = 0.012$$

$$\frac{\partial \sigma_{Ex}}{\partial(T)} = \frac{\sum_{all\ gases} \rho_i F_{syngas} y_i\left(a + b(\frac{1}{T}) + 2cT + 3T^2 + 4eT^3\right)}{\beta.\,LHV \times (m - m_w)} = 0.189$$

$$\frac{\partial \sigma_{Ex}}{\partial(m)} = -\frac{\sum_{all\ gases} y_i \rho_i F_s \gamma_{T_i}}{\beta.\,LHV \times (m - m_w)^2} = -0.189$$

$$\frac{\partial \sigma_{Ex}}{\partial(m_w)} = \frac{\sum_{all\ gases} y_i \rho_i F_s \gamma_{T_i}}{\beta.\,LHV \times (m - m_w)^2} = 0.189$$

Finally, the uncertainty in exergy balance can be calculated using the following relation:

$$U_{\sigma_{Ex}} = \sqrt{\begin{array}{c} \left(\frac{\partial \sigma_{Ex}}{\partial F_s} \cdot u_{F_s}\right)^2 + \sum_{\text{all gases}}\left(\frac{\partial \sigma_{Ex}}{\partial y_i} \cdot u_{y_i}\right)^2 + \left(\frac{\partial \sigma_{Ex}}{\partial T} \cdot u_T\right)^2 \\ + \left(\frac{\partial \sigma_{Ex}}{\partial m} \cdot u_m\right)^2 + \left(\frac{\partial \sigma_{Ex}}{\partial m_w} \cdot u_{m_w}\right)^2 \end{array}}$$

$U_{\sigma_{Ex}} = 0.0246$

Using those values and the above equation, uncertainty in exergy balance was determined to be 0.0246.

REFERENCES

[1] E.O. Doebelin, Measurement Systems: Application and Design, 5th ed., McGraw-Hill, 2003.

[2] K.J. Ptasinski, M.J. Prins, A. Pierik, Exergetic evaluation of biomass gasification, Energy, 32 (2007) 568-574.